11-6-2023

DYNAMIC REGULATION OF STORE-OPERATED CALCIUM ENTRY BY PROTEIN S-ACYLATION

Goutham Kodakandla
Rowan University

DYNAMIC REGULATION OF STORE-OPERATED CALCIUM ENTRY BY PROTEIN S-ACYLATION

by

Goutham Kodakandla

A Dissertation

Submitted to the
Department of Molecular Cell Biology and Neuroscience
School of Translation Biomedical Engineering and Science
In partial fulfillment of the requirement
For the degree of
Doctor of Philosophy
at
Rowan University
August 25, 2023

Dissertation Chair: Darren Boehning, Ph.D., Professor and Head, Cooper Medical School

Committee Members:
Askar Akimzhanov, Ph.D., Associate Professor, McGovern Medical School
Val Carabetta, Ph.D., Assistant Professor, Cooper Medical School
Amanda Fakira, Ph.D., Assistant Professor, Cooper Medical School
Jim Holaska, Ph.D., Professor, Cooper Medical School
Manoj Pandey, Ph.D., Assistant Professor, Cooper Medical School

Dedication

To my mom. And my dad.

Acknowledgments

I would like to thank Dr. Darren Boehning for his unwavering support, encouragement, and guidance. I would also like to thank my committee members Dr. Askar Akimzhanov, Dr. Val Carabetta, Dr. Amanda Fakira, Dr. Jim Holaska, and Dr. Manoj Pandey. I would like to express my sincerest thanks to lab members of the Boehning and Akimzhanov labs for their input and useful discussion. I would also like to thank Dr. Mark Byrne and Dr. Vince Beachley at the School of Translational Biomedical Engineering and Sciences, and Dr. Daniel Chandler at the GSBS. Finally, I want to thank the members of Department of Biomedical Sciences at Cooper Medical School of Rowan University for promoting a friendly and welcoming atmosphere during my academics. This work was supported by National Institute of General Medical Sciences (NIGMS) of the National Institutes of Health (NIH) under award numbers R01GM130840 (to D. B. and A. M. A.), R01GM115446 (to A. M. A.), and R01GM081685 (to D. B.). The content is solely the responsibility of the authors and does not necessarily represent the official views of the National Institutes of Health.

Abstract

Goutham Kodakandla
DYNAMIC REGULATION OF STORE-OPERATED CALCIUM ENTRY BY PROTEIN S-ACYLATION
2023-2024
Darren Boehning, Ph.D.
Doctor of Philosophy

Cytosolic calcium levels are finely tuned by calcium ion channels, pumps, and intracellular organelles. Store-operated calcium entry (SOCE) happens when the depletion of endoplasmic reticulum (ER) calcium stores activates a calcium sensor known as stromal interaction molecule 1 (STIM1). Activation of STIM1 leads to a conformational change from a compact state to an extended state. This extended state of STIM1 allows it to bind to a calcium channel in the plasma membrane (PM) known as Orai1. The binding of Orai1 and STIM1 leads to the opening of Orai1 channels and calcium entry into the cell. This is known as the calcium-release activated calcium (CRAC) current. Multiple subunits of Orai1 and STIM1 coalesce together at the ER:PM junctions to form oligomers known as “puncta”. Despite being discovered over two decades ago, the precise mechanism of how these two proteins in different organelles in the cell colocalize to promote calcium entry remains elusive. In this dissertation, we propose that the posttranslational addition of lipid moieties to the cysteine residues of target proteins, known as S-acylation, as a governing mechanism for the directed movement of Orai1 and STIM1 proteins to the ER:PM junctions. Our data show that the store depletion induces S-acylation of Orai1 and STIM1. We also found that S-acylation is required for puncta formation, CRAC channel assembly, and SOCE. These results reveal a new paradigm regulating calcium entry after store depletion.

Table of Contents

Abstract v

List of Figures xi

List of Tables xiii

Chapter 1: Regulation of Store-Operated Calcium Entry 1

Abstract 1

Introduction 2

History of SOCE 5

IP3-Mediated Calcium Release 6

CRAC Channel Characterization and Models of Activation 7

Calcium Influx Factor (CIF) 9

Membrane Fusion of Active CRAC Channels 9

Conformational Coupling of an ER Calcium Sensor and a PM Calcium Channel 10

TRP Channels as Potential CRAC Channels 10

The Superfamily of Drosophila TRP Channels 11

Mechanism of Drosophila TRP Activation and Function 12

Mammalian TRP Channels 13

TRP Channels and their Role in SOCE 14

Discovery and Cloning of Orai1 and STIM1 18

Orai1/STIM1 Clustering/Puncta 22

Clinical Implications of Mutations in Orai1 and STIM1 23

Mechanism of Activation of SOCE 27

STIM1 27

Orai1 33

SARAF 39

Models of CRAC Channel Assembly 42

ATP-Dependent Puncta Formation 42

Table of Contents (Continued)

Microtube-Associated STIM1 Translocation 42

Phosphatidylinositol-Mediated Membrane Sorting....43

Diffusion-Trap Model....43

S-Acylation as a Regulator of Orai1/STIM1 Assembly 45

Chapter 2: S-Acylation of Orai1 Regulates Store-Operated Calcium Entry 51

Summary Statement 51

Abstract 51

Introduction 52

Results and Discussion....53

Orai1 Is Transiently S-Acylated at Cysteine 143 53

Orai1 S-Acylation Is Necessary for Store-Operated Calcium Entry....54

S-Acylation of Orai1 is Required for Clustering and Recruitment to STIM1....55

Orai1 S-Acylation is Required for the Recruitment of Active Calcium Channels to Puncta 57

Materials and Methods 60

Cells, Antibodies, and Constructs....60

Acyl Biotin Exchange (ABE) Assay 61

Western Blotting 62

Cell Surface Biotinylation 62

Electrophysiology....63

Calcium Imaging 64

Total Internal Reflection Fluorescence (TIRF) Imaging 65

Confocal Imaging 67

Co-Immunoprecipitation 67

Acknowledgements 68

Funding....68

Table of Contents (Continued)

Competing Interests....68

Data Availability....68

Figures....69

Chapter 3: Dynamic S-Acylation of the ER-Resident Protein Stromal Interaction Molecule 1 (STIM1) is Required for Store-Operated Calcium Entry....73

Abstract....73

Introduction....74

Results....76

STIM1 is Dynamically S-Acylated After Store Depletion at Cysteine 437....76

S-Acylation of STIM1 at Cysteine 437 is Required for SOCE....77

S-Acylation of STIM1 is Required for Orai1/STIM1 Assembly....78

Formation of Functional Orai1/STIM1 Puncta is Compromised by the STIM1 C437S Mutant....78

Discussion....79

Material and Methods....82

Cells, Antibodies, and Constructs....82

Electrophysiology....83

Fura-2 Imaging....84

Confocal Imaging....85

Acyl-Resin-Assisted Capture (Acyl-RAC) Assay....85

Total Internal Reflection Imaging (TIRF)....86

Figures....88

Chapter 4: DHHC21 is a STIM1 Palmitoyl Acyltransferase....93

Abstract....93

Introduction....94

Material and Methods....96

Cells, Antibodies, and Constructs....96

Table of Contents (Continued)

Co-Immunoprecipitation 98

Super-Resolution Imaging 99

Fura-2 Imaging 99

Total Internal Reflection Fluorescence Imaging (TIRF) 100

Confocal Imaging 101

Results 101

DHHC21 is Required STIM1 S-Acylation 101

DHHC21 is Required for Store-Operated Calcium Entry 102

Co-Localization of WT and ΔF233 DHHC21 with STIM1 102

Discussion 103

Acknowledgements 106

Funding 106

Data Availability 106

Figures 107

Chapter 5: S-Acylation of SOCE-Associated Regulatory Factor Regulates Store-Operated Calcium Entry 114

Introduction 114

Results and Discussion 115

SARAF Undergoes S-Acylation Upon Store-Depletion 115

SARAF Knockout in HEK293 Cells Affects Basal Cytosolic Calcium Levels 117

SARAF C320S Shows Impaired SOCE 119

SARAF Colocalizes to CRAC Puncta Upon Store Depletion 121

Chapter 6: Conclusions and Future Directions 125

Conclusions from Orai1, STIM1, and DHHC21 Projects 125

Unanswered Questions and Future Directions 129

References 133

Table of Contents (Continued)

Appendix A: Abbreviations.....157

Appendix B: Attributes.....159

Appendix C: Supplementary Figures.....160

List of Figures

Figure Page

Figure 1.1 General overview of store-operated calcium entry (SOCE).....3

Figure 1.2 STIM1-lipid binding at the nexus of CRAC channels 32

Figure 1.3 Mechanism of DHHC enzyme catalysis.....46

Figure 1.4 S-acylation regulates CRAC puncta formation and stabilization at ER:PM junctions.....48

Figure 2.1 Orai1 is transiently S-acylated at cysteine 143.....69

Figure 2.2 Orai1 S-acylation is necessary for store-operated calcium entry 70

Figure 2.3 S-acylation of Orai1 is required for clustering and recruitment to STIM1 71

Figure 2.4 Orai1 S-acylation is required for the recruitment of active calcium channels to puncta.....72

Figure 3.1 STIM1 is dynamically S-acylated at cysteine 437 88

Figure 3.2 S-acylation of STIM1 facilitates store operated calcium entry 89

Figure 3.3 S-acylation of STIM1 is required for colocalization with Orai1.....90

Figure 3.4. STIM1 S-acylation is required for the recruitment of active Orai1 to puncta.....91

Figure 3.5 S-acylation of STIM1 C437 and CRAC channel function.....92

Figure 4.1 DHHC21 is the STIM1 protein acyltransferase 107

Figure 4.2 *Depilated* splenocytes show abnormal SOCE.....108

Figure 4.3 DHHC21 KO cells have impaired SOCE.....109

Figure 4.4 DHHC21-ΔF233 expression leads to a reduction in SOCE.....110

Figure 4.5 DHHC21-ΔF233 shows increased colocalization with STIM1 upon store-depletion.....111

Figure 4.6 DHHC21 colocalizes with STIM1 in *depilated* splenocytes.....112

List of Figures (Continued)

Figure Page

Figure 4.7 DHHC21 regulates SOCE by S-acylating STIM1 113

Figure 5.1 SARAF undergoes S-acylation at C320 residue 117

Figure 5.2 SARAF CRISPR knockout affects ER calcium levels and SOCE.....118

Figure 5.3 S-acylation of SARAF regulates store-operated calcium entry and peak calcium entry.....120

Figure 5.4 SARAF is recruited into CRAC puncta.....122

List of Tables

Table Page

Table 1. Common Mutations in Orai1 and STIM1 Associated with Genetic Diseases in Humans 25

Chapter 1

Regulation of Store-Operated Calcium Entry[1]

Abstract

Calcium influx through plasma membrane ion channels is crucial for many events in cellular physiology. Cell surface stimuli lead to the production of inositol 1,4,5-trisphosphate (IP_3), which binds to IP_3 receptors (IP_3R) in the endoplasmic reticulum (ER) to release calcium pools from the ER lumen. This leads to the depletion of ER calcium pools, which has been termed store depletion. Store depletion leads to the dissociation of calcium ions from the EF-hand motif of the ER calcium sensor Stromal Interaction Molecule 1 (STIM1). This leads to a conformational change in STIM1, which helps it to interact with plasma membrane (PM) at ER:PM junctions. At these ER:PM junctions, STIM1 binds to and activates a calcium channel known as Orai1 to form calcium-release activated calcium (CRAC) channels. Activation of Orai1 leads to calcium influx, known as store-operated calcium entry (SOCE). In addition to Orai1 and STIM1, the homologs of Orai1 and STIM1, such as Orai2/3 and STIM2, also play a crucial role in calcium homeostasis. The influx of calcium through the Orai channel activates a calcium current that has been termed CRAC current. CRAC channels form multimers and cluster together in large macromolecular assemblies termed "puncta". How CRAC channels form puncta has been contentious since their discovery. In this

[1] Goutham Kodakandla, Askar M. Akimzhanov, Darren Boehning
Cooper Medical School of Rowan University, Camden, NJ, USA, 08103
Department of Biochemistry and Molecular Biology, McGovern Medical School, University of Texas Health Sciences Center at Houston, Houston, Texas, USA, 77030

https://doi.org/10.48550/arXiv.2309.06907

review, we will outline the history of SOCE, the molecular players involved in this process, as well as the models that have been proposed to explain this critical mechanism in cellular physiology.

Introduction

Calcium is a crucial secondary messenger that serves a multitude of functions ranging from subcellular signaling to organ system-level changes. It serves many roles in biological processes, including growth, disease, and death [1-3]. Calcium levels in the cytosol are maintained at ~100nM in many ways, including calcium pumps and exchangers on the plasma membrane and various organelles. The extracellular calcium concentration is 1-1.5 mM [1]. The calcium ion gradient across the plasma membrane (PM) is maintained by calcium efflux pumps and ion channels, in addition to calcium reuptake mechanisms in ER. Sarco-endoplasmic reticulum calcium ATPase (SERCA) pumps use an active transport mechanism to move calcium across the concentration gradient from the cytosol into the ER lumen [4, 5]. Upon cellular stimulation by agonist actions at plasma membrane receptors, a multitude of signaling cascades starts that lead to the production of inositol 1,4,5-trisphosphate (IP_3) due to phospholipase-C-mediated cleavage of membrane phosphatidylinositol 4,5-bisphosphate (PIP_2) [6]. Once produced, IP_3 binds to and activates the IP_3 receptors (IP_3Rs) on the ER membrane to promote calcium release from the ER lumen into the cytosol. This decrease in calcium levels in the ER leads to intracellular calcium store depletion [7]. Store depletion leads to the activation of an ER transmembrane protein known as stromal interaction molecule 1 (STIM1), which then binds to Orai1 channels on the plasma membrane to promote store-operated calcium entry (SOCE) [7, 8]. The channel formed by Orai1 and STIM1 is

known as the calcium release-activated calcium (CRAC) channel. A general overview of SOCE is presented in **Figure 1.1**.

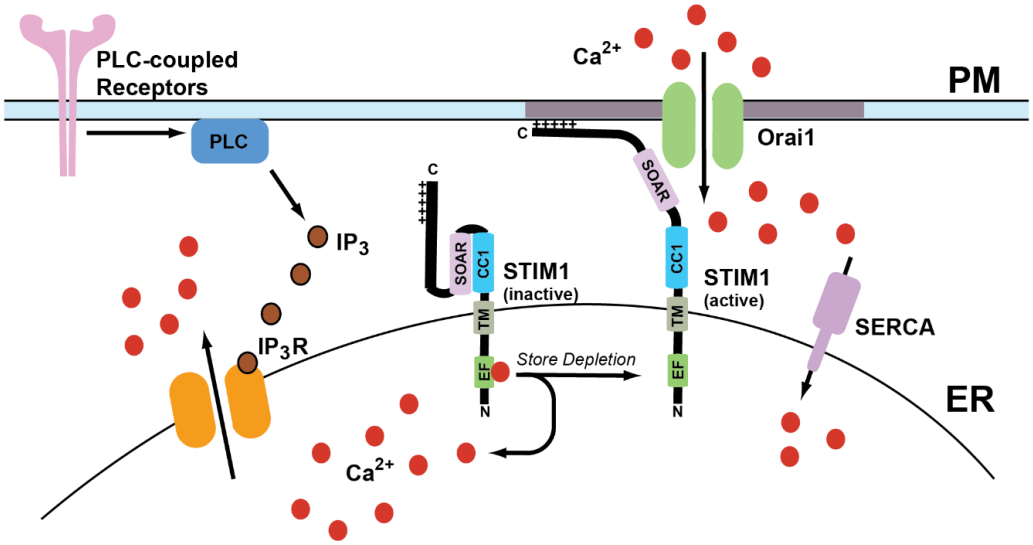

Figure 1.1. General overview of store-operated calcium entry (SOCE). Agonist stimulation through the PLC-coupled receptors leads to IP3-mediated calcium release which leads to ER calcium store depletion. As a result, calcium dissociates from the EF-hand of STIM1 and leads to its activation. This leads to a conformation change in STIM1 which extends its C-terminus toward plasma membrane where it binds to Orai1 channels and form calcium-release activated calcium (CRAC) channels. CRAC channels promote calcium entry from extracellular milieu into the cells. One subunit of STIM1 dimer is shown here for simplicity.

Store-operated calcium entry is a predominant mechanism for calcium entry from the extracellular milieu to increase cytosolic calcium after store depletion. It also serves to refill the ER calcium stores after IP_3-mediated calcium release [9, 10]. The most important role SOCE plays is a sustained calcium entry that can last from several seconds

to up to an hour in some cellular systems [11, 12]. One specific case where this differential role of calcium entry plays a crucial role is the activation of T cells. For example, the activation of nuclear factor of activated T cells (NFAT), which regulates IL-2 production, a sustained calcium entry is needed, which lasts for several minutes [13]. While for activation of NF-KB, calcium oscillations of lower frequency from Orai1 channels are required. Finally, CaMKII, a calcium sensitive kinase, needs calcium oscillations of higher frequency for its activation. Thus, cellular functions regulated by calcium are mediated by changes in both frequency and amplitude [14]. Calcium entry from the plasma membrane is essential for shaping the spatiotemporal aspects of calcium transients, including the amplitude and duration of calcium release events. Calcium entry contributes to many cellular functions such as secretion, gene transcription, and enzyme activation. Efficient SOCE requires the formation of multiple Orai1-STIM1 complexes at defined ER:PM junctions known as “puncta” [15-18]. A key difference between CRAC channels and other calcium channels such as voltage or ligand gated ion channels is their ability to conduct calcium currents at resting membrane potentials without ligand binding [19]. This property allows CRAC channels to be gated in non-excitable cells by exclusively by binding to STIM1. This facilitates precise spatiotemporal regulation of cellular calcium signaling by store depletion.

In this review, we look at the historical origins of SOCE and summarize a few landmark studies that established the characteristics of SOCE. We will delve into the proteins that form the CRAC channel complex, such as Orai1 and STIM1, and how these proteins are regulated. In addition to STIM1, STIM2 is another member of ER resident calcium sensor that promotes SOCE. Orai2 and Orai3 are genes in the Orai family with Orai1.

Proteins outside these two families such as TRP channels also play a role in SOCE. Finally, we will also review the effect of SOCE-associated regulatory factor (SARAF) and role it plays in SOCE. SARAF promotes calcium dependent inactivation, but how it functions as an inactivator of SOCE is not well known. Our review outlines the key modulators of SOCE. We will conclude with a discussion of very recent work indicating the protein S-acylation is a key mediator of CRAC channel assembly and function.

History of SOCE

The earliest known proposal for SOCE was introduced by the Putney group in 1985 as outlined by their model for receptor-regulated calcium entry, in which they proposed the mechanism for sustained calcium entry from extracellular matrix upon agonist binding to G-protein coupled receptors [20]. Termed as the capacitive calcium entry model, they carefully analyzed the calcium release from the ER and entry from extracellular milieu, and the coupling between these two processes. A few years later, Hoth and Penner identified a similar inward rectifying calcium current in mast cells upon depletion of intracellular calcium stores using IP_3 [21]. Zweifach and Lewis then showed store depletion in T cells leads to a similar calcium current using thapsigargin, a SERCA pump inhibitor [22]. Later, studies published by Liou et al, and Roos J et al, identified STIM proteins as sensors of ER luminal calcium [23, 24]. A year later, studies by Feske et al showed how a mutation in Orai1 protein causes immune deficiency by affecting SOCE [25]. Other studies during this same period also showed Orai1 is crucial for SOCE [26]. A genome wide RNAi screen in drosophila S2 cells showed the role of both Orai1 and STIM1 in SOCE. They demonstrated that RNAi of olf186-f, the *drosophila* Orai1 homologue, reduced thapsigargin-evoked SOCE, which was improved by 3-fold upon its

overexpression. In addition, co-expression of STIM with olf186-f increased SOCE by approximately 8-fold [27, 28]. These seminal studies identified the key regulatory proteins involved in SOCE. What followed is an expansion of studies involving Orai and STIM proteins and their role in CRAC channel formation to promote SOCE.

IP3-Mediated Calcium Release

Cleavage of membrane phospholipids by phospholipase C (PLC) leads to production of IP_3 and glycerol [6]. Liberated IP_3 binds to IP_3 receptor calcium channels on ER membranes, and leads to calcium efflux from the ER lumen [29]. Depending on the strength and duration of agonist stimulation, IP_3R activation leads to decrease of calcium levels in the ER lumen which is termed as store depletion [7, 29]. The role of IP_3 in activating calcium release from endoplasmic reticulum was initially discovered by experiments by the Berridge group in blowfly salivary glands based on the ability of those tissues to respond to hydrolysis of PIP_2 [30]. Subsequently, the role of IP_3 as a secondary messenger was to mobilize internal calcium stores in mammalian cells was demonstrated in saponin-permeabilized hepatocytes [31]. Application of IP_3 led to a brief rise in intracellular calcium levels followed by a sustained calcium plateau [31]. Capacitive calcium entry was the first model proposed to explain the calcium entry observed in cells upon emptying intracellular calcium pools [20]. This idea originated from the observation that calcium entry from the extracellular milieu lasted for a long duration after the levels of IP_3 returned to the baseline. These observations were made in rat parotid gland upon carbachol [32] application, and rabbit ear artery upon application of noradrenaline [33]. Based on the biphasic nature of agonist-induced increase in the cytosolic calcium, it was proposed that the initial increase is a result of calcium release

from the ER due to the action of IP_3 followed by influx of calcium through channels in the plasma membrane until the levels of calcium in the ER reaches to a significant level that stops the entry [20].

CRAC Channel Characterization and Models of Activation

An effort to accurately define the mechanism of SOCE and to distinguish it from other calcium currents led to further research into the channels underlying these currents. CRAC channels conduct calcium currents at a negative membrane potential. The voltage independence of CRAC channel gating was first observed in patch recordings conducted on Jurkat T cells treated with various cell mitogens such as phytohaemagglutinin (PHA), a substance known to activate T-cell signaling pathway [19]. A similar current was also observed in these cells recorded in low extracellular calcium. In a separate set of experiments conducted in mast cells, intracellular dialysis with IP_3 and extracellular application of substance P generated a similar low-noise current (1-2pA) in patch-clamp recordings [34, 35]. This current developed in these cells with a concomitant increase of intracellular calcium. The currents observed by both groups showed similar features such as inward rectifying current-voltage relationship, voltage-independent gating, very high calcium selectivity, an extremely low unitary conductance, and extracellular calcium-dependent feedback inhibition.

The discovery of thapsigargin as a potent, selective, and irreversible SERCA pump inhibitor helped in delineating the difference between CRAC currents and other calcium currents [36]. Thapsigargin promotes a slow calcium leak from the ER lumen into the cytosol, and thereby passively depletes ER calcium stores, possibly through the Sec61 translocon on the ER membranes [37]. In addition, the development of calcium sensitive

fluorescent dyes made live-calcium imaging feasible without the need for electrophysiological recordings [38]. One established model of isolating SOCE currents using calcium-sensitive dyes involves depletion of ER calcium stores by treatment with thapsigargin in calcium-free buffer. Subsequent treatment of these cells with calcium replete buffer results in calcium entry from extracellular milieu which can easily be monitored using microscopy in live cells. Using this methodology, along with other imaging paradigms, many groups have reported SOCE in both excitable and non-excitable cells. It was discovered that PLC-mediated IP_3 production was dispensable for SOCE [39-41]. A seminal observation made in parotid acinar cells using thapsigargin to deplete stores garnered evidence that the ER calcium store levels and activate SOCE independently of IP_3 production [42]. A subsequent set of experiments done on T cells using thapsigargin established the role of ER calcium store depletion and T-cell activation. The term I_{CRAC} was coined by Hoth and Penner after identifying calcium currents in whole cell currents elicited by a number of agents such as ionomycin, IP_3, and EGTA [21]. The crucial experiments conducted by Lewis and colleagues using perforated-patch clamp and thapsigargin in T cells showed the similarity between TCR-mediated calcium currents and CRAC currents [22, 43, 44]. These studies led to the definitive conclusion that CRAC currents are controlled by intracellular ER calcium stores.

The research into how ER calcium depletion leads to CRAC channel activation led to three main hypotheses: 1) diffusion of an activating factor released from the ER to the plasma membrane, 2) targeting of active CRAC channels to the PM by membrane fusion,

and 3) conformational coupling between a putative ER calcium sensor and a PM calcium channel. Here we will discuss these proposals in detail.

Calcium Influx Factor (CIF)

The earliest proposal for a diffusible mediator that is released from the ER into the cytosol and/or the extracellular milieu to activate calcium influx was presented in early 1990s. Application of phytohaemagglutinin (PHA)-treated Jurkat T cell extracts to P388D1 macrophage cells showed a sustained but fluctuating calcium increase. A diluted version of the extract decreased the amplitude and increased the latency of the calcium flux [45]. Interestingly, NG115-401L cells did not show CIF-induced calcium entry [46]. In later studies, it was shown that NG115-401L cells do not express endogenous STIM1 [47]. The treatment of putative CIF-containing extracts with alkaline phosphatase neutralized the effect of these extracts. These observations led to a proposal where cellular stimulation leads to the production of a diffusible factor that activates extracellular influx of calcium [7, 8].

Membrane Fusion of Active CRAC Channels

It was found that acid extracts from thapsigargin-treated Jurkat cells leads to a chloride current in *Xenopus* oocytes [46]. Microinjection of Xenopus oocytes with the Rho GTPase inhibitor clostridium C3 transferase potentiated a calcium entry current termed I_{SOC}. In addition, the expression of wild-type or constitutively active Rho inhibited I_{SOC}. Interestingly, botulinum neurotoxin A and dominant negative SNAP-25 mutants activated I_{SOC}. Treatment of these cells with brefeldin A, an agent that blocks exocytosis by inhibiting protein maturation and exit from Golgi apparatus, has no effect on I_{SOC}. Based

on these results, Tsien and colleagues proposed the model where SOCE is mediated by exocytosis, leading to CRAC channels being inserted into the plasma membrane [48].

Conformational Coupling of an ER Calcium Sensor and a PM Calcium Channel

The IP_3 receptor has calcium binding sites in its luminal domain. This calcium binding site on the IP_3 receptor was proposed to regulate calcium efflux from the ER into the cytosol [49, 50]. Based on these observations, it was proposed that the IP_3R was a sensor for ER calcium levels. Upon depletion of ER calcium stores, a cytosolic domain of the receptor binds to the plasma membrane to promote calcium influx. In this hypothesis, the IP_3 receptor is the regulator of calcium homeostasis in the cells, resulting in release from the ER lumen, as well as influx from extracellular milieu [51]. The role the IP_3R plays in this conformational coupling model is analogous to the role of ryanodine receptors and dihydropyridine receptors in muscle cells [52].

The identification of the mechanism(s) of CRAC channel activation ultimately required the cloning and characterization of the relevant calcium channel(s) activated by store depletion. In the next section we will discuss the putative role of transient receptor potential (TRP) channels in mediating SOCE.

TRP Channels as Potential CRAC Channels

Transient receptor potential (TRP) channels are ion channels that show diverse ion selectivity, activation mechanisms, and physiological functions. All TRP channels share some common features such as six transmembrane domains, tetrameric structure, cation selectivity, and sequence homology. The first TRP channels were characterized in *Drosophila* visual transduction mutants [53, 54]. The *Drosophila trp* and *trpl* mutants have a significant decrease in light-induced calcium influx [55, 56]. Combined with other

mutants in the PLC pathway which also affected vision, it was hypothesized that *trp/trpl* channels are putative SOCE channels. Cloning and characterization of these channels showed that the protein encoded by the *trp* gene localizes to the eye, contains four N-terminal ankyrin repeats, and a transmembrane topology similar to voltage-gated ion channels. [57, 58]. Whole cells currents recorded from Sf9 insect cells showed the channels encoded by *trp* gene are activated upon ER calcium store depletion and are moderately selective for calcium over monovalent cations such as sodium (P_{Ca}:P_{Na} ~ 10:1) [59].

The Superfamily of Drosophila TRP Channels

There are seven subfamilies of TRP channels, all with 6 transmembrane domains. These channels likely form tetrameric assemblies similar to voltage-dependent channels [60-62]. TRP channels do not have positively charged residues on the fourth TM domain and thus do not have a traditional voltage sensor for gating [63]. TRP channels are highly conserved across animal kingdom ranging from worms to humans. The nomenclature of TRP channels is based on the first recognized member within each subfamily. The classical or canonical TRPs are grouped in to TRPC subfamily. TRPC, TRPV (transient receptor potential vanilloid), TRPM (transient receptor potential melastatin), TRPN (transient receptor potential nompC), and TRPA (transient receptor potential ankyrin) are group 1 TRP channels and share sequence identity in the TM domains. Of these, TRPC, TRPM, and TRPN have a 23-25 amino acid TRP domain in the C terminus after the sixth TM domain. TRPP (transient receptor potential polycystin) and TRPML (transient receptor potential mucolipin) are group 2 subfamily TRP channels vary from group 1 TRP channels in low sequence similarity and the presence of a large extracellular loop

between TM1 and TM2 domains [64]. The TRPN subfamily of TRP channels are found in invertebrates [65] and zebrafish [66]. Some distantly related TRP channels are also found in fungi, characterized into the TRPY subfamily [67, 68].

In *Drosophila*, three TRPC members are expressed in the eye that play an important role in phototransduction. TRP, TRPL, and TRPγ are the three proteins work in concert for successful operation of fly vision [69, 70]. TRPL and TRPγ have ~50% sequence identity with TRP in the six TM domains, and only differ in the TRP domain, which contains highly conserved regions known as TRP boxes 1 and 2. Loss-of-function and dominant-negative mutations in *Drosophila* TRPCs have demonstrated the importance of these channels in calcium influx in photoreceptors of *Drosophila* upon light stimulus. The *trpl* mutant flies affect the specificity of different cation influx and a decreased response to light stimulus of long duration. In addition, *trp/trpl* double mutant flies cannot respond to light, showing the importance of these channels. Finally, TRPγ heteromultimerizes with TRPL to form light-regulated channels, and a dominant-negative form of TRPγ suppresses TRPL currents [70-73].

Mechanism of Drosophila TRP Activation and Function

The *Drosophila* TRP can be activated in tissue culture setting by blocking the SERCA (sarcoplasmic endoplasmic reticulum calcium ATPase) pumps that maintain the calcium gradient between ER lumen and cytosol [59, 69]. Thapsigargin irreversibly blocks SERCA pumps and causes a passive ER calcium leak, which will then activates store-operated calcium channels [36, 74]. However, *in vivo* observations do not support the *in vitro* analyses. Thapsigargin-mediated SERCA blockade or IP_3 receptor activation does

not promote calcium influx or affect phototransduction [75-77]. Some studies also evaluated the potential effect of diacylglycerol, another product of PLC hydrolysis of PIP_2, on calcium influx and phototransduction. Isolated photoreceptor cells from drosophila wild type and *rdgA* (DAG kinase) mutants show constitutive TRP activity. Recently, endocannabinoids produced in Drosophila photoreceptor cells in response to light have been shown to activate TRP channels [78]. In addition, using flies engineered to express genetically encoded ER calcium indicator, the sodium/calcium exchanger has been shown to result in rapid calcium release from the ER upon light exposure [79].

Mammalian TRP Channels

The seven TRPC proteins in mammals are divided into four groups based on sequence homology [80, 81]. Like *Drosophila* TRPC proteins, the mammalian counterparts also include three to four ankyrin repeats, 6 TM domains, and high sequence homology in the TRP box domain in the N-terminus [82-86]. Like Drosophila TRPCs, the activation of mammalian TRP channels can be activated in cultured cells through PLC activation [85, 87]. The specific mediator in the PLC pathway that ultimately activates these channels is still unknown, and hypotheses include activation by IP_3, DAG, and calcium. TRPC1-4 proteins have been shown to be activated upon store depletion, either by IP_3 or thapsigargin treatment in cultured cells expressing these proteins [85, 87, 88]. Calcium influx factor was proposed to be a factor to activate these channels to promote calcium influx [45, 46, 89]. Additional hypotheses also included conformational coupling between IP_3R and the TRP channels [51]. Some models also suggested internalization of TRPC1/3/4 channels upon store depletion [90, 91]. Other TRPC proteins, such as

TRP6/7, are activated by DAG and show similarities to *Drosophila* TRP channels [90, 92].

Another complexity in mammalian TRPC channel activation comes from context and cell type-specific activation mechanisms. For example, mouse TRPC2 in vomeronasal neurons has been shown to be activated by DAG, whereas the same protein in mouse sperm has been shown to be activated by calcium release [93, 94]. Whether this differential activation is due to alternate splicing or different multimerization is unknown [95, 96]. TRPC3 also shows similar differential activation between DAG and store depletion. Some reports also suggest direct binding between TRPC3 and IP_3R as a mode of activation of these channels [87, 92, 97]..

TRP Channels and their Role in SOCE

Of the many roles TRP channels play in cellular physiology, a crucial one is store-operated calcium entry [98]. TRP channels have low calcium selectivity, which distinguishes them from conventional CRAC channels or voltage-gated calcium channels. As such, TRP channels are high conductance and non-selective cation channels with varying permeability ratios between calcium, potassium, and sodium [99, 100]. The mechanism of TRP channel activation and gating ranges from changes in cytosolic calcium concentration, to membrane depolarization, and external cellular stimuli [21]. The loop between transmembrane domains 5 and 6 form the channel pore of these TRP channels. Four individual TRP subunits form an active channel complex to promote calcium entry [101, 102]. The domain architecture of different TRP family proteins regulates the functions of these proteins. For example, TRPC, TRPV, and TRPA channels

have repeats of ankyrin regions in their N-terminus [102] and TRPC and TRPM channels have a conserved TRP domain adjacent to the last transmembrane domain [53]. TRPM subfamily of TRP channels have a catalytic kinase domain in their C-terminus. These proteins also have a highly conserved TRP box sequence (Glu-Trp-Lys-Phe-Ala-Arg) and proline-rich sequence that regulates signal transduction and gating [103]. In addition, coiled-coil domains in C- and N- terminal domains aid in the assembly of some TRP channel subfamilies [104]. These coiled-coil domains also regulate the channel binding to STIM1, the ER calcium sensor, to regulate SOCE [105]. A C-terminal calmodulin and IP_3R binding region in TRPC channels is known to regulate both store-independent, and store-dependent calcium entry [106, 107].

Different subfamilies of TRP channels are expressed in different cell types and carry out specific functions in only these cell types. For example, TRPC channels are expressed in endothelial cells, where they mediate cell shape, blood vessel tone and permeability, angiogenesis, and leukocyte trafficking by modulating calcium entry in these cells [108-112]. TRPC4 knockout mice show impaired vasorelaxation of the aortic rings and no IP_3 and BAPTA-induced calcium influx in aortic endothelial cells [113]. TRPC subfamily proteins are also expressed in other non-excitable cells where they regulate SOCE such as platelets, pancreatic beta cells, salivary gland cells [114, 115]. Another important process where SOCE plays an important role is in fertilization of the mammalian egg. A signaling cascade is activated following fusion of the sperm with the egg the results in activation of several GPCR signaling mediators finally resulting in store-operated calcium influx. A putative isoform of TRPC2 helps in the calcium influx in the egg cell that is mediated by the glycoprotein ZP3 in mice [94].

Several TRPC proteins has been found in brain and tissues in the central nervous system [116, 117]. In rodents, expression of TRPC2 is involved in the pheromone detection response [96, 118]. In mammalian brains, TRPC3 is activated following brain derived nerve growth factor (BDNF) activation of receptor tyrosine kinase TrkB [119]. This pathway is known to aid in neuronal differentiation, synaptic plasticity, and neurotransmitter release. TRP channels play roles across animal kingdom in sensory physiology such a visual transduction in Drosophila [120], olfaction, mechanosensation, and osmosensation in C. elegans [121], and acid, heat, and pain responses in mice [122].

Support for TRP channels acting as store-operated channels came from the studies done using TRPC1 expression in vitro which showed increased calcium entry after store depletion [87, 88, 123]. One key difference in these experiments was even though these cells showed calcium entry upon store depletion, this current was different from the biophysical properties observed in CRAC currents (I_{CRAC}) [88, 124, 125]. Experiments later determined that TRPC1 is assembled with the Orai1-STIM1 complex [126, 127]. Immunofluorescence and confocal microscopy in human salivary gland cells showed colocalization of Orai1, STIM1, and TRPC1 at the plasma membrane upon store depletion [126].. Activation and gating of TRPC1 is mediated by negatively charged aspartate residues which bind STIM1 at both the SOAR domain as the polybasic domain [128]. Examination of how calcium entry observed from Orai1:STIM1 complex upon store depletion differs from TRPC1:STIM1 complex led to many interesting hypotheses. One hypothesis is that the local increase of cytosolic calcium near ER:PM junctions upon store depletion activates cytosolic TRPC1 channels, which then gets embedded into the plasma membrane to be activated by STIM1 [11, 129]. This model can explain the

spatiotemporal differences observed in calcium oscillations in Orai1:STIM1 complexes versus TRPC1:STIM1 complexes. These differences also affect the physiological and pathological outcomes of cytosolic calcium transients. One specific example is the activation of nuclear factor of activated T-cells (NFAT) versus activation of NF-kB. Calcium entry mediated by Orai1 after T-cell stimulation leads to activation of NFAT [130-132], while TRPC1-dependent calcium entry leads to activation of NFkB [133]. Interestingly, knockdown of Orai1 in Jurkat cells inhibits both SOC and CRAC currents, with no effect upon knockdown of TRPC1 or TRPC3 [134]. In addition, calcium entry observed from the Orai1:STIM1:TRPC1 complex leads to insulin release from pancreatic beta cells, platelet activation during blood clotting, and SNARE complex formation for adipocyte differentiation and adiponectin secretion [135-137]. Furthermore, calcium entry from this complex contributes to prostate and colon cancer cell migration [138, 139]. Finally, calcium entry observed in STIM1-Orai1-TRPC1-TRPC4 complexes plays a pivotal role in right ventricular hypertrophy [140].

Decades of research has now shown the pivotal role of TRP channels modulating the spatiotemporal aspects of calcium release in many systems. This includes activation by store depletion and other IP_3-mediated signaling pathways. However, TRP channels do not re-capitulate the "classic" biophysical properties of store-operated calcium currents originally described T cells, including small unitary conductance and very high calcium selectivity. We will next describe the cloning of Orai1 and STIM1 as mediators of this specific type of SOCE with direct implications for human disease.

Discovery and Cloning of Orai1 and STIM1

Feske and colleagues reported abnormalities in T-cell activation in infants born to consanguineous parents that manifested as severe combined immunodeficiency (SCID) [25]. They found increased CD4+ T cell counts and inability of these T cells to produce IL-2 upon stimulation with phorbol 12-myristate 13-acetate (PMA), concanavalin A, and anti-CD3 stimulation. Exogenous application of IL-2 restored the proliferative deficiencies of these cells. Further analyses into the DNA binding activity of transcription factors showed a lack of NFAT binding to DNA with no difference in AP-1, NF-kB, and Octamer binding proteins. They also found no differences in the expression of NFAT, but the dephosphorylation and nuclear translocation was affected in these T cells [141]. In subsequent experiments using PMA+ionomycin and increasing concentrations of extracellular calcium, they found that higher levels of extracellular calcium rescued IL-2 production in these T cells [142]. They concluded that dysregulation in upstream signaling events play a role in NFAT binding to DNA elements that ultimately results in SCID [25].

During this time, it was discovered that there exist two different calcium mobilization patterns in T cells after stimulation. An immediate transient calcium spike [143] followed by a sustained calcium influx from extracellular milieu [20, 144]. The transient calcium release activates NF-kB and JNK, but NFAT activation needs sustained elevations to promote dephosphorylation by the calcium-dependent phosphatase calcineurin [145-148]. Calcium imaging of T cells obtained from the patients with SCID showed dysregulated calcium entry upon stimulation with anti-CD3, ionomycin, and thapsigargin. More importantly, membrane hyperpolarization with valinomycin did not alter calcium entry

abnormalities found in these cells, suggesting the lack of calcium entry is not a result of depolarization [149]. These intriguing results warranted further research into the calcium entry in T cells upon their activation and the ion channels that promote sustained calcium entry.

Development of RNAi screening as a research tool in early 2000s opened avenues for high throughput identification of proteins that mediate specific signaling pathways [150, 151]. Two important siRNA screens performed at this time identified the proteins involved in mediating I_{CRAC} and pinpointed the possible mechanism of activation [27, 152]. These two screens were performed in the Drosophila S2 cells, which were known to have a store-operated channel with low conductance and high calcium selectivity similar to I_{CRAC} in mammalian cells [153]. The siRNA screen performed by Feske and colleagues identified known proteins that affect calcium influx in addition to NFAT regulatory proteins [27]. When they used this RNAi screen to identify potential regulators of Ca^{+2}/calcineurin mediated NFAT activation, they found a kinase that negatively regulated exogenously expressed NFAT. In addition, they also found other candidates in this screen that alter calcium levels in the cytosol such as SERCA, Homer, and STIM. Concurrently, Zhang and colleagues independently performed a similar genome-wide RNAi screen [152]. Probing for hits that resulted in an inhibition of calcium influx after store depletion by thapsigargin, they identified 11 transmembrane proteins including STIM. Of note was another four transmembrane protein olf186-F, which showed a reduction in SOCE and CRAC currents. They followed up this experiment with an overexpression paradigm, which showed a three-fold increase in CRAC currents, which was further increased to

eight-fold upon co-expression with STIM [152]. These two pivotal experiments identified Orai1 and STIM1 as the core proteins that form the CRAC channel.

At the same time these RNAi experiments were being conducted, Feske and colleagues continued their research into understand the T-cell activation abnormalities in SCID infants. Using whole-cell patch-clamp electrophysiology performed on T cells from control and SCID patients, they showed that T cells obtained from some SCID patients lacked SOCE. Furthermore, they also found that exogenous expression of STIM1 in these SCID cells did not rescue SOCE in these cells [131]. Next, they used a combined approach of *Drosophila* RNAi screening and linkage analysis with a single-nucleotide polymorphism (SNP) array to screen for regulators of SOCE and nuclear import of NFAT. T cells obtained from SCID infants and relatives of these infants were analyzed for SOCE deficits and SNP mapping arrays using their genomic DNA. This, in conjunction with *Drosophila* RNAi screen for NFAT regulators, pointed to a gene olf186-f in Drosophila and to the *TMEM142A* gene on chromosome 12 in humans which they named Orai1 [154]. Genomic DNA sequencing showed a mutation of an arginine to tryptophan at residue 91 (R91W) on Orai1, identifying the molecular defect in these patients leading to reduced SOCE. Finally, exogenous expression of wild-type Orai1 in T cells from SCID patients restored CRAC channel activity.

STIM1 is mammalian homolog of *Drosophila* STIM, which is essential for CRAC channel activation in human T cells. Roos and colleagues showed in S2, HEK293, and Jurkat cell lines that silencing of STIM1 abrogates SOCE [155]. Zhang et. al. determined the role of the luminal EF hand motif by expressing calcium binding mutants in Jurkat T cells and analyzing SOCE. The STIM1 EF hand calcium binding mutants 1A3A and 12Q

were found to be constitutively active STIM1 mutants [24]. At the time, the pore forming Orai1 subunit had not been cloned and it was hypothesized that STIM1 may traffic to the PM upon store depletion to activate a channel or form a channel itself. The critical role of the EF hand in SOCE and puncta formation was independently confirmed by another group in HeLa cells using a D76A mutant [23]. This discovery, along with the discovery of Orai1 as CRAC channel pore forming subunit, potentiated a barrage of research into these proteins in SOCE.

The discovery of Orai1 as pore-forming subunit of CRAC channels was a direct result of the RNAi approaches in *Drosophila* S2 cells by several groups as outline above. Following the research into calcium deficits observed in SCID human patients, two different groups pursued RNAi screens focused toward decreases in NFAT translocation into nucleus, and they individually found the same four transmembrane plasma membrane protein with intracellular C and N termini olf186-F [26, 149], and named it CRACM1 [26]. The human homolog of this protein was eventually named Orai1. There are three homologs of Orai proteins with high sequence identity, with up to 90% identity in the transmembrane regions. Overexpression of Orai1 and STIM1 in HEK293 cells helped identify the pore forming subunit of CRAC channels. The definitive proof for Orai1 as the pore forming subunit came from experiments that showed the importance of acidic residues in the transmembrane domains of Orai1. Residues E106 and E190 are two important glutamic acid residues that line the pore of Orai1 channel. Mutation of these residues to aspartate and glutamine respectively decreased the calcium influx, increased monovalent cation current, and made the channel cesium permeable [156]. These experiments strongly supported Orai1 as the pore forming unit of CRAC channel.

Orai1/STIM1 Clustering/Puncta

Orai1 in the plasma membrane and STIM1 in the ER membrane are diffusely distributed in cells with replete ER calcium stores. Upon store depletion, Orai1-STIM1 complexes are recruited to ER:PM junctions where they form CRAC channel clusters to promote efficient calcium entry upon store depletion [16]. These clusters were denoted as "puncta" upon observation under fluorescence microscopy of tagged-STIM1 [18, 23, 24, 157-159]. These ER:PM junctions are regions within the cell where PM and ER are held in close apposition (~10-20 nm) [18, 160]. Upon store depletion, STIM1 accumulates near the thin cortical tubules of the ER [160]. An interesting observation in CRAC puncta formation is the longevity of these puncta. Depending on the downstream effect of calcium influx, the puncta can be active for a few minutes or up to an hour. How these puncta can stay active to promote calcium entry for this duration is still not completely understood. Even more compelling is the ability of STIM1 to translocate to the sites of already formed puncta repeatedly upon subsequent store depletion [161]. A multitude of factors regulate this behavior to increase the number of cortical ER tubules near the plasma membrane. One mechanism is a secretion-like coupling model which includes redistribution of F-actin into cortical layers [162]. STIM1 has been known to interact with microtube attachment protein EB1 and maintain ER tubule length [163]. STIM1 also binds to plasma membrane using its polybasic domain, which might strengthen the STIM1 localization in the puncta [16]. The SOAR region of STIM1 also has a cholesterol binding domain which has been shown to bind to cholesterol rich regions in the plasma membrane [164]. Several additional proteins like synaptogamins and septins maintain the integrity of these ER:PM junctions [165, 166]. Cytosolic calcium elevation leads to

increased translocation of E-Syt1 to ER:PM junctions, which subsequently recruits the phosphatidylinositol transfer protein (PITP) Nir2 to these junctions to strengthen ER:PM junction stability [166]. E-Syt2 and E-Syt3 also regulate the ER:PM junctions, in a calcium-independent manner [167]. Interestingly, siRNA-mediated knockdown of E-Syt proteins decreases the number of ER:PM contact sites but does not affect SOCE [167]. This explains the possibility that E-Syt proteins maintain the stability of ER:PM junctions with no specific effect on Orai1 or STIM1. Another protein that has shown a role in regulating SOCE as well as long-term maintenance of ER:PM junctions is an ER transmembrane protein TMEM110, also known as junctate [168]. Junctate is a calcium binding protein in the ER membrane that forms supramolecular complexes with IP_3 receptors and TRPC3 calcium channels. Junctate has an EF-hand domain in its ER luminal side, which is required for CRAC channel activation independently of store depletion [169, 170]. In addition to these proteins mentioned above, many other proteins play a crucial role in maintenance of stable ER:PM junctions that help CRAC channel formation and function [171].

Clinical Implications of Mutations in Orai1 and STIM1

Mutations observed in Orai1 and STIM1 lead to several diseases in humans, and the phenotype is broadly based upon whether the mutations are loss-of-function or gain-of-function. The loss-of-function mutations show immunological deficits such as immunodeficiency, ectodermal dysplasia autoimmunity, muscular hypotonia, and defects in tooth formation. The gain-of-function mutations show constitutive CRAC channel activity and abnormal cytosolic calcium levels which lead to diseases affecting musculoskeletal system. Gain-of-function mutations lead to the disorders tubular

aggregate myopathy (TAM), York platelet syndrome, Stormorken syndrome, thrombocytopenia, and bleeding disorders. The common mutations involved in CRAC channelopathies and associated references are listed in **Table 1**.

Table 1

Common Mutations in Orai1 and STIM1 Associated with Genetic Diseases in Humans

Gene Name	**Protein Mutation**	**Disease**	**OMIM**
ORAI1	G98S	Myopathy, tubular aggregate, 2	610277.0003
ORAI1	P245L	Myopathy, tubular aggregate, 2	610277.0002
ORAI1	R91W	Immune dysfunction with T-cell inactivation due to calcium entry defect 1	610277.0001
ORAI1	A103E	Immune dysfunction with T-cell inactivation due to calcium entry defect 1	610277.0006
ORAI1	L138F	Myopathy, tubular aggregate, 2	610277.0004
ORAI1	L194P	Immune dysfunction with T-cell inactivation due to calcium entry defect 1	610277.0007
ORAI1	S97C	Myopathy, tubular aggregate, 2	610277.0008
ORAI1	T184M	myopathy, tubular aggregate, 2	610277
ORAI1	V107M	myopathy, tubular aggregate, 2	610277
STIM1	D84G	Myopathy with tubular aggregates	605921.0004
STIM1	H109N	Myopathy with tubular aggregates	605921.0005
STIM1	H109R	Myopathy with tubular aggregates	605921.0006

Gene Name	Protein Mutation	Disease	OMIM
STIM1	H72Q	Myopathy with tubular aggregates	605921.0007
STIM1	I115F	Myopathy with tubular aggregates, Stormorken syndrome	605921.0009
STIM1	N80T	Myopathy with tubular aggregates	605921.0010
STIM1	R304W	Stormorken syndrome	605921.0008
STIM1	R429C	Immune dysfunction with T-cell inactivation due to calcium entry defect 2	605921.0003
STIM1	R426C	Immune dysfunction with T-cell inactivation due to calcium entry defect 2	605921.00011
STIM1	L74P	Immune dysfunction with T-cell inactivation due to calcium entry defect 2	605921.00012
STIM1	F108I	myopathy, tubular aggregate, 1	605921
STIM1	F108L	myopathy, tubular aggregate, 1	605921
STIM1	G81D	myopathy, tubular aggregate, 1	605921
STIM1	L96V	myopathy, tubular aggregate, 1	605921

Mechanism of Activation of SOCE

The discovery of STIM1 as ER calcium sensor that activates SOCE upon store depletion was a pivotal moment in furthering the field of store-operated calcium entry [23]. Soon after the discovery of STIM1, multiple research groups discovered a four transmembrane cell surface protein in *Drosophila* and its homologs in mammalian cells which would ultimately be known as Orai [26, 152, 154]. Overexpression of Orai1 in T cells isolated from patients with SCID restored the calcium entry deficits in those cells. In addition, co-expression of Orai1 with STIM1 in HEK293 cells showed calcium currents in these cells that matched the biophysical properties of CRAC currents [172]. CRAC channel formation is interesting in that is requires the assembly of proteins from two different membranous subcellular compartments to form the active channel complex [24, 126, 173-175]. In this next section, we will discuss how this mechanism of activation was discovered.

STIM1

Depletion of ER calcium stores initiates a cascade of events starting with the activation of STIM1 and culminates with calcium entry from the extracellular milieu. STIM1 is a dimer of two single pass type I ER transmembrane proteins. In the N-terminus, there is a canonical and a noncanonical EF hand motifs that play a role in calcium sensing in the ER [176, 177]. Immediately adjacent to the EF hand motifs, there is a sterile alpha motif (SAM) domain. On the cytosolic side, there is a calcium-activating domain (CAD) which is also known as STIM-Orai activation region (SOAR), which binds to the Orai1 channel [178]. The cytosolic C-terminus also contains three coiled-coil domains (CC1, CC2,

CC3) that help maintaining STIM1 in its inactive conformation when ER calcium store are full. Near the C-terminus, there is a polybasic domain which binds to the PIP_2 in the plasma membrane [178]. In addition to these domains, STIM1 also has and inhibitory domain (ID), a proline-serine rich domain (P/S domain), EB1 binding domain (EB) in its cytosolic side. These domains act in conjunction with each other upon store depletion to colocalize with Orai1 to form CRAC channels.

The calcium binding EF hand motifs are required for STIM1 to sense ER calcium store levels. This was confirmed using experiments with mutations in the EF hand motif. The mutations D76A, D78A, and E87A reduce the affinity of this motif to bind to calcium and show constitutive puncta formation as well as CRAC currents in resting cells [23, 24, 172]. The EF-SAM domains of STIM1 and STIM2 show similar affinities to calcium *in vitro*, however, structural differences in the two proteins results in dramatically different abilities to oligomerize in response to store depletion [176, 179].

The first step in the CRAC channel activation after ER calcium store depletion is the conformational change in STIM1. This was elucidated in experiments conducted using the cytosolic fragment composed of amino acids 233-685, which is capable of activating SOCE regardless of store depletion [180]. Further experiments involving truncation mutants of STIM1 led to identification of STIM1-Orai1 activating region (SOAR/CAD), the stretch of amino acids that can activate SOCE without store depletion. It is, however, interesting to note the difference in the amino acid sequences identified by individual groups ranged from 342-448 [181], 344-442 [178], and 339-444 [182]. Despite these differences, the consensus is that the SOAR/CAD region can activate CRAC currents independently of store depletion. Further research into CAD domain also showed that

CAD binds both the N- and C-termini of Orai1, but the strength of binding is higher at the C-terminus [181]. This binding between Orai1 and CAD is mediated by a coiled-coil interaction between the CC2 region of STIM1-CAD and the polar residues in the C terminus of Orai1 [183].

In resting conditions, STIM1 is diffusely localized throughout the ER, but upon store depletion redistributes into clusters that are termed “puncta” [181]. In resting conditions, STIM1 is in a compact conformation that keeps it from interacting with Orai1. Upon store depletion, a conformational change in STIM1 leads to an extended conformation with its N-terminus reaching toward the plasma membrane where it binds to the C-terminus of Orai1 [18, 24, 157]. Following store depletion, a complex choreography of intramolecular events happens between several domains of STIM1 that stabilizes STIM1 in its extended conformation to promote binding with Orai1. The ER:PM sites of cells are held in close apposition to promote STIM1 and Orai1 binding to promote CRAC channel formation by a multitude of accessory proteins such a septins, synptogamins, junctate, and others as described above [18]. The extended conformation of STIM1 was proposed to trap Orai1 into puncta, leading to channel gating to promote SOCE [184, 185]. This is known as the “diffusion-trap” model.

STIM1 exists as a dimer in cells with calcium replete stores in the resting state. This was confirmed using the C-terminal cytosolic fractions *in vitro* which formed dimers in solution. The specific domains involved in dimerization of STIM1 were further resolved using co-immunoprecipitation and fluorescence photobleaching of individual fragments [186]. The coiled-coiled domain fragments and CAD domain independently can form dimers *in vitro*. The CAD domain dimerization is interesting because STIM1 binding to

Orai1 is also mediated by this domain. The CC1 domains alone can form dimers, but they are weak and unstable [186, 187]. This supports the conclusion that STIM1 dimerization is a complex process requiring the interaction of multiple domains in the protein.

The CAD domain of STIM1 can independently and constitutively activate Orai1 and promote CRAC currents. Based on a crystal structure of CAD domain, hydrophobic residues form hydrogen bonds between the two monomers to stabilize the dimer [182]. In addition, interactions between the CC2 and CC3 regions of the STIM1 are purported to stabilize the extended conformation of STIM1. One interesting finding in the structure of CAD domain is the role of the CC2 and CC3 helices in binding to and activating Orai1 channels. In resting inactive state, the two CC2 helices (in a dimer) are in a parallel configuration in a tight hairpin structure with CC3 helices. Upon store depletion, these CC2 helices pivot and twist to an antiparallel orientation, allowing CC3 to extend out and allow for binding with Orai1 [183, 188-190]. These are highly complex and precise molecular movements in a restricted space between ER and PM within seconds of store depletion.

The EF hand domains of STIM1 residing in the ER lumen also undergo dimerization upon release of calcium from their binding pockets. In resting state, these domains exist as compact monomers bound to calcium [176]. NMR-resolved calcium-bound STIM1/2 EF-SAM fragments show an α-helical structure with a canonical (cEF) and non-canonical (nEF) EF hand domains. The cEF domain contains a helix-loop-helix structure that binds to calcium and nEF domain does not bind to calcium but stabilizes the cEF through hydrogen bonding [191]. Upon calcium release, the EF-SAM domains unfold leading to conformational changes in luminal and cytosolic domains of STIM1. Mutations in the

glutamate (E87A) or leucine residues (L195R) individually, and phenylalanine and glycine (F108D & G110D) together, in the EF-hand domain led to puncta formation irrespective of calcium depletion [189]. This led to a proposal that calcium release from EF-hands leads to STIM1 oligomerization upon store depletion. Live-cell imaging and FRET studies using STIM1 mutants added credence to this hypothesis, as they show increased FRET between STIM1 fused with YFP and CFP in RBL cells, which was reverse upon calcium addback [16]. Furthermore, FRET experiments conducted using Orai1-CFP and STIM1-YFP also show a spatiotemporal correlation between STIM1 oligomerization and Orai1-STIM1 binding [192].

Taken together, how calcium depletion in the ER leads to activation of STIM1 shows a complicated picture of multiple events happening in a precise sequential order mediated by several domains of STIM1. First, the binding of calcium ions to the EF-hand keeps the EF-SAM in a compact state which helps interactions between CC1 and CAD regions of STIM1 in the cytosolic side. An inhibitory clamp formed by intramolecular interactions between CC1/2/3 regions of STIM1 helps keep it in inactive state [157, 190, 193]. Store depletion and calcium dissociation from EF-hands leads to a conformational change that releases this clamp and formation of a coiled-coil dimer between CC1 domains. Experiments done using isolated cytosolic STIM1 fragments show that in resting state, these cytosolic fragments are tightly bound, which are extended upon binding to Orai1 [194]. Mutations in the CC1 regions that cause spontaneous activation of STIM1 also show a similar phenotype [188]. Finally, several leucine residues (L251, L261, L419, and L416) in the CAD region play a crucial role in extension of STIM1 toward plasma membrane for STIM1 binding to Orai1 [188, 195, 196]. This intra-and-intermolecular

choreography of STIM1 proteins upon store depletion controls SOCE. An overview of important binding events between STIM1 and plasma membrane lipids is shown in **Figure 1.2**.

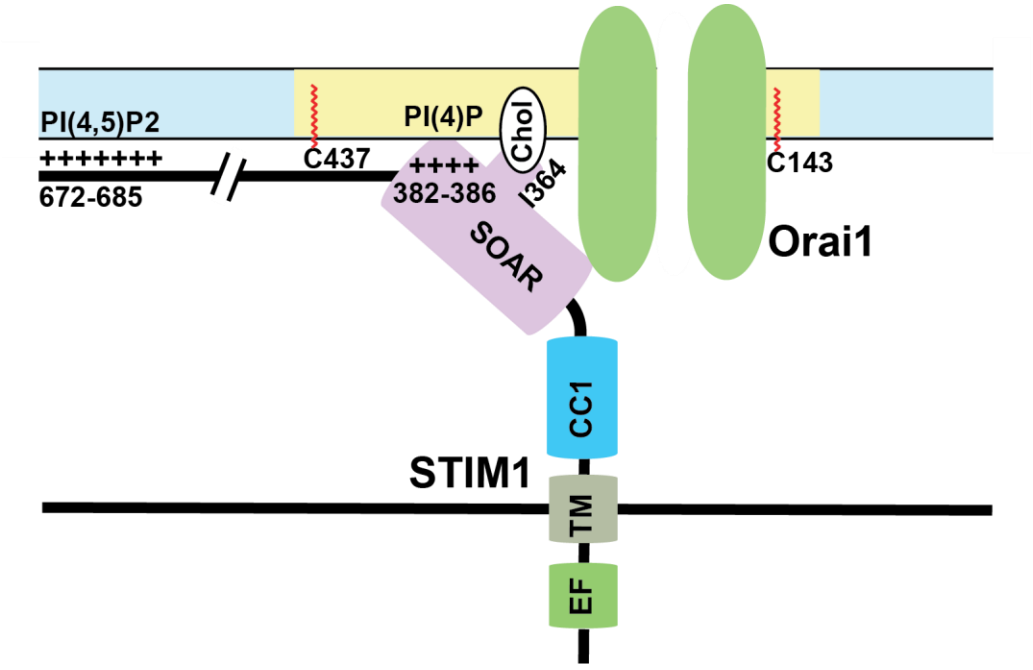

Figure 1.2. STIM1-lipid binding at the nexus of CRAC channels. The CRAC channels are stabilized at the ER:PM junctions by a multitude of bindings between different domains of Orai1 and STIM1 with plasma membrane lipids upon store depletion. Orai1 undergoes S-acylation at its C143 residue which shuttles the channels to lipid rafts. The SOAR domain of STIM1 binds to the N-terminus region of Orai1 and leads to activation of Orai1 channels. The cholesterol binding domain (CBD) in the SOAR domain also binds to the cholesterol rich phospholipids in the plasma membrane, which is mediated by I364 residue. The polybasic domain of STIM1 binds to the PI(4,5)P2 phospholipids in the plasma membrane which is mediated by the positively charged amino acids in the C-terminal tail of STIM1. Finally, STIM1 undergoes S-acylation at its C437 residue which is crucial for SOCE. One subunit of STIM1 dimer is shown here for simplicity.

Orai1

There are three homologs of Orai proteins (Orai1, Orai2, Orai3) in humans, and all three proteins promote calcium entry upon store depletion with varying biophysical properties. They can also form both homo- and hetero-multimers. For example, Orai1 and Orai3 can assemble as heteromultimers to promote store-independent calcium channels that are regulated by arachidonic acid or leukotriene C_4 [197-200]. These are called ARC channels and LRC channels, respectively.

Orai protein subunits are composed of approximately 300 amino acids. Early evidence from co-immunoprecipitation and FRET experiments suggested that these proteins are oligomers in functional CRAC channels [192, 201-203]. Experiments using preassembled tandem Orai1 multimers and co-expression with dominant-negative Orai1 mutants showed that Orai1 may form homotetramers in CRAC channels similar to other ion channels [204]. Using photo-bleaching of individual fluorophores in tandem Orai1-STIM1 multimers suggested a similar result of four Orai1 molecules with two STIM1 dimers, which was confirmed using FRET [205]. These results were replicated in live mammalian cells as well as cellular lysates obtained from lymphocytes [17, 206]. However, the X-ray crystallographic structure of Drosophila Orai revealed a hexameric stoichiometry challenging these observations [207].

Channel Gating and Biophysical Properties of Orai1 Channel. The X-ray and CryoEM structures of the *Drosophila* Orai channel helped resolve the oligomeric status of Orai and revealed the mechanisms for gating and ion permeation [207-209]. This structure shows Orai1 as a four transmembrane protein with cytosolic C and N termini.

The TM1 forms the channel pore with the Orai1 N terminus. TM2 and TM3 shield the pore from the membrane and TM4 and C terminus extend away from the channel pore. The channel pore has a ring of glutamate residues on TM1 (E178 is Drosophila, E106 in humans) that form a highly negative electrostatic region and serves as a selectivity filter. The side chains of these glutamate residues extend into the central pore, where the oxygen atoms of the carboxylic groups are in close proximity (~6 Å). Below the selectivity filter is a region of hydrophobic amino acids followed by positively charged residues that extend into the cytosolic lumen. One interesting observation from the crystal structure is that the C terminal tails of Orai1 helices form anti-parallel helices with each other in the hexamer. These interactions are held together by hydrophobic interactions between leucine residues at 316 and 219 (273 and 276 in humans). Mutations at these residues, such as L273S/D and L276D, lower the coiled-coil probability of the C terminus as well as inhibit STIM1 binding and channel activity [202, 210, 211]. However, an NMR structure between Orai1 272-292 fragment and 312-387 STIM1 fragment shows that the anti-parrel orientation doesn't change upon binding, but only leads to a small change in the angle or Orai1 helices [183]. The information obtained from these multitude of experimental approaches gave a picture, despite a hazy one, of how CRAC channels are gated, especially how the allosteric modulators regulate Orai1 channel function. This was eventually clarified in a cryo-EM structure published recently [208].

It has been shown that store depletion leads to the relatively slow activation of Orai1 channels (seconds to tens of seconds) [212]. A non-linear gating mechanism has been proposed to regulate CRAC channel gating, where these channels exhibit a 'modal

gating' mechanism where the channels alternate between silent and high open probability [213]. Modal gating mechanism was based on an observation that 2-APB, a widely used as I_{CRAC} inhibitor, elicits strong SOCE at low concentrations and inhibition at high concentrations. This hypothesis proposed that STIM1 binding to the Orai1 channel increases the time spent by these channels in the high open probability state. And because the frequency of these transitions is lower, calcium entry is enhanced [213].

The research into identifying the location of CRAC channel gate was hindered due to a lack of structural information until recently. Four seminal studies helped us elucidate the structural features regulating gating and ion permeation in the Orai channel [207-209]. Glutamate residues in the extracellular side of TM1 (E106, E178 in *Drosophila*), as explained earlier in the review, were hypothesized to form a selectivity filter by selectively binding calcium over other divalent cations. Mutation of a valine at position 102 (V174 in *Drosophila*) in the TM1 domain to alanine or serine made the channels constitutively active [214]. The *Drosophila* Orai structure also shows the hydrophobic valine residues making extensive connections protruding into the ion permeation pathway that presents a de-solvation barrier for ions in closed configuration of the channel [207, 215]. Using Terbium luminescence and disulfide crosslinking, others have also shown that STIM1 binding to Orai1 leads to a conformational change in the extracellular side near E106 and V102, and that this short segment forms a STIM1-dependent barrier [216]. Based on these observations, V102 was proposed as a hydrophobic gate, which was eventually refuted and F171 is now considered to be the hydrophobic gate (discussed in more detail below). Surprisingly, mutation of glycine and arginine residues in the intracellular side of TM1 region of Orai1, at 98 and 91 respectively, resulted in

constitutive activation of Orai1 channels. This led to a speculation whether there is another gate in the in the cytosolic side of the channel [217]. Based on these observations, R91 was thought to be the physical gate at the intracellular side that leads to dilation of the helices upon STIM1 binding. G98 was suggested to serve as a hinge, upon which the N terminus can rotate to allow for calcium entry. In addition, a phenyl alanine at 99 is on the opposite side of the pore helix to G98. STIM1 binding has been proposed to evoke a conformational change that exposes G98 while concealing F99 away from the channel pore [218]. The *Drosophila* Orai crystal structure revealed basic residues in the immediate inner cytosolic end of channel pore which led to another hypothesis where these residues stabilize the closed channel through either binding of anions or electrostatic repulsion of cations near this pore [207]. With the knowledge obtained from structural and functional studies using Orai1 and STIM1 mutants, several hypotheses have been put forward to explain the mechanism of activation of Orai1 by STIM1. STIM1 has been proposed to activate Orai1 in stepwise manner, first by initial binding to the C terminus for docking and a subsequent weaker binding to the N terminus to initiate conformational changes in the TM pore leading to pore opening [219].

A stretch of conserved acidic amino acids of Orai1 have been shown to confer calcium selectivity. These include residues at E106, E190, D110, D112, and D114 all of which are either in the TM1 or TM1-2 loop. Mutation of aspartate residues to alanine resulted in increased cesium permeability in these channels [220, 221]. In addition, mutation of E106 residue in the channel pore resulted in the same increase in cesium permeability. These mutants also increase the pore diameter as evidenced by increased permeability of

methylammonium derivatives[221]. Finally, E106D mutant also increases the fast calcium dependent inactivation time latency compared to wild-type Orai1[221].

The structure of the open conformation of Orai1 was recently resolved at 3.3 Å using cryo-electron microscopy [208]. As mentioned earlier, the hydrophobic amino acids F99 and V102 (F171 and V174 in human) within the channel pore were thought to function as channel gate [207]. This structure shows the channel pore lined by acidic residues facing the extracellular entrance by D184, D182, Q180 and E178 followed by hydrophobic residues V174, F171, and L167 lining the middle of the pore, and positively charged K163 and K159 lining the pore on the intracellular side. A comparison of the open and closed structures revealed that F171 is the primary gate, with the side chain rotating into the ion conduction pathway in the closed state [208]. Amino acids Q180, D182, and D184 on the extracellular surface create a negative electrostatic surface to attract cations near the mouth of the pore with E178 acting as a selectivity filter at the entrance to the ion conduction pathway.

Selectivity and Permeation of CRAC Channels. One of the most distinguishing properties of CRAC channels is their very high selectivity toward calcium over other cations. CRAC channels show 1,000 times higher selectivity over sodium. Mutagenesis of the residues lining the channel pore have provided insights into the mechanisms mediating the remarkable selectivity of Orai1 channels toward calcium. Alanine substitutions of E106 in TM1 region, D110, D112, and D114 residues in the TM1-TM2 loop, and E190 in the TM2-TM3 loop all result in a loss of calcium selectivity and increased cesium permeating. In addition, these mutations also diminish calcium-dependent inactivation of these channels. Cesium permeability reveals that the loss of

selectivity is likely due to an increase in pore diameter [221]. The E190Q mutation in the TM2-TM3 loop also resulted in loss of calcium selectivity [201] [156]. Also, alanine substitution of the D180 residue changed these channels from calcium selective and inward rectifying channels to sodium/cesium selective and outward rectifying channels [28]. These observations highlight the selectivity filter in the Orai1 channels is formed by the conserved acidic residues lining the outer pore of the channel.

Cysteine scanning experiments showed that the channel pore diameter is largely responsible for the low conductance and high calcium selectivity. Lack of cysteine reactivity suggests that the E190 residue doesn't form the channel pore. Molecular dynamics simulation suggested that mutating this residue to glutamate (E190Q) decreases the pore hydration of the channel [222]. In addition, mutating this residue to a cysteine (E190C) decreased the calcium selectivity of Orai1 channel [223]. It is possible this residue helps in maintaining the pore size by regulating hydration of the ion conduction pathway. Finally, cysteine substitution of aspartate residues at 110, 112, 114 in the TM1-TM2 loop did not change calcium selectivity of these channels [175, 224]. These results show that TM1 lines the channel pore and a E106 residue (E178 dOrai1) from each monomer forms the selectivity filter in the extracellular side of Orai1 channel.

The combination of electrophysiological analysis and high-resolution structures have resolved many questions regarding Orai structure/function. Orai is unique with regards to subunit composition, ion permeation properties, and the kinetics of gating compared to other calcium channels. Indeed, they have very little sequence homology to other calcium channel families such as voltage-gated calcium channels and ligand-gated channels. Orai

channels may have evolved from the very large and ubiquitous Cation Diffusion Facilitator (CDF) carrier family [225].

SARAF

SARAF (SOCE-associated regulatory factor) is an ER transmembrane protein known to be bind to STIM1, keeping it in an inactive state. It primarily localizes to the ER membrane and possibly to the plasma membrane [226, 227]. SARAF was discovered in a functional expression screen to identify proteins that affect mitochondrial calcium homeostasis [226]. HEK293 cells transfected with SARAF cDNA showed lower baseline cytosolic, ER, and mitochondrial calcium levels. In addition, siRNA-based knockdown of SARAF resulted in an increase of basal cytosolic and ER calcium levels. This suggested a role for SARAF in cellular calcium homeostasis. Further experiments conducted using SARAF in conjunction with Orai1 and STIM1 led to deciphering its role in calcium entry. Electrophysiology recordings of Jurkat T cells and HEK293 cells showed SARAF regulates SOCE, specifically the slow calcium-dependent inactivation of CRAC channels [226]. Subsequent experiments conducted in SH-SY5Y and NG115-401L cell lines also showed that SARAF is expressed in the plasma membrane where it interacts with and negatively regulates ARC channels [228]. In addition, SARAF can also inhibit calcium entry mediated by TRPC1 channels [229].

How SARAF affects STIM1 structure and function is still not completely understood. Several reports indicate that SARAF interacts with STIM1 in resting conditions to keep STIM1 in its inactive state [230, 231]. Co-immunoprecipitation studies have shown that SARAF binds to STIM1, and this binding is mediated by the C-terminus of SARAF. The

TM and ER-luminal domains are not required for this interaction [226]. Interestingly, constitutively active STIM1 which has four glutamates mutated to alanine in its SOAR domain does not bind to SARAF and has deficits in slow calcium-dependent inactivation [230]. The physical interaction between STIM1 and SARAF has been confirmed by multiple reports [227, 230-232]. In addition, SARAF has been shown to bind Orai1 and EFHB (EF hand containing family member B) [230-234].

The nature of SARAF binding to STIM1 and Orai1 is interesting, especially when put into the context of SOCE. SARAF binds to STIM1 in resting conditions to keep it from spontaneously activating. Upon store depletion, co-immunoprecipitation experiments have shown that SARAF immediately dissociates from STIM1 within the first minute, but then they re-associate rapidly [231, 233, 234]. It is possible that SARAF binds to Orai1 after store depletion, not STIM1. The exact sequence of events by which SARAF binds/releases STIM1 and Orai1 during SOCE is difficult to determine using existing techniques. Experiments conducted using fragments of these proteins show that SARAF interacts with STIM1 at the CC1 and the C-terminal inhibitory domain (CTID) of STIM1 [230]. TIRF microscopy using STIM1-mCherry and SARAF-GFP show that these two proteins co-localize at the ER:PM junctions upon store depletion using thapsigargin. Co-immunoprecipitation of the SARAF N- and C-termini with STIM1 shows that SARAF binds to the C-terminus of STIM1 [226].

Membrane phospholipids play a crucial role in the interaction between SARAF and STIM1/Orai1. Phosphatidylinositol 4,5-bisphosphate ($PI(4,5)P_2$) is a membrane phospholipid that mediates many functions in cellular signaling. It has been shown that the CRAC complex translocates between $PI(4,5)P_2$ poor and rich microdomains during

SOCE, and this regulates SOCE [235] . STIM1 interactions with Orai1 and $PI(4,5)P_2$ are both dependent on SARAF [233]. In addition, localization of Oria1/STIM1 in $PI(4,5)P_2$ microdomains are maintained by stabilizing proteins such as extended synaptogamin 1 (E-Syt1) and septin4 [233]. The dynamic regulation of this complex in membrane microdomains during store depletion has yet to be determined with suitable kinetic resolution. More recently, the SOAR domain of STIM1 has been shown to bind interact with plasma membrane phospholipids. Interactions between lysine residues 382, 384, 385, and 386 in the SOAR domain with plasma membrane phospholipids $PI(3,4)P_2$, $PI(3,5)P_2$, $PI(4,5)P_2$, and $PI(3,4,5)P_2$ are crucial for the stability of ER:PM junctions as well as SOCE [230]. The Orai1/STIM1 complex localized to the PI(4,5)P2 rich subdomains binds to SARAF and this localization and binding is crucial for SARAF to regulate slow calcium dependent inactivation [233]. These complex binding interactions between the SOAR and CTID domains of STIM1 and membrane phospholipids are crucial for the activity of SARAF.

How SARAF regulates slow calcium-dependent inactivation is still unknown. Multiple hypotheses have been proposed to explain this behavior. One of them is that an additional calcium-binding protein mediates SARAF activation in slow calcium-dependent inactivation [236]. Calcium binding proteins have been known to modulate SOCE, and some of them have been discussed earlier in the review such as EFHB and calmodulin [237]. Other hypotheses include modulation by the calcium sensing abilities of STIM1 and Orai1.

Models of CRAC Channel Assembly

ATP-Dependent Puncta Formation

Based on the observation in live cells that STIM1 translocates to the plasma membrane from the ER membrane and an earlier hypothesis that STIM1 is transported to PM via a secretory pathway [238], puncta formation was hypothesized to be ATP-dependent. Mitochondria are known to accumulate near the ER:PM junctions and regulate calcium homeostasis [12, 239]. In addition, depletion of intracellular ATP leads to decreased calcium entry in rat lymphocytes [240]. ATP depletion can also lead to translocation of STIM1 to puncta. However, this required depletion of $PI(4,5)P_2$ in addition to ATP depletion [241].

Microtube-Associated STIM1 Translocation

As discussed earlier in the review, STIM1 binds to the EB1 protein that is known to modulate microtubule growth. In B cells, treatment with the anti-mitotic agent nocodazole, which inhibits polymerization of microtubules, did not show the puncta formation observed in untreated cells [158]. Pull down assay with EB1, EB2, and EB3 proteins showed STIM1 binds to EB1. This was also confirmed using immunocytochemistry and co-immunoprecipitation experiments [163]. In addition, treatment of cells with ML-9, a myosin light chain kinase inhibitor, led to reversal of CRAC puncta as well inhibition of SOCE [161]. These observations led to a hypothesis that STIM1 traffics to the ER:PM junctions by microtubule-assisted transport mediated by its binding to EB1. However, this model shows that STIM1 and Orai1 proteins are

confined at the junctions after store depletion but does not offer any explanation to why this happens.

Phosphatidylinositol-Mediated Membrane Sorting

Early experiments conducted on STIM proteins led to discovery of a C-terminal polybasic domain that interact with PM phospholipids, such as $PI(4,5)P_2$ [235, 242]. This polybasic domain was also found to mediate the inward rectification of SOCE currents [178]. HeLa cells treated with wortmannin and LY294002, inhibitors of phosphatidyl inositol 3-kinase (PI3K) and PI4K respectively, led to inhibition of STIM1 puncta formation as well as SOCE [243]. In addition, the binding between STIM1 and Orai1 was differentially modulated by the levels of $PI(4,5)P_2$ [235]. Decreased $PI(4,5)P_2$ concentrations resulted in reduced thapsigargin-mediated Orai1-STIM1 binding in the PM liquid-ordered phase/rafts, and this affinity was reversed in membrane disordered regions [243]. This led a hypothesis that membrane phospholipids play a role in CRAC channel formation and SOCE. However, depletion of phosphoinositides in cells overexpressing Orai1 did not affect either STIM1 puncta formation or SOCE [243]. In addition, the experiments showing a role for phosphoinositides was shown using inhibitors which do not discriminate between direct effects on Orai1/STIM versus general effects due to severely perturbing PM phospholipid composition.

Diffusion-Trap Model

The diffusion-trap model postulates that STIM1 undergoes a conformational change that exposes its C-terminal domains toward plasma membrane, where it binds to membrane phospholipids and stochastically binds to Orai1 channels laterally diffusing in the PM

[184, 185]. In agreement with this hypothesis, super-resolution microscopy experiments conducted using tagged Orai1 and STIM1 constructs showed that these proteins diffuse randomly in resting conditions. Upon store depletion, these proteins slow down at distinct ER:PM junctions allowing them to accumulate and form puncta [184]. Additionally, single particle tracking analysis shows single STIM1 and Orai1 particles diffusing freely before getting trapped at the junctions. Deletion of the polybasic domain in the C-terminus of STIM1 showed altered puncta formation after store depletion, suggesting a direct role for this domain. These experiments also demonstrated that STIM1 and Orai1 particles have a long half-life in puncta once trapped [184, 244].

The diffusion-trap model fails to explain some aspects of puncta formation and SOCE. The polybasic domain was hypothesized to act as a trap to attract Orai1 to STIM1. However, a mutant STIM1 devoid of this polybasic domain is capable of binding with Orai1. Orai1 binding by itself can also trap STIM1 within ER:PM junctions which raises the possibility that Orai1 may be trapping STIM1 [243]. Interestingly, we have found that STIM1 can form puncta in the absence of Orai1, but Orai1 cannot form puncta in the absence of STIM1 [245, 246] . The strong binding between Orai1 and STIM1 in the puncta could also mean there is an equivalent amount of protein particles enter and leave the puncta, thereby maintaining a dynamic equilibrium at these ER:PM junctions [184]. Finally, single particle tracking and polydispersity analyses conducted on Orai1 and STIM1 proteins show that the mobility of these proteins decreases after store depletion, but these proteins are also confined in compartmentalized membrane regions before and after store depletion [244]. Based on these observations, the binding of Orai1 and STIM1 upon store depletion appears to be more complicated than a simple diffusion model.

S-Acylation as a Regulator of Orai1/STIM1 Assembly

Orai1 and STIM1 accumulate in lipid raft domains upon depletion of intracellular calcium stores. Depletion of PM cholesterol with methyl-beta-cyclodextrin impairs SOCE, implying a role for lipid rafts in SOCE [247, 248]. Our group found that signaling through the Fas death receptor in T cells requires dynamic S-acylation of the kinase Lck, leading to translocation to rafts where it activates PLC-y1-mediated IP_3 production [249] [249]. Subsequently, we found that many TCR components such as Lck, Fyn, ZAP70, and PLCy1 undergo dynamic S-acylation upon T cell activation [130, 250, 251]. This S-acylation was required the calcium/calmodulin-dependent activation of the protein acyltransferase DHHC21. We next investigated T cell function in the mutant mouse *depilated*, which carry a functionally deficient DHHC21 with an in-frame deletion of phenylalanine 233 (F233) eliminated calmodulin binding. *Depilated* mice have severe deficits in T cell differentiation, including differentiation into Th1, Th2, and Th17 lineages [252]. TCR signaling in *depilated* mice is severely disrupted due to reduced activation of ZAP70, Lck, PLCγ1, JNK, ERK1/2, and p38 in response to TCR stimulation [252, 253]. As Orai1 and STIM1 are essential for TCR signaling, we hypothesized that Orai1 and STIM1 undergo S-acylation to regulate CRAC channel formation and function in T cells.

S-acylation is a reversible addition of lipid moieties to cysteine residues of target proteins that affects protein stability, function, conformation, and trafficking between compartments within a cell [254, 255]. S-acylation is a post translational modification that is mediated by specific group of enzymes known as protein acyltransferases (PATs). PATs are also known as DHHC enzymes owing to the conserved aspartate-histidine-

histidine-cysteine motif in their active site that carries out this reaction [254]. The different classes of DHHC enzymes distinguish among themselves by their selectivity toward substrates, lipid preferences, and mechanisms that activate and inactivate them [255]. Deficiencies in DHHC enzyme functions leads to a range of diseases ranging from cancers such as adenocarcinomas, lung cancer, bladder cancer, and breast cancer, to diseases that affect neurological functions such as epilepsy and schizophrenia, glioblastoma, and X-linked intellectual disability [255-259]. The subsequent process of removal of lipid moieties from protein substrates, known as deacylation, is mediated by another set of enzymes known as acyl protein thioesterases (APTs) [260, 261]. These enzymes act in concert to dynamically regulate protein function in a stimulus-dependent manner. How most DHHC and APT enzymes are activated and inactivated is still unclear.

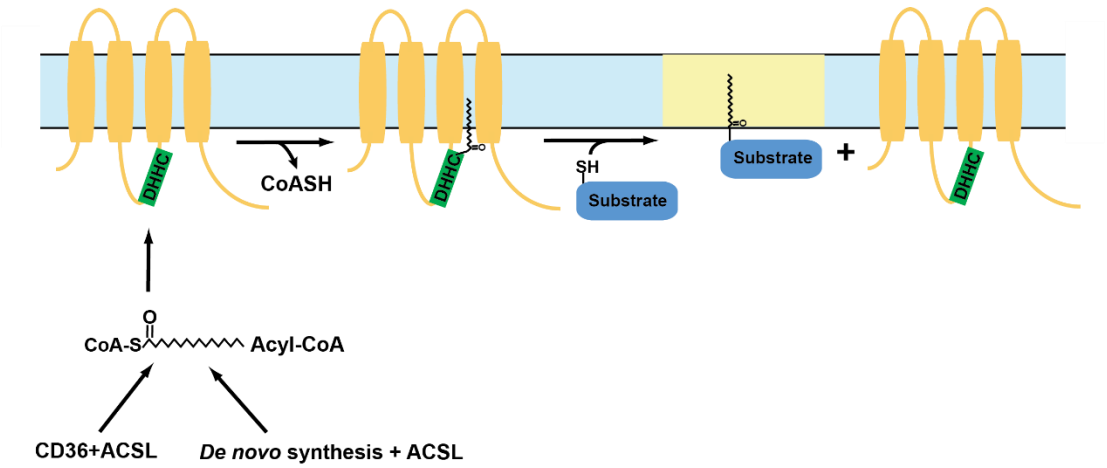

Figure 1.3. Mechanism of DHHC enzyme catalysis. DHHC enzymes S-acylate their substrates by a two-step mechanism which involves these enzymes undergoing auto acylation followed by transfer of the acyl group to target proteins.

DHHC enzymes catalyze the addition of lipid moieties to proteins through a two-step mechanism, where the cysteine residue in the active site of the enzyme receives the lipid group and then transfers it to the cysteine residues of target proteins [262]. This first step, known as auto-acylation, is followed by the transfer of acyl group to target proteins. The DHHC enzymatic reaction is sometimes referred as a “ping-pong” reaction, however, this may be a misnomer. Ping-pong mechanisms (also known as double-displacement reactions) always involved two substrates and two products, with binding of the second substrate dependent upon successful completion of the first reaction [263, 264]. The reaction mechanism for DHHC enzymes is highlighted in **Figure 1.3**. For the DHHC reaction to be considered ping-pong, we would have to accept that CoA is product #1, and that substrate #2 binding (the protein be S-acylated) depends upon autoacylation of the DHHC enzyme. We would argue that the autoacylated DHHC enzyme is an intermediate, not an enzyme newly capable of binding substrate #2. Regardless, the ultimate result is the S-acylation of the target protein.

Following the hypothesis that Orai1 and STIM1 undergo S-acylation upon store depletion, we found that treatment of Jurkat T cells with anti-CD3 or HEK293 cells with thapsigargin (an irreversible SERCA pump inhibitor that leads to ER calcium store depletion) leads to stimulus-dependent S-acylation of Orai1 and STIM1. The kinetics of S-acylation Orai1 and STIM1 are very rapid consistent with the assembly of puncta and channel activation. The cysteine-mutant versions of Orai1 and STIM1 that are incapable of undergoing S-acylation have significantly reduced puncta formation and SOCE, indicating a direct role for S-acylation in CRAC channel assembly [245, 246].

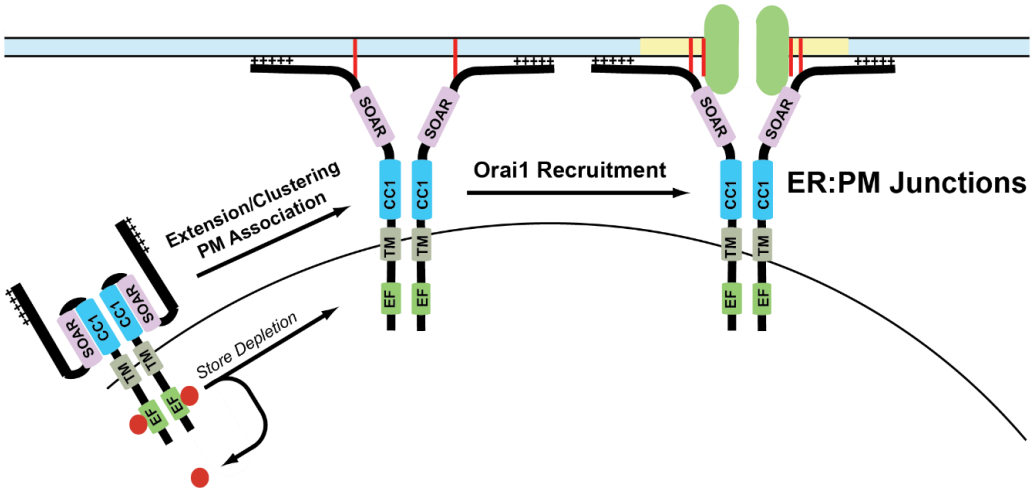

Figure 1.4. S-acylation regulates CRAC puncta formation and stabilization at ER:PM junctions. S-acylation of Orai1 and STIM1 leads to CRAC puncta formation and stabilization of CRAC channels. Calcium dissociation from the EF-hand of STIM1 leads to conformation change in STIM1 which extends the C-terminal tail toward plasma membrane, where multiple domains of STIM1 interact with plasma membrane, including S-acylation of STIM1. Orai1 is then recruited to lipid rafts through its S-acylation. Together, STIM1 and Orai1 form CRAC channels.

One interesting observation between the cysteine mutants of Orai1 and STIM1 is that the Orai1 cysteine mutant (C143S) was an almost complete loss of function phenotype, whereas mutant STIM1 (C437S) retained some residual activity. The residue where STIM1 undergoes S-acylation is at the proximal end of its SOAR domain. As explained earlier in the review, the SOAR domain of STIM1 is crucial in the tethering of STIM1 to plasma membrane. The C-terminus of STIM1 also has the polybasic membrane binding domain. We hypothesize the S-acylation of STIM1 stabilizes the C-terminus in the plasma membrane. Due to redundant membrane-binding domains in the C-terminus, we postulate that the loss of S-acylation would only partially reduce the affinity of the C-

terminus for the membrane, thus possibly explaining our partial loss-of-function phenotype (**Figure 1.2**) [164]. Our model is that a plasma membrane resident DHHC enzyme, probably DHHC21, S-acylates STIM1 and anchors its C-terminus in the plasma membrane, thereby stabilizing the CRAC complex at these ER:PM junctions to facilitate SOCE [245, 246]. An overview of the role of S-acylation of Orai1 and STIM1 in CRAC puncta formation is depicted in **Figure 1.4**.

At the same time as our research into S-acylation of Orai1 and STIM1, the Demaurex group also showed that Orai1 undergoes S-acylation [265]. I was found that S-acylation of Orai1 is critical for its recruitment to the immunological synapse as well as TCR-mediated calcium entry in Jurkat T cells. Using TIRF and confocal imaging techniques, they showed that S-acylation of Orai1 is critical for channel clustering as well as their trafficking to the lipid rafts. Finally, using overexpression analysis, they show that DHHC20 is the enzyme that mediates S-acylation of Orai1 in the plasma membrane, at least under resting conditions. We hypothesize that DHHC20 may mediate Orai1 S-acylation under resting conditions, whereas store depletion leads to calcium/calmodulin-dependent activation of DHHC21 leading to increased Orai1/STIM1 S-acylation and active partitioning to ER:PM junctions. This would be consistent with our data in *depilated* DHHC21 mutant mice showing altered T cell calcium signaling in response TCR activation [252, 253, 266].

The regulation of CRAC channel formation and SOCE by S-acylation adds a regulatory step for channel assembly during store depletion. S-acylation also allows for the enzymatic control of CRAC channel assembly and disassembly. This further allows for

the fine tuning of the spatiotemporal aspects of calcium signaling in cells expressing Orai1/STIM1.

S-acylation governing CRAC channel formation and SOCE adds another layer in regulating calcium signals in cell physiology. This secondary regulation of channel formation and function gives an additional way to fine tune calcium levels upon receptor activation to effectively process signaling events. Our results provide an alternative model for CRAC channel assembly and disassembly that is enzymatically regulated. This allows fine-tuning of SOCE and resultant spatio-temporal aspects of the calcium signal.

Chapter 2

S-Acylation of Orai1 Regulates Store-Operated Calcium Entry[2]

Summary Statement

Dynamic S-acylation of calcium-release activated channel Orai1 is required for its recruitment to the plasma membrane subdomains and subsequent activation.

Abstract

Store-operated calcium entry is a central component of intracellular calcium signaling pathways. The calcium release-activated channel (CRAC) mediates store-operated calcium entry in many different cell types. The CRAC channel is composed of plasma membrane (PM)-localized Orai1 channel and endoplasmic reticulum (ER)-localized STIM1 calcium sensor. Upon ER calcium store depletion Orai1 and STIM1 form complexes at ER-PM junctions, leading to the formation of activated CRAC channels. While the importance of CRAC channels is well described, the underlying mechanisms which regulate the recruitment of Orai1 to ER-PM junctions are not fully understood. Here we describe the rapid and transient S-acylation of Orai1. Using biochemical

---

[2] Savannah J. West[*], Goutham Kodakandla[*], Qioachu Wang, Ritika Tewari, Michael X. Zhu, Darren Boehning[,a], and Askar M. Akimzhanov[,a]
Department of Biochemistry and Molecular Biology, McGovern Medical School, University of Texas Health Science Center at Houston
Department of Biomedical Sciences, Cooper Medical School of Rowan University
Department of Integrative Biology and Pharmacology, McGovern Medical School, University of Texas Health Science Center at Houston
[*]These authors contributed equally
[a]Correspondence to DB (boehning@rowan.edu) or AMA (Askar.M.Akimzhanov@uth.tmc.edu)
Running title: Orai1 is S-acylated
Key words: palmitoylation, S-acylation, calcium, calcium channel, Orai1

approaches, we show that Orai1 is rapidly S-acylated at cysteine 143 upon ER calcium store depletion. Importantly, S-acylation of cysteine 143 was required for Orai1-mediated calcium entry and recruitment to STIM1 puncta. We conclude that store depletion-induced S-acylation of Orai1 is necessary for recruitment to ER-PM junctions, subsequent binding to STIM1, and channel activation.

Introduction

Orai1 and STIM1 form calcium release-activated channels (CRAC) which are required for store-operated calcium entry (SOCE). Orai1, the pore-forming subunit of the CRAC channel [28, 154, 156], is a plasma membrane (PM)-localized protein, while STIM1 is localized to the endoplasmic reticulum (ER) membrane and has a calcium sensing EF hand within the ER lumen and a cytosolic domain which binds Orai1 [23, 155]. At rest, STIM1 is in a folded conformation as a dimer with calcium bound to the EF hands. Upon cellular stimulation ER calcium stores are depleted, leading to a loss of STIM1 binding to calcium. Loss of calcium binding to STIM1 leads to an extended conformation in the cytosolic domain which allows it to bind to Orai1 at ER-PM junctions [18, 158]. The binding of Orai1 to STIM1 activates the channel causing temporally distinct calcium elevations in the cytosol which modulate downstream cellular signaling pathways such as cell migration, proliferation, and apoptosis [156, 267]. The importance of Orai1/STIM1-mediated SOCE has been well described [268], however, it is still not fully understood what mechanisms regulate the recruitment of Orai1 to ER-PM junctions allowing for CRAC channel formation and SOCE. Orai1 and STIM1 are critical regulators of T cell function, and mutations in these proteins cause primary immunodeficiencies, myopathy

with tubular aggregates, and Stormorken syndrome [267, 269]. Thus, understanding how CRAC channels are activated has high relevance to human disease.

S-acylation is the reversible post-translational lipidation of a cysteine residue and can regulate protein trafficking, function, and stability. Many transmembrane proteins are S-acylated, such as BK channels [270], G protein-coupled receptors [271, 272], calnexin [273], and others [274]. It has been suggested that at 15% of the human proteome may be S-acylated [275]. Although this S-acylation was discovered over 30 years ago[276], it was not until recently that it has been appreciated as a highly dynamic regulator of signaling pathways. This discovery has been facilitated by the development of highly sensitive and reliable methods for detecting S-acylation [277]. Our group and others have shown that dynamic acylation is a critical regulator of T cell signaling and function [251, 253, 258, 266, 278-281].

Here we show that Orai1 is rapidly S-acylated on cysteine 143 after store depletion. Mutation of cysteine 143 to serine eliminated S-acylation of Orai1, and led to severely reduced store-operated calcium entry. The C143S mutant could not be efficiently recruited to STIM1 after store depletion, indicating that S-acylation of Orai1 is necessary for recruitment to PM-ER subdomains and subsequent activation of the channel.

Results and Discussion

Orai1 Is Transiently S-Acylated at Cysteine 143

During a proteomic screen for S-acylated proteins, we found that Orai1 is S-acylated in Jurkat T cells. Orai1 has three cysteine residues, C126 within the second transmembrane domain, C143 within the cytosol in the TM2/TM3 loop, and C195 in the third

transmembrane domain facing the extracellular space (**Fig. 2.1A**). S-acylation only occurs on the cytosolic side of membranes, and thus we hypothesized that C143 is the site of S-acylation. We used acyl-biotin exchange (ABE) to determine if recombinant Orai1-YFP was S-acylated. As a positive control we used the well-established and stably S-acylated protein calnexin. As shown in **Fig. 2.1B** wild-type Orai1, but not the C143S mutant, was acylated when expressed in HEK293T cells. Next, we used Jurkat T cells to assess the effects of agonist-induced calcium release on S-acylation of endogenous Orai1. Stimulation of the T cell receptor (TCR) activates phospholipase C- γ1 (PLC- γ1), which then produces the second messenger, inositol 1,4,5-trisphosphate (IP_3), leading to activation of the IP_3 receptor/calcium channel and subsequent depletion of ER stores [269]. We found that treatment of the TCR with OKT3 (anti-CD3) antibody resulted in a significant, approximately 4-fold, increase in Orai1 S-acylation (**Fig 2.1C, D)**. Similar to phosphorylation of PLC-γ1 (**Fig. 2.1C, input**), the increase in Orai1 S-acylation was transient, peaking at 2 minutes and returning to baseline levels after prolonged stimulation. These data indicate that Orai1 is rapidly and transiently S-acylated at C143, and this S-acylation is triggered by ER calcium store depletion upon engagement of the TCR.

Orai1 S-Acylation Is Necessary for Store-Operated Calcium Entry

To determine if Orai1 S-acylation affects CRAC channel function, we performed whole-cell voltage clamp recordings in cells co-expressing wild-type STIM1-mRFP and either wild-type or C143S Orai1-YFP. In **Fig. 2.2A**, representative traces of wild-type (red) and C143S (blue) currents collected at -100mV are shown. ER calcium store depletion was initiated by inclusion of 50 μM IP_3 in the patch pipette. Wild-type Orai1 activation

developed with three phases: activation (0-45 s), inactivation (50-100 s), and a plateau (100-150 s). In contrast, C143S Orai1 channels displayed a slowly developing low amplitude response to IP_3. Representative basal and peak current-voltage relationships are shown (**Fig. 2.2B**), with labeling indicating the time point the I-V curve was collected on the trace in Fig. 2A. The average peak current density of wild-type Orai1 channels (-58.23 pA/pS) was significantly higher than C143S Orai1 channels (-8.80 pA/pS) (**Fig. 2.2C**).

We next characterized Orai1 function using Fura-2 calcium imaging in Orai triple knockout (TKO) HEK cells [282]. The TKO cells were co-transfected with STIM1-mRFP and either wild-type or C143S Orai1-YFP channels. Store depletion was induced by the addition of 10 μM thapsigargin in calcium free media. Calcium entry through recombinant Orai1 channels was initiated by the addition of 1 mM calcium. Using this calcium add-back experimental paradigm, there is no calcium entry in TKO cells unless recombinant Orai channels are expressed [282, 283]. Cells expressing wild-type Orai1 had robust calcium entry after calcium add-back (**Fig. 2.2D**). In contrast, cells expressing C143S Orai1 had significantly reduced calcium entry (**Fig 2.2D,E**). The time to peak for C143S channels was also significantly shorter compared to wild-type Orai1, consistent with decreased calcium entry (**Fig. 2.2F**). In total, S-acylation deficient C143S channels are not able to efficiently support store-operated calcium entry.

S-Acylation of Orai1 is Required for Clustering and Recruitment to STIM1

S-acylation can function to sequester proteins in plasma membrane subdomains [284]. We hypothesized that the C143S mutation may inhibit recruitment to PM/ER subdomains

where Orai1 binds to STIM1. We examined the plasma membrane distribution of wild-type Orai1-YFP, C143S Orai1-YFP, and STIM1-mRFP in Orai TKO cells using total internal reflection fluorescence (TIRF) microscopy. Wild-type Orai1-YFP and the C143S-YFP mutant were both present in the TIRF plane, indicating expression and localization to the plasma membrane was not compromised in the C143S mutant channel (**Figs. 2.3A**). Cells were stimulated with 10 μM thapsigargin to induce ER calcium store depletion and subsequent clustering of Orai1 with STIM1. Thapsigargin treatment led to the rapid recruitment of wild-type Orai1-YFP into puncta with STIM1, as expected (**Fig. 2.3A and C2.3**). This was reduced in the C143S acylation-deficient mutant. We calculated the Pearson correlation coefficient to quantify co-localization between YFP-tagged Orai1 and mRFP-tagged STIM1 proteins. Upon ER store depletion, there was rapid co-localization of wild-type Orai1-YFP and STIM1-mRFP. In contrast, the C143S Orai1-YFP mutant channel had deficient recruitment to STIM1-mRFP in the TIRF plane (**Fig. 3B**). This was quantitatively reflected in the significantly lower peak co-localization of the C143S mutant with STIM1 (**Fig. 2.3C**). We also performed a co-immunoprecipitation assay with WT and C143S Orai1-YFP overexpressed in HEK293T cells. The transfected cells were stimulated with 10 μM thapsigargin for 0 or 5 minutes, and immunoprecipitated using a STIM1 antibody (**Fig. C2.2**). Although we observed an upward trend in WT Orai1-YFP/STIM1 binding after thapsigargin treatment that was not seen in C143S Orai1-YFP, there were no significant changes between groups. This is likely due to the formation of self-activating Orai1/STIM1 complexes observed in cells overexpressing Orai1 protein [210, 285]. Due to these limitations, we conclude that the coimmunoprecipitation assay is unsuitable for assessment of Orai1/STIM1 interaction

when overexpressed. Overall, our TIRF data strongly suggest that the lack of Orai1 S-acylation results in significantly less co-localization with STIM1 at ER-PM junctions after store depletion.

Orai1 S-Acylation is Required for the Recruitment of Active Calcium Channels to Puncta

Using Orai1 fused to the calcium indicator protein GCaMP6f, it is possible to specifically measure the activity of Orai1 individual channels or clusters of channels (**Fig. 2.4A**; [286]). We hypothesized that this protein could be used to simultaneously evaluate the combined effects of the C143S mutant on activity and assembly with STIM1. Orai1-GCaMP6f is only fluorescent when the Orai1 channel is open, and thus there is little fluorescence under resting conditions (**Figs. 2.4A and C2.4**). Addition of thapsigargin in calcium free solution marginally increased the fluorescence of Orai1-GCaMP6f, consistent with the specificity of this fusion protein in measuring calcium exiting the cytosolic pore of the channel (**Fig. 2.4B**). Calcium add-back to induce calcium entry resulted in a large increase in Orai1-GCaMP6f fluorescent puncta, indicating both increased activity and clustering of channels (**Fig. 2.4A-C**). The C143S mutant had reduced fluorescence when compared to the wild-type channel upon calcium add-back, consistent with reduced activity. The total number of Orai1-GCaMP6f particles appearing after calcium add-back is representative of the number of active channels being recruited to puncta/STIM1. We found a significantly reduced number of active C143S puncta after calcium add-back indicative of defective recruitment to STIM1 (**Fig. 2.4D**). The few C143S mutant channels which are active suggest a small pool of C143S channels bound to STIM1 in a store depletion-independent manner or are stochastically localized with

puncta during add-back. We conclude that Orai1 C143S mutant channels are capable of gating, however they have dysregulated recruitment to STIM1 after store depletion resulting in the activation of fewer channels.

Here we have shown that store depletion-induced S-acylation of Orai1 at cysteine 143 (C143) is required for recruitment to STIM1 and subsequent store-operated calcium entry. Using the ABE assay, we find that a significant fraction of endogenous Orai1 is rapidly and transiently S-acylated at C143 in response to TCR stimulation, indicating that reversible S-acylation of Orai1 can serve as a signal transduction mechanism mediating T cell immune responses.

Cysteine residues are the target of several post-translational modifications. In Orai1, the only previously known modification of cysteine residues is oxidation. Several reports have systematically analyzed the oxidation state of the three cysteine residues in Orai1 [287, 288]. These studies have shown that cysteine 195 is the redox sensor, and cysteine 143 is not subject to this modification [287, 288]. We conclude that changes in Orai1 function in the C143S mutant are most likely due to the lack of S-acylation (as shown in **Fig. 2.1B**) and not other modifications. We also found that this mutation does not affect protein expression or trafficking to the plasma membrane, and thus our observed effects on function are not due to low protein expression, protein degradation, or intracellular retention **(Figs. 2.1B, 2.3A, 2.4A, and C2.1**). Instead, our data suggest the effects of the C143S mutant are due to a lack of lateral recruitment to STIM1. Our data can be explained by a model where the initial calcium release from the ER stores, triggered by antigenic stimulation, activates a protein acyltransferase which then rapidly S-acylates Orai1. Orai1 then translocates to the specialized membrane microdomains where it can

interact with STIM1. We have shown that the protein acyltransferase DHHC21 mediates TCR and Fas signaling in T cells [251, 253], and is activated by calcium-calmodulin to dynamically S-acylate TCR components *in vitro* and *in vivo* [252]. Thus, DHHC21 is an obvious target in future studies examining the enzymatic mechanisms by which Orai1 is S-acylated in T cells.

How Orai1 and STIM1 are recruited to plasma membrane/ER contact sites is still incompletely understood. Several models have been suggested for the recruitment of Orai1 to these junctions, of which the diffusion-trap model is the most predominant [184, 289]. In this model, Orai1 diffusing in the plasma membrane becomes trapped at PM/ER junctions through interaction with STIM1. It is known that store depletion greatly reduces the lateral mobility of both Orai1 and STIM1, and this is associated with stable yet transient interactions at PM/ER junctions [159, 244, 290]. Our data suggest there may be an additional mechanism to facilitate sequestration of Orai1 in membrane subdomains: S-acylation and translocation to lipid rafts which would facilitate both oligomerization and association with STIM1. This would be particularly relevant for the function of Orai1 in T cell signaling, as the immunological synapse is known to concentrate S-acylated signaling proteins to modulate downstream responses such as NFAT activation and IL-2 production [258]. As such, our findings may provide insight into defects on Orai1 function in T cells in human primary immunodeficiencies and reveal new targets for therapeutic intervention.

Materials and Methods

Cells, Antibodies, and Constructs

The HEK293T cell line was obtained from American Type Culture Collection and maintained in Dulbecco's Modified Eagle's Media supplemented with 10% fetal bovine serum, 1% L-glutamine, and 1% penicillin/streptomycin. Orai triple knockout (TKO) HEK293T cells [282] (Yoast et al., 2020) were the kind gift of Dr. Mohamed Trebak (Penn State University Medical Center) and maintained in the same media. Cells were passed every three days until passage 30. The cells were plated on either polystyrene tissue culture dishes (Corning) or on poly-L-lysine (Sigma-Aldrich, P-8920) coated glass coverslips. Cells were transfected with Lipofectamine 3000 according to the manufacturer's instructions with 0.75 μg Orai1 plasmid and/or 2.25 μg STIM1 plasmid per 35mm well. All cells were maintained at 37°C and 5% CO_2. Imaging was carried out 18 hours after transfection. The following antibodies were purchased from Cell Signaling Technology: STIM1 (#4916S), Calnexin (#2679), Lck (#2787), GFP (#2955), PLC-γ1 (#2822), pPLC-γ1 (#2821), and anti-rabbit IgG, HRP-linked secondary antibody (#7074S). Anti-human CD3 antibody was purchased from eBioscience, #14-0037-82. The Orai1 antibody was produced by Alomone Labs, #ACC-062. Orai1-YFP was a gift from Anjana Rao (Addgene plasmid #19756). Orai1-C143S-YFP and Orai1-C143S-GCaMP6f were built using a q5 mutagenesis kit (NEB) and the primers 5'-CATGATCAGCACCTCCATCCTGCCCAAC-3' and 5'-GTTGGGCAGGATGGATGGAGGTGCTGATCATG-3'. Orai1-GCaMP6f was a gift from Michael Cahalan (Addgene #73564). STIM1-mRFP was a gift from David Holowka and Barbara Baird (Cornell University).

Acyl Biotin Exchange (ABE) Assay

Protein S-acylation was determined by acyl biotin exchange (ABE), as previously described in [291] and modified from [278]. Prior to cell lysis for ABE, HEK293T cells were stimulated with 10 μM thapsigargin for 0, 2, 5, or 15 minutes; 1 X 10^7 Jurkat cells were stimulated with 10 μg/mL anti-CD3 (OKT3) antibody for 0, 2, 5, or 15 minutes. Cells were lysed in 1% Dodecyl β-D-maltoside in phosphate buffered saline, supplemented with cOmplete Protease Inhibitor Cocktail, acyl protein thioesterases inhibitor ML211, and the serine protease inhibitor phenylmethylsulfonyl fluoride (10 mM). The lysate was then cleared by centrifugation, protein concentration was determined using BIO-RAD Protein Assay Dye Reagent Concentrate, according to the manufacturer's directions, and 500 μg of protein was used. Input was retained to confirm stimulation. The lysate was subjected to chloroform-methanol (CM) precipitation, then was incubated in 0.2% S-methyl methanethiosulfonate (MMTS) for 15 min at 42°C. MMTS was removed by three rounds of CM precipitation, and the protein pellets were dissolved in 2SB buffer (2% SDS, 5 mM EDTA, 100 mM HEPES, pH 7.2). Approximately 1/10 of each sample was retained for input control. To cleave thioester bonds and capture free thiol groups, freshly prepared, neutral hydroxylamine (400 mM, pH 7.2) and HPDP-biotin (0.4mM) were added to the experimental samples. Negative control samples were treated with 2M neutral sodium chloride instead of hydroxylamine. Samples were incubated while rotating at room temperature for 1.5 h, followed by two CM precipitations to remove excess biotin. Samples were then incubated with streptavidin agarose beads in conjugation buffer (5 mM EDTA, 100 mM HEPES, 0.2% TX-100, 0.1% SDS, pH 7.2) at room temperature overnight. The beads were then washed

and collected, and protein was eluted by incubation in SDS sample buffer (50 mM Tris-HCl (pH 6.8), 2 % SDS, 10 % glycerol, 5 % β-mercaptoethanol and 0.01 % bromophenol blue) supplemented with 5 mM DTT for 15 min at 80°C. Eluted proteins were then analyzed by Western blotting.

Western Blotting

Eluted proteins were resolved by SDS-PAGE and transferred to nitrocellulose membrane. After transfer, membranes were blocked with 5% bovine serum albumin in TBS-T (0.1 % Tween-20 in TBS buffer) at room temperature for 1 h. Membranes were then incubated with primary antibodies (1:1000 for all primary antibodies, except Orai1, which was 1:500) overnight at 4°C, followed by three washes with TBS-T. Membranes were then incubated with secondary HRP-conjugated antibodies (1:5000) for 1 h at room temperature, followed by three washes in TBS-T. BIO-RAD Clarity Western ECL (#1705061) was used to develop membranes and they were imaged on the LI-COR Odyssey Scanner (LI-COR Biosciences; Lincoln, NE). Brightness and contrast were adjusted in the linear range using the Image Studio software (LI-COR).

Cell Surface Biotinylation

Cell surface biotinylation was performed as described previously [292]. HEK293 Orai TKO cells were plated on 10 cm plates and transfected with WT Orai1-YFP + WT STIM1-mRFP or Orai1-YFP C143S+ WT STIM1-mRFP plasmids using Lipofectamine 3000 according to manufacturer's protocol. Next day, the media was removed, and the cells were washed two times with sterile ice-cold PBS. Cell impermeant Biotin (Sulfo-NHS-SS-Biotin; Pierce) was dissolved in ice-cold PBS/$MgCl_2$/$CaCl_2$ to prepare labeling

solution at a final concentration of 1 mM. 6 mL of this solution was added to each plate and was incubated at 4ºC for 3 hours for cell surface proteins to be biotinylated. After 3h, the labeling solution was removed and the cells were incubated in quenching buffer (PBS, 10 mM Tris, 100 mM glycine) for 10 min at 4ºC. Cells were then lysed using 250 µl lysis buffer containing protease inhibitors. Whole cell lysates were obtained by centrifuging these samples at 10,000 xg for 20 min at 4ºC. 1000 µg of protein (~2mg/mL in lysis buffer) was added to a 25 µL bed-volume of Neutravidin agarose resin (Pierce). The resin was incubated overnight at 4ºC with rotation. Next day, the resin was washed 10 times with wash buffer (PBS + protease inhibitors) and biotinylated samples were eluted using 25 µL 2X SDS sample buffer. The samples were analyzed using SDS-PAGE and western blotting as described above.

Electrophysiology

HEK293T cells were seeded in 35-mm culture dishes and co-transfected with STIM1-mRFP and Orai1-YFP or C143S-Orai1-YFP when cell density reached 60-70% confluence using the polyethylenimine (PEI) method as previously described [293]. At 6-8 hrs after the transfection, cells were reseeded on glass coverslips placed in 35-mm dishes and then used for recording within 24 hrs. Whole-cell voltage clamp recordings were conducted with an EPC-10 amplifier (HEKA) controlled by Patchmaster software (HEKA). Recording pipettes were pulled from standard wall borosilicate tubing with filament (Sutter Instrument) and fire polished. The pipette and bath solutions followed the previous description [287] and contained (in mM): pipette solution, 120 cesium glutamate, 20 cesium· BAPTA [1,2-bis(2-aminophenoxy)ethane- N,N,N’,N’-tetraacetic acid], 3 $MgCl_2$, 0.05 potassium inositol 1,4,5-trisphosphate (IP_3), and 10 HEPES (pH 7.2

adjusted with CsOH); bath solution, 120 NaCl, 10 $CaCl_2$, 2 $MgCl_2$, 10 tetraethylammonium chloride (TEA-HCl), 10 glucose, and 10 HEPES (pH 7.2 adjusted with NaOH).Pipette resistance was 5 - 8 MΩ when filled with the pipette solution and placed in the bath. Cells with membrane resistance of 3 - 5 GΩ were made into whole-cell by applying negative pressure and those with >1 GΩ resistance were used for further analysis. All voltages were corrected for a liquid junction potential of −10 mV. Whole-cell currents were elicited by repeated 100-ms voltage ramps from −100 to +100 mV at a sampling rate of 1 Hz. The holding potential was kept at 0 mV and the sampling frequency was 10 kHz filtered at 1 kHz. Inward currents at -100 mV were calculated for current density by dividing cell capacitance and plotted against time.

Calcium Imaging

Calcium imaging on HEK293 cells was done as described previously [130, 294]. Briefly, two days before calcium imaging, 300,000 cells were seeded onto glass coverslips. After 24 hours, the cells were co-transfected with Orai1-YFP or C143S-Orai1-YFP and STIM1-mRFP plasmids. Before loading with Fura-2AM (Invitrogen), the coverslips were rinsed twice with imaging solution (1% BSA, 107 mM NaCl, 20 mM HEPES, 2.5 mM MgCl2, 7.5 mM KCl, 11.5 mM glucose, and 1 mM CaCl2). The cells were incubated with 5 µM Fura-2AM in imaging solution for 30 minutes. After 30 minutes, the cells were incubated in imaging solution without Fura-2 for an additional 10-30 minutes. Coverslips were mounted onto a Nikon Eclipse Ti2 microscope. Images were captured with an ORCA-Fusion CMOS digital camera. Time-lapse images were obtained using a 40X oil immersion objective every 2 seconds for 16 minutes with alternative excitation at 340 and 380 nm. The first minute of the recording was used as baseline. After one

minute, the imaging solution was replaced with calcium free imaging solution with 10 μM thapsigargin (TG). After 7 minutes, the same solution with 1 mM calcium was added. The ratio of Fura-2 absorbance at 340 nm to 380 nm was used to quantify cytosolic calcium. Some cells were unresponsive to thapsigargin-induced ER calcium release. These cells were excluded from analysis to remove cells with already depleted calcium stores. The cells that showed TG-induced calcium release were evaluated for Orai1-mediated calcium entry after calcium add back. Peak entry was calculated by subtracting the maximum 340/380 ratio from the 340/380 ratio immediately prior to calcium add back. Time to peak entry was calculated by quantifying the time it took to reach the peak 340/380 ratio. A t-test was used to calculate the significance in peak entry and time to peak between the WT and C143S Orai1 channels. Orai TKO HEK293 cells which were not expressing recombinant Orai1 did not respond to calcium add back.

Total Internal Reflection Fluorescence (TIRF) Imaging

HEK293 Orai TKO cells were seeded on poly-L-lysine coated coverslips two days before imaging. After 24 h, the cells were co-transfected with Orai1-YFP and STIM1-mRFP plasmids as described above. The TIRF imaging was performed on a Nikon Eclipse Ti microscope with a TIRF illumination system and a Nikon 60X TIRF objective. Cells were excited with 488nm and 561nm lasers. A Photometrics Prime 95B camera was used for image acquisition. Images were acquired every 10 seconds for 16 minutes. The first minute of the recording was used as a baseline. Thapsigargin (10 μM) was added in calcium free imaging solution after 1 minute to deplete ER calcium stores.

In experiments evaluating Orai1-GCaMP6f activity, HEK293 Orai triple knockout cells on glass coverslips were transfected using Lipofectamine 3000 following manufacturer's protocol. The following day the cells were used for TIRF imaging. Store depletion was induced by 10 μM thapsigargin in calcium free medium. After 7 minutes the same solution with 1 mM calcium was added to induce calcium entry through Orai1 channels. We found that cells expressing high levels of Orai1 and STIM1 had significant clustering and co-localization under resting conditions, therefore these cells were excluded from further analysis. The fluorescence from the GCaMP6f channel was used to quantify calcium levels. Regions of Interest (ROI) were drawn around each cell to calculate relative fluorescent units (RFUs) at a given point of recording. For calculating peak calcium entry, the maximum fluorescence value (Cmax) was subtracted from the fluorescence value before calcium addition (Co) and was normalized by dividing with the fluorescence just before calcium addition (Co), Cmax-Co/Co. A t test was used to calculate the significance between the peak calcium entry between WT and C143S cells.

Co-localization between the Orai1 and STIM1 fluorophores was accomplished using the Pearson correlation coefficient analysis in the Nikon NIS-Elements software. Regions of interest (ROI) were drawn on single cells and the correlation was calculated in the time lapse series. From the obtained Pearson Correlation values, we normalized correlation for the time series by dividing the nth time point (Rn) by the correlation value for that frame by the first time point (Ro). The normalized correlation values for each time point were then averaged and plotted against time to obtain the co-localization curve. Peak Pearson correlation was then calculated by subtracting the maximum normalized correlation

(Rmax) after adding TG from correlation immediately before TG addition (Ro) and dividing it with Ro.

For Orai1-GCaMP6f particle number analyses, we utilized the 'Spot Detection' tool in the Binary Image Analysis section of NIS Elements software. We chose the first image captured and 550 seconds into recording, which is the time point of maximum calcium entry in our protocol. The difference between the number of puncta at time zero and 550 seconds was plotted to determine the change in puncta corresponding to the number of active Orai1-GCaMP6f channels. All image processing and measurements were performed using Nikon NIS-Elements AR software 5.21.02. Additional calculations were performed in Microsoft Excel, and graphs and statistical analysis were accomplished using GraphPad Prism 9 and the ‘ggpubr' package in RStudio.

Confocal Imaging

Confocal images of HEK293 T cells expressing WT or C143S Orai1-YFP were taken on a Nikon Ti2 spinning disk confocal microscope with a Plan Apo λ 60x oil objective and a Photometrics Prime 95B sCMOS camera. The numerical aperture was 1.4, and the exposure time was 600 ms.

Co-Immunoprecipitation

HEK293T cells expressing either WT or C143S Orai1-YFP were treated with 10 μM thapsigargin for 0 or 5 minutes, followed by lysis as described above. Protein concentration was determined using Bio-Rad Protein Assay Dye Reagent Concentrate, according to the manufacturer’s directions. 50μg of protein was used for each sample. The lysates were then incubated with 1μg of STIM1 antibody while rotating at 4°C

overnight. Protein A beads were then added, and the samples rotated at 4°C for three hours. The beads were then washed with lysis buffer three times, then the protein was eluted using the elution buffer described above. Samples were then subjected to Western blot analysis.

Acknowledgements

The authors wish to thank Dr. Mohamed Trebak (Penn State University Medical Center) for the kind gift of Orai triple knockout HEK293 cells.

Funding

Research reported in this publication was supported by the National Institute of General Medical Sciences of the National Institutes of Health under Award Number F31GM140644 (to S.J.W.). The content is solely the responsibility of the authors and does not necessarily represent the official views of the National Institutes of Health. This work was also supported by R01GM130840 (to D.B. and A.M.A.), R01GM115446 (to A.M.A.), and R01GM081685 (D.B.).

Competing Interests

The authors declare that no competing interest exists.

Data Availability

N/A

Figures

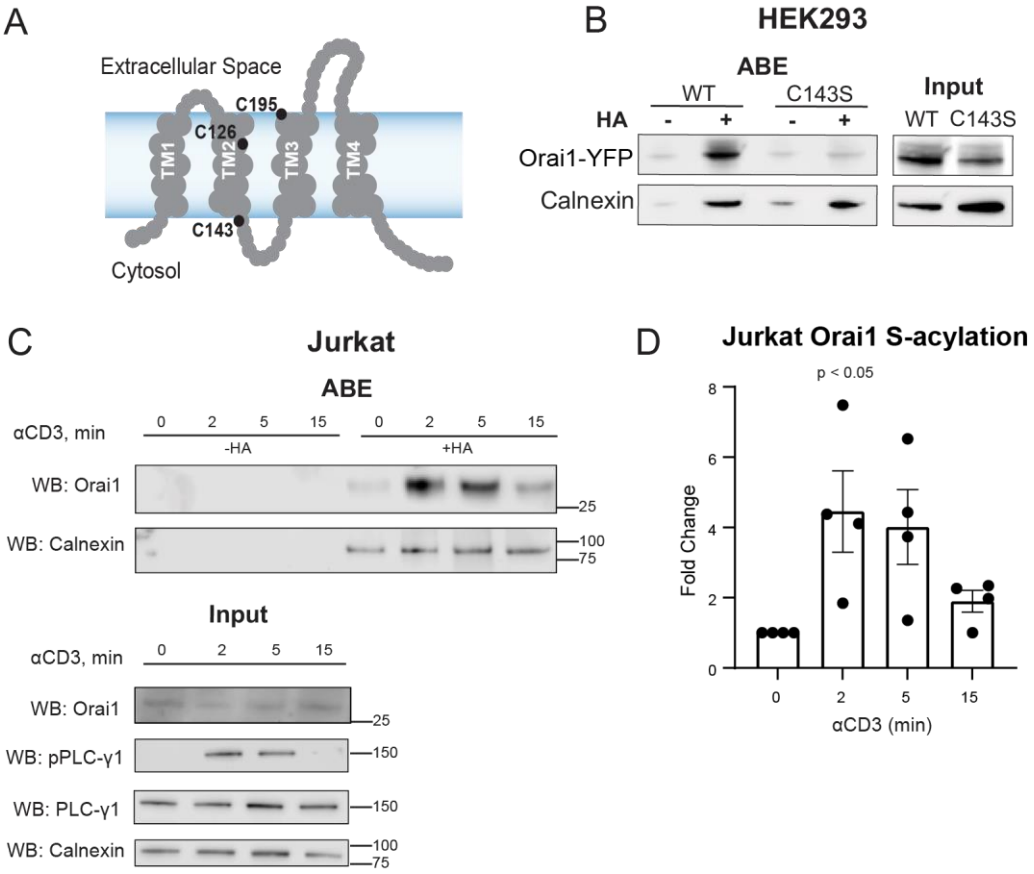

Figure 2.1. Orai1 is transiently S-acylated at cysteine 143. A) Schematic of the localization of the three Orai1 cysteine residues. B) HEK293T cells were transfected with WT or C143S Orai1-YFP, and ABE was performed. The absence of hydroxylamine (-HA) was used as a control for non-specific binding to the resin. Calnexin is used as a positive control for S-acylation. (n=3) C) Jurkat cells were treated with αCD3 for 0, 2, 5, or 15 minutes, followed by ABE. A representative western blot of three experiments is shown. Calnexin is used as a positive control for S-acylation. In this experiment calnexin also functions as a loading control for quantification of changes in Orai1 S-acylation because its levels do not change during cellular stimulation. Representative input blots show levels of Orai1, pPLC-γ1 (proof of cellular stimulation), total PLC-γ1, and calnexin prior to ABE. **D)** Quantification of fold change in Orai1 S-acylation normalized to calnexin (n=4). Error bars indicate S.E.M

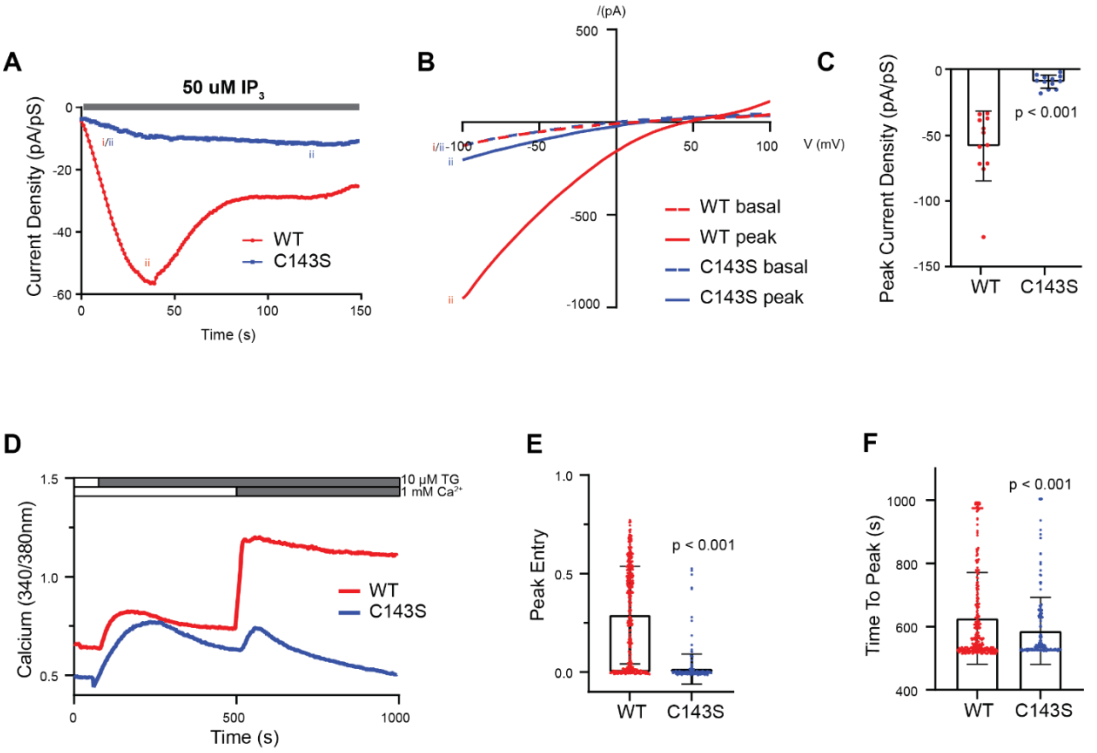

Figure 2.2. Orai1 S-acylation is necessary for store-operated calcium entry. Whole cell recordings were done on HEK 293T cells co-expressing STIM1-mRFP and either WT Orai1-YFP or C143S Orai1-YFP. **(A)** Representative traces of WT (red) and acylation-deficient mutant C143S (blue) Orai1 channel currents were collected at -100mV immediately upon whole cell configuration set up. 50 µM IP_3 was included in the pipettes to activate IP_3Rs to induce ER calcium store depletion. **(B)** Representative current-voltage relationships of WT and C143S Orai1 channels. Labeling on the left corresponds to the time point that the I/V curve was collected on the trace in (A). **(C)** Quantification of average peak current density of wild-type and C143S Orai1-YFP channels (n=12 cells for each condition). Error bars indicate S.E.M. **D)** Fura-2 experiments were conducted on Orai TKO HEK293 cells expressing WT or C143S Orai1-YFP and WT STIM1-mRFP. Cells were first imaged in calcium-free media, then treated with 10 µM thapsigargin (TG) in the absence of calcium to induce calcium store depletion. Cells were then treated with 10 µM TG in the presence of 1 mM calcium to induce calcium entry. Representative single cell traces are shown. There was no difference in basal calcium or peak TG-induced calcium release from the pooled data. **E)** Quantification of peak calcium entry of WT and C143S Orai1-YFP channels. **F)** Quantification of the time to peak calcium entry of WT and C143S Orai1-YFP channels. In E and F, each data point represents a single cell, and the data is pooled from three experiments. Error bars indicate st. dev.

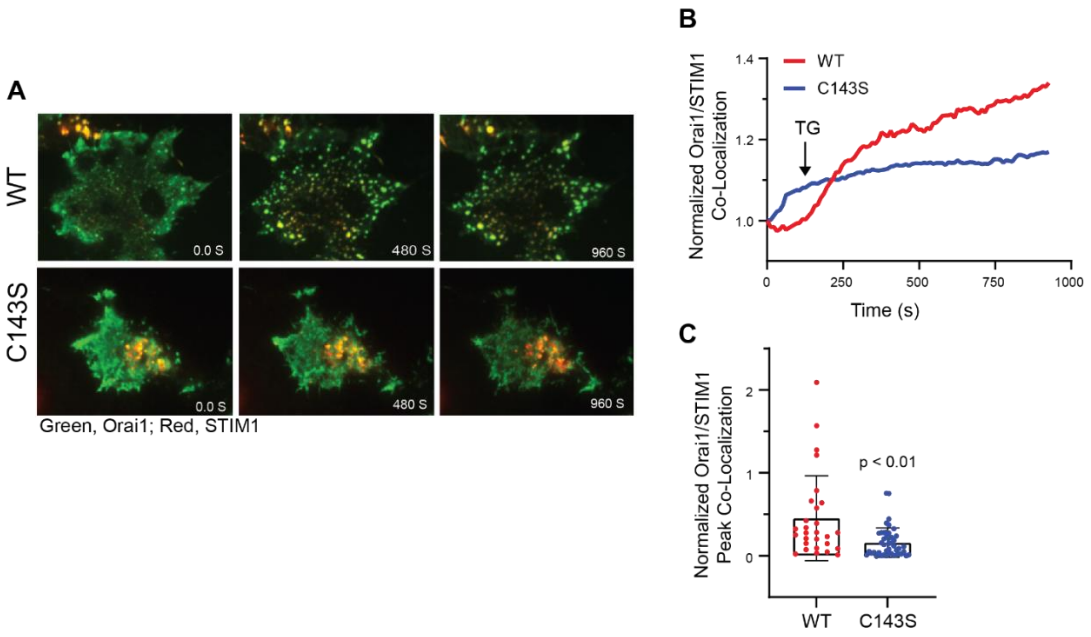

Figure 2.3. S-acylation of Orai1 is required for clustering and recruitment to STIM1. A) Representative TIRF images of Orai TKO HEK293 cells expressing wild-type (top) or C143S (bottom) Orai1-YFP (green) and STIM1-mRFP (red). Thapsigargin was added at 60 s. Representative experiments can be viewed in Supplementary Movies 1 and 2. B) Quantification of wild-type and C143S Orai1-YFP/STIM1-mRFP co-localization using Pearson's correlation coefficient over time. Traces represent averages pooled from at least three separate experiments. The data was normalized at time zero. C) Peak normalized co-localization quantification of WT and C143S Orai1-YFP with WT STIM1-mRFP. Each data point represents a single cell, and the data is pooled from three experiments. Error bars indicate st. dev.

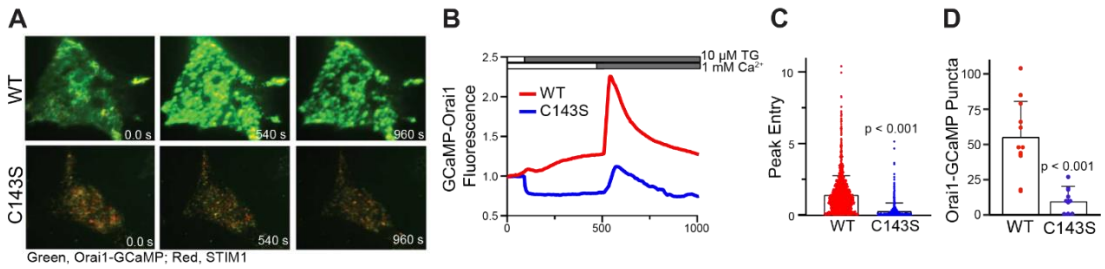

Figure 2.4. Orai1 S-acylation is required for the recruitment of active calcium channels to puncta. A) Representative TIRF images of WT (top) or C143S (bottom) Orai1-GCaMP6f (green) and WT STIM1-mRFP (red) expressed in Orai TKO HEK293 cells. Thapsigargin (10 μM) was added at 60 s. Representative experiments can be viewed in Supplementary Movies 3 and 4. B) Averaged GCaMP6f fluorescence of wild-type and C143S Orai1-GCaMP6f channels over time during a calcium add-back experiment pooled from at least three separate experiments. C) Quantification of peak calcium entry from traces shown in (B) Each data point represents a single cell, and the data is pooled from at least three experiments. D) Quantification of the number of Orai1-GCaMP6f puncta which appear after calcium add-back. Each data point represents a single cell, and the data is pooled from three experiments. Error bars indicate st. dev.

Chapter 3

Dynamic S-Acylation of the ER-Resident Protein Stromal Interaction Molecule 1 (STIM1) is Required for Store-Operated Calcium Entry[3]

Abstract

Many cell surface stimuli cause calcium release from endoplasmic reticulum (ER) stores to regulate cellular physiology. Upon ER calcium store depletion, the ER-resident protein STIM1 physically interacts with plasma membrane protein Orai1 to induce calcium release-activated calcium (CRAC) currents that conduct calcium influx from the extracellular milieu. Although the physiological relevance of this process is well established, the mechanism supporting the assembly of these proteins is incompletely understood. Earlier we demonstrated a previously unknown post-translational modification of Orai1 with long chain fatty acids, known as S-acylation. We found that S-acylation of Orai1 is dynamically regulated in a stimulus-dependent manner and essential for its function as a calcium channel. Here we show that STIM1 is also rapidly and transiently S-acylated at cysteine 437 upon ER calcium store depletion. S-acylation of STIM1 is required for the assembly of STIM1 into puncta with Orai1 and full CRAC

[3] Goutham Kodkandla[*], Savannah J West[*], Qioachu Wang, Ritika Tewari, Michael X Zhu, Askar M. Akimzhanov[‡], and Darren Boehning[‡]
Department of Biomedical Sciences, Cooper Medical School of Rowan University, Camden, NJ 08103, USA
Department of Biochemistry and Molecular Biology, McGovern Medical School, Department of Integrative Biology and Pharmacology, McGovern Medical School, University of Texas Health Science Center at Houston, Houston, TX 77030, USA
*These authors contributed equally to this work
[‡]Authors for correspondence (Askar.M.Akimzhanov@uth.tmc.edu; boehning@rowan.edu)

channel function. Together with the S-acylation of Orai1, our data suggest that stimulus-dependent S-acylation of CRAC channel components Orai1 and STIM1 is a critical mechanism facilitating CRAC channel assembly and function.

Introduction

Calcium depletion in the endoplasmic reticulum (ER) upon IP_3-induced calcium release leads to a rapid, highly controlled, and concerted convergence of plasma membrane (PM) calcium channel Orai1 and ER membrane calcium sensing protein STIM1 to form calcium release-activated current (CRAC) channel puncta to promote calcium entry [174]. The term puncta is used to define these complexes of Orai1 and STIM1 at the ER-PM junctions [15]. Calcium entry through these puncta after store depletion is called store-operated calcium entry (SOCE). The luminal EF hand domain of STIM1 prevents its spontaneous activation by binding to calcium and keeping STIM1 in an inactive conformation [23, 295]. Dissociation of calcium from the EF hand of STIM1 after store depletion results in a conformational change that exposes its STIM1-ORAI activating region (SOAR) [296]. STIM1 then oligomerizes and translocates to PM subdomains where it binds to Orai1 [173, 297]. Subsequent calcium entry through Orai1 channels is essential for shaping the spatiotemporal aspects of calcium signaling leading to diverse cellular outcomes.

The mechanism that directs Orai1 and STIM1 into CRAC puncta is still incompletely understood. The prevailing hypothesis is a diffusion trap model, which postulates that a STIM1 conformational change leads STIM1 binding to Orai1 in a stochastic manner at ER-PM contact sites to promote SOCE [184, 185]. STIM1 can bind phosphatidylinositol

4,5-bisphosphate (PIP_2) via a lysine-rich C-terminal domain, and studies have shown that STIM1 translocates and binds PIP_2 present specifically in lipid rafts [235]. This indicates an active mechanism for targeting STIM1 to lipid rafts, as we and others have shown previously for Orai1 [245, 265]. Perhaps not surprising, it has also been shown that there is reduced mobility of Orai1 and STIM1 after store depletion at ER-PM contact sites [244, 290]. However, both proteins are in a state of dynamic equilibrium, and both proteins can "escape" a puncta and join other puncta [184]. Put together, the assembly of Orai1 and STIM1 at ER-PM junctions is likely more complicated than a simple diffusion trap model with several factors regulating the assembly and disassembly of the CRAC complex.

S-acylation is a reversible post-translational modification of cysteine residues that is mediated by a specific set of enzymes called palmitoyl acyltransferases (PATs) [298]. All known PATs belong to the family of DHHC enzymes owing their name to the aspartate-histidine-histidine-cysteine motif in their catalytic site. S-acylation is known to affect protein stability, trafficking, and recruitment to membrane subdomains [298-300]. In contrast to other post-translational lipid modifications like prenylation, myristoylation, or others, S-acylation is reversible and highly labile [298]. We have recently shown that Orai1 is dynamically S-acylated after store depletion and during initial stages of T cell activation [245]. This was required for Orai1 activation and recruitment into puncta. Here we show that the dynamic S-acylation of STIM1 also mediates SOCE. STIM1 is rapidly and transiently S-acylated after store depletion at cysteine 437, and this is required for recruitment into puncta and SOCE. Our results are consistent with the central role of lipid

rafts in mediating the macromolecular assembly of the T-cell receptor (TCR) and other signaling complexes to orchestrate cellular calcium signaling [255].

Results

STIM1 is Dynamically S-Acylated After Store Depletion at Cysteine 437

Previously, we found that S-acylation of Orai1 is increased after stimulation of the T cell receptor (TCR) in Jurkat T cells [245]. We tested the hypothesis that STIM1 also undergoes S-acylation after T cell activation. STIM1 has only one cytosolic cysteine residue (C437) that can potentially be a substrate for DHHC enzymes (Fig. 1A). We treated Jurkat T cells with anti-CD3 (OKT3) antibody to stimulate the TCR in these cells. We obtained cell lysates after different time points and selectively enriched the S-acylated proteins using the acyl-resin-assisted capture (acyl-RAC) assay [278]. We found that STIM1 is S-acylated after T cell activation which peaked at 5 minutes and then returned to baseline by 15 minutes (Fig. 1B-C). These kinetics are consistent with the activation of the downstream TCR signaling cascade indicated by phosphorylation of PLC-γ1 (Fig. 1D). Next, to show that C437 is the S-acylated residue in STIM1, we transfected HEK293 STIM double knockout (DKO) cells with WT Orai1-Myc and WT or C437S versions of STIM1-Flag. ER calcium store depletion was induced using thapsigargin (TG), and acyl-RAC was performed. Using this approach, we show that WT STIM1, but not the C437S STIM1, is S-acylated after ER calcium store depletion (Fig. 1E). Importantly, the expression levels and ER localization of STIM1 was not compromised by the C437S mutant (Fig. S1). Thus, our data suggests that STIM1 is S-acylated at C437 in a stimulus-dependent manner.

S-Acylation of STIM1 at Cysteine 437 is Required for SOCE

To evaluate the effect of S-acylation of STIM1 on CRAC channel function, we monitored whole cell currents in cells co-expressing Orai1-YFP and either WT or the C437S mutant of STIM1-mRFP. Patch pipettes included 50μM IP_3 to deplete internal stores and activate CRAC currents. As shown in Fig. 2A for current density at −100 mV, cells co-expressing Orai1 and WT STIM1 (grey trace) displayed current developments with three distinct phases: activation (0–45 s), inactivation (50–100 s) and a plateau (100–150 s). In comparison, the activation phase was markedly slowed for cells co-expressing Orai1 and C437S STIM1 (black trace) and the peak current density was also reduced. The current-voltage relationships obtained from voltage ramps at the beginning of whole-cell breaking-in and at the peak of current development showed an inward rectification and reversal potentials at >+40mV (Fig 2B), consistent with the features of CRAC channels. Peak current density and the time to 90% peak at -100mV from multiple cells revealed significant decreases in cells that express C437S STIM1 compared to cells that express WT STIM1 (Fig 2C, D).

To further evaluate the effect of S-acylation of STIM1 on SOCE, we used Fura-2 imaging in STIM DKO cells. As shown by others, knockout of STIM1 and STIM2 in these cells resulted in a loss of SOCE upon store depletion (Fig. S2; [301]). We rescued STIM1 expression in these cells with either WT or C437S mutant versions of STIM1-mRFP and co-expressed Orai1-YFP. Thapsigargin (TG) in calcium-free buffer was used to induce ER calcium store depletion. Calcium addback was achieved using imaging buffer supplemented with 1mM calcium. Expression of WT STIM1-mRFP rescued SOCE in STIM DKO cells (Fig. 2E). In contrast, cells expressing the C437S version of

STIM1-mRFP showed significantly reduced calcium entry (Fig 2E). The peak calcium entry in C437S expressing cells was significantly lower compared to the WT counterpart (Fig. 2F), whereas the time to peak was not affected (Fig. 5G). We conclude that cysteine 437 on STIM1 is required for SOCE.

S-Acylation of STIM1 is Required for Orai1/STIM1 Assembly

We previously showed that preventing S-acylation of Orai1 results in loss of puncta formation and colocalization with STIM1 upon store depletion [245]. We next tested whether S-acylation of STIM1 is required for assembly with Orai1. We co-transfected STIM DKO cells with Orai1-YFP and either WT or C437S versions of STIM1-mRFP and depleted ER stores using 10μM TG. Cells co-transfected with Orai1-YFP and WT STIM1-mRFP showed a rapid and stimulus-dependent colocalization by TIRF imaging (Fig. 3A-C; Fig. S3). In contrast, cells expressing the C437S version of STIM1 showed slower kinetics of colocalization with Orai1 and significantly reduced peak colocalization (Fig. 3A-C; Fig. S3).

Formation of Functional Orai1/STIM1 Puncta is Compromised by the STIM1 C437S Mutant

Orai1 fused to the calcium indicator GCaMP6f allows the direct and local imaging of calcium entry through individual or clusters of Orai1 channels by TIRF imaging [285]. We have previously used this approach to investigate how S-acylation of Orai1 affects the formation of active Orai1 puncta [245]. To investigate how STIM1 S-acylation affects the Orai1 channel activation and puncta formation, we co-transfected STIM DKO cells with WT Orai1-GCaMP6f and either the WT or C437S version of STIM1-mRFP.

The addition of 10μM TG in calcium free media led to puncta formation in WT STIM1 expressing cells, with much fewer puncta in C437S expressing cells (Fig. 4A-C; Fig. S4). Thapsigargin treatment in calcium free media resulted in no increase in Orai1-GCaMP6f fluorescence in either WT or C437S STIM1 expressing cells, consistent with the specificity of this protein in measuring calcium entry through the mouth of the channel (Fig. 4A-B; Fig. S4). Calcium addback caused a significant increase in Orai1-GCaMP6f fluorescence in cells expressing WT STIM1, indicative of calcium entry through Orai1 channels. In contrast, cells expressing C437S STIM1 did not show a significant increase in fluorescence after calcium addback, but only recovered to the level comparable to that of before extracellular calcium removal (Fig 4A-B,D; Fig. S4). We conclude that the STIM1-C437S mutant has defects in both the recruitment to Orai1 puncta and gating the channel.

Discussion

Store-operated calcium entry is an important mechanism for calcium refilling after ER calcium store depletion and contributes significantly to shaping the spatiotemporal aspects of calcium signaling [302, 303]. The mechanisms behind how the CRAC channel components are translocated to the ER-PM junctions to form puncta are not fully understood. Previously, our group demonstrated that Orai1 is dynamically S-acylated after store depletion and a cysteine mutant version of this protein that cannot undergo S-acylation effects CRAC channel assembly and SOCE [245], findings that have also been validated by others [265]. Here we show that S-acylation of STIM1 also plays a crucial role in CRAC puncta formation and that it contributes to SOCE.

The S-acylation of Orai1 in the PM targets the channel to lipid rafts where it forms CRAC channels with STIM1 to promote calcium entry [245, 265]. We hypothesize S-acylation of STIM1 regulates SOCE in two possible ways. One model postulates that STIM1 is S-acylated by an ER-localized DHHC enzyme to promote and/or stabilize the extended conformation of STIM1 (Fig. 5). Another possible model hypothesizes the S-acylation of the C-terminus of STIM1 in the extended conformation by a PM-localized DHHC enzyme. In this model, S-acylation would function not only to anchor the SOAR/CAD domain of STIM1 in the PM but also promote localization to lipid rafts to promote binding to raft-localized Orai1 (Fig. 5). Importantly, this model proposes that both the assembly and disassembly of CRAC channels is an enzymatically regulated process. If this model is correct, a significant revision to the diffusion-trap model of CRAC channel assembly would be required.

Active STIM1 adopts an extended conformation upon store depletion. This fully extended conformation facilitates binding of the polybasic domain of STIM1 to the PIP_2-rich domains specifically in PM lipid rafts [235]. In addition, STIM1 has a cholesterol binding domain in the SOAR region, of which isoleucine 364 plays a critical role [164]. Thus, in addition to S-acylation, there are multiple structural features in the C-terminus of STIM1 which promotes binding and segregation to lipid rafts. This redundancy in function is a likely explanation for the partial loss of SOCE we describe here with the C437S mutant STIM1. Interestingly, it has been shown that STIM1 encompassing only residues 1-442 still forms puncta in Orai1 triple knockout cells, whereas STIM1 encompassing residues 1-342 does not [304]. These results indicate that Orai1 and the

polybasic domain of STIM1 are dispensable for puncta formation, however the SOAR domain (containing C437 and I364 residues) is absolutely required.

It is possible that the same plasma membrane DHHC enzyme mediates the S-acylation of both Orai1 and STIM1. This hypothesis is supported by our findings that both Orai1 and STIM1 reach peak S-acylation levels at the same time point after T cell stimulation (Fig. 1B-C; [245]). Similarly, we have observed in TIRF time lapse imaging experiments that the peak colocalization of Orai1 and STIM1 happens approximately at the same time after store depletion (Fig. 3B; [245]). It has been shown that DHHC20 S-acylates Orai1 [265]. We have shown that many TCR pathway components are S-acylated by the PM-localized DHHC21 [251-253, 266]. Future work will evaluate if Orai1 can also be S-acylated by DHHC21 and determine the DHHC enzyme(s) responsible for STIM1 S-acylation. Of note, we have shown dramatic defects in T cell function in DHHC21 mutant mice *in vitro* and *in vivo* which may be consistent with alterations in SOCE [252].

Another important observation from S-acylation of STIM1 and Orai1 is the importance of immunological synapse formation in the TCR-mediated immune response [12, 305, 306]. S-acylation of Orai1 is important for segregation of the channel to the immunological synapse [265]. In our previous studies, we have shown that several TCR components are rapidly and transiently S-acylated during T cell activation to regulate immune responses [130, 252, 253, 266]. T cell signaling proteins such as Lck and ZAP70 are recruited into the immunological synapse, and we have shown that S-acylation is an important mechanism behind this recruitment and activation [251, 266]. We can now include the Orai1/STIM1 complex in the dynamically S-acylated proteome of T cells. As such, CRAC components are co-localized to the immunological synapse with TCR signaling

proteins following cellular stimulation to promote sustained calcium entry that is required for immune responses [174, 306]. Our results also indicate that the S-acylation enzymatic machinery may be a viable therapeutic target for diseases of immune cell function.

Material and Methods

Cells, Antibodies, and Constructs

HEK293 STIM DKO cells were a kind gift of Dr. Mohamed Trebak [301] (University of Pittsburgh, Pittsburgh, PA, USA) and were maintained in Dulbecco's modified eagle medium (DMEM) supplemented with 10% fetal bovine serum, 1% L-glutamine, and 1% penicillin-streptomycin. Jurkat T cells were obtained from ATCC and cultured in RPMI media supplemented with 10% fetal bovine serum, 1% L-glutamine, 1% penicillin-streptomycin. Cells were plated on polystyrene tissue culture dishes or 6 well plates for experiments. For some experiments, cells were plated on poly-L-lysine coated coverslips for imaging. Cells were transfected with Lipofectamine 3000 (Invitrogen) according to manufacturer's protocol with 0.75µg Orai1 plasmid and/or 2.25µg STIM1 plasmid per 35mm well. Cells were maintained at 37ºC and 5% CO2. For immunoblotting, the antibodies were purchased from commercially available sources: STIM1 (#4961S), calnexin (#2679), phospholipase Cγ1 (PLCγ1) (#2822S), phospho-PLCγ1 (Tyr783) (#2821S), anti-rabbit IgG, HRP-linked secondary antibody (#7074S), anti-mouse IgG, HRP-linked secondary antibody (#7076P2) were from Cell Signaling Technology; anti-CD3 human antibody (14-0037-82) was from eBiosciences. Orai1-YFP was a generous gift from Anjana Rao (Addgene plasmid #19756). Orai1-GCamp6f was a plasmid deposited in Addgene by Michael Cahalan (Addgene #73564; [285]). STIM1-mRFP was

a generous gift from David Holowka and Barbara Baird (Cornell University, Ithaca, NY, USA). The C437S mutant version of STIM1-mRFP and STIM1-Flag were prepared using q5 site-directed mutagenesis kit from New England Biolabs. The following primers for mutagenesis were designed using the NEB tool 5'-GAGATCAACCTTGCTAAGCAGG-3' and 5'- GAAACACACTCTTTGGCACCTT-3'. The mutation was confirmed using Sanger sequencing (Eton Biosciences). Thiol-sepharose beads used for acyl-RAC were obtained from Nanocs Inc and activated according to manufacturer's protocol before continuing with acyl-RAC protocol listed below. All other chemicals and reagents were purchased from Sigma-Aldrich or VWR.

Electrophysiology

We performed whole-cell recording using HEK293 cells co-expressing Orai1-YFP with WT or C437S STIM1-mRFP as described previously[245]. Patch-clamping was conducted with an EPC-10 amplifier controlled by PatchMaster software (HEKA) within 24 hours after transfection. The resistance of fire polished pipettes was between 5 megohm to 8 megohm. The pipette solution contained 120mM cesium glutamate, 20mM cesium, BAPTA [1,2-bis(2-aminophenoxy)ethane-N,N,N',N'-tetraacetic acid], 3mM $MgCl_2$, 0.05mM IP_3 (K^+-salt), and 10mM HEPES (pH 7.2 with CsOH). The bath solution contained 120mM NaCl, 10mM $CaCl_2$, 2 mM$MgCl_2$, 10mM TEA-HCl (tetraethylammonium chloride), 10mM glucose, and 10mM HEPES (pH 7.2 with NaOH). Cells were held at the holding potential of 0mV and currents recorded at a sampling frequency of 10kHz with 1kHz filtering. Currents were elicited by voltage ramps from −100 to +100mV in 100mS, repeated every second. To capture current development immediately after IP_3 dialysis, the recording began before the establishment of the whole-

cell configuration and continued throughout the breaking-in and afterwards. Patches with seal resistance up to 3 gigohm to 5 gigohm were broken by applying negative pressure and only cells that maintained gigohm resistance after the breaking-in were used for analysis. All voltages were corrected for a liquid junction potential of −10 mV.

Fura-2 Imaging

Calcium imaging on HEK293 cells was performed as previously described [307]. Briefly, two days before imaging, approximately 300,000 HEK293 STIM DKO cells were seeded on coverslips in a 6 well culture plate. After 24h, these cells were transfected with WT Orai1-YFP and either WT or C437S STIM1-mRFP plasmids. All calcium imaging was performed in 1% BSA, 107mM NaCl, 20mM HEPES, 2.5mM $MgCl_2$, 7.5mM KCl, and 11.5mM glucose with or without the presence of 1mM $CaCl_2$. Time-lapse images were obtained every two seconds for 16 minutes using a 40X oil immersion objective lens. Cells were excited using 340nm and 380nm wavelengths alternatively every two seconds and emission was collected at 525nm. The first minute of recording was used as baseline. After 1 min, 10μM thapsigargin (TG) in calcium free imaging solution was added to induce ER calcium store depletion. This was continued for 7 minutes and imaging solution with calcium and thapsigargin was added back to induce calcium entry. The ratio of fluorescence at 340nm to 380nm was used to quantify cytosolic calcium. We excluded the cells which did not respond to thapsigargin in our analysis. For calculating Peak Entry, we subtracted the maximum fluorescence ratio (R_{max}) after calcium addback from the fluorescence ratio at time zero (R_0) and normalized to R_0.

Confocal Imaging

HEK293 STIM DKO cells were plated on coverslips in a 6 well plate at a density of 350,000 cells per coverslip. Next day, they were transfected with WT or C437S version of STIM1-mRFP using Lipofectamine 3000 per manufacturer's protocol. The next day, cells were imaged using Nikon Ti2 confocal microscope with a plan apo lambda 60x oil objective at 1.5 magnification factor. Exposure parameters were identical between the WT and STIM1 expressing cells.

Acyl-Resin-Assisted Capture (Acyl-RAC) Assay

We performed the acyl-RAC assay as described by our group elsewhere [278]. Cells were transfected with WT Orai1-Myc and either WT or C437S version of STIM1-Flag plasmids. For Jurkat T cells, 10 million cells per treatment were used for endogenous STIM1 S-acylation experiments and were treated with 5µg/ml anti-CD3 (OKT3) antibody. For STIM1 exogenous expression paradigms, we used 10µM thapsigargin for 5 minutes to induce ER calcium store depletion. Cell lysates were collected after the specific time points using 1% dodecyl ß-D-maltoside in PBS, supplemented with cOmplete protease inhibitor cocktail (Roche), acyl protein thioesterase inhibitor ML211, and serine protease inhibitor PMSF (10mM). The lysates were cleared at 20,000 xg for 30 minutes at 4ºC by centrifugation. Approximately 500 µg of cell lysates were used for the assay. The lysates were precipitated using 2:1 methanol and chloroform, and the resulting protein pellets were incubated with 0.2% methylmethanethiosulfonate (MMTS) for 15 minutes at 42ºC. MMTS was removed using three rounds of methanol chloroform precipitation. After the last round of precipitation, the pellets were dissolved in 2SHB

buffer (2% SDS, 5mM EDTA, 100mM HEPES, pH 7.4). 20µl of lysate was saved for input. The lysates were incubated with 400mM hydroxylamine (HA) to cleave the thioester bonds and incubated with thiolsepharose resin overnight at 4ºC. For the minus HA controls, lysates were incubated with 400mM sodium chloride in place of HA. Next day, the samples were washed four times using 1% SDS solution in Buffer A (5mM EDTA, 100mM HEPES, pH 7.4) and eluted using 10mM dithiothrietol (DTT) in SDS buffer (1% SDS, 50mM Tris-HCl, 10% glycerol, 1% Bromophenol Blue). The samples were resolved on 10% SDS-PAGE gels and analyzed using western blotting.

Total Internal Reflection Imaging (TIRF)

HEK293 STIM DKO cells were seeded on coverslips treated with poly-L-lysine two days before imaging at 300,000 cells per coverslip. Next day, these cells were transfected with WT Orai1-YFP or either WT or C437S STIM1-mRFP. For TIRF imaging, we used a Nikon Eclipse Ti microscope equipped with TIRF illumination system and a 60X oil objective. The cells were mounted on the microscope and alternatively excited using 488nm and 561nm lasers every ten seconds. The images were acquired for 16 minutes using a Photometrics Prime 95B camera. The first minute of the recording was used as baseline. Thapsigargin in calcium free imaging solution was added after the first minute to observe Orai1 and STIM1 PM targeting and recruitment to CRAC puncta. For the experiments in Fig. 4, we used Orai1-GCaMP6f with WT or C437S version of STIM1-mRFP to evaluate the effect of STIM1 S-acylation on Orai1 channel activity. We altered the protocol to evaluate calcium entry and imaged every 5 seconds. Imaging was done for 16 minutes and the first minute was used as baseline. After 1 minute, thapsigargin in calcium free imaging solution was added to observe STIM1 colocalization with Orai1.

After 8 minutes, the solution was replaced with imaging solution with calcium to observe calcium entry. We excluded all cells with aggregates under resting conditions from our analyses. We used Nikon NIS Elements software for fluorescence data analysis. We drew regions of interest (ROI) around cells to calculate relative fluorescence units (RFU) at any point during the timelapse. We normalized the RFU of specific cell to itself by dividing a specific timepoint fluorescence (Cn) value to time zero (C0). We use these normalized fluorescence values to plot Orai1 channel fluorescence over the time course of thapsigargin addition and calcium addback. To calculate the peak entry, we obtained the maximum fluorescence value (Cmax) after calcium addback and subtracted it from the fluorescence value at time zero (C0) and normalized the difference by dividing it to time zero (C0) (Cmax-C0/C0). To calculate the colocalization between Orai1 and STIM1, we used colocalization analysis on Nikon NIS Elements software. The software uses Pearson's correlation coefficient as an estimate for colocalization between two fluorophores. We drew ROIs around cells of interest and obtained correlation coefficients for the time series of all cells. We followed the similar method of normalized correlation by dividing correlation coefficient at a given time point (Rn) by time zero (R0). We used these values to plot the colocalization curve. To calculate peak colocalization, we used the similar method to that of peak entry, we subtracted the peak colocalization after thapsigargin addition (Rmax) from time zero (R0) and divided the difference to time zero (R_0) (Rmax-R0/R0).

Figures

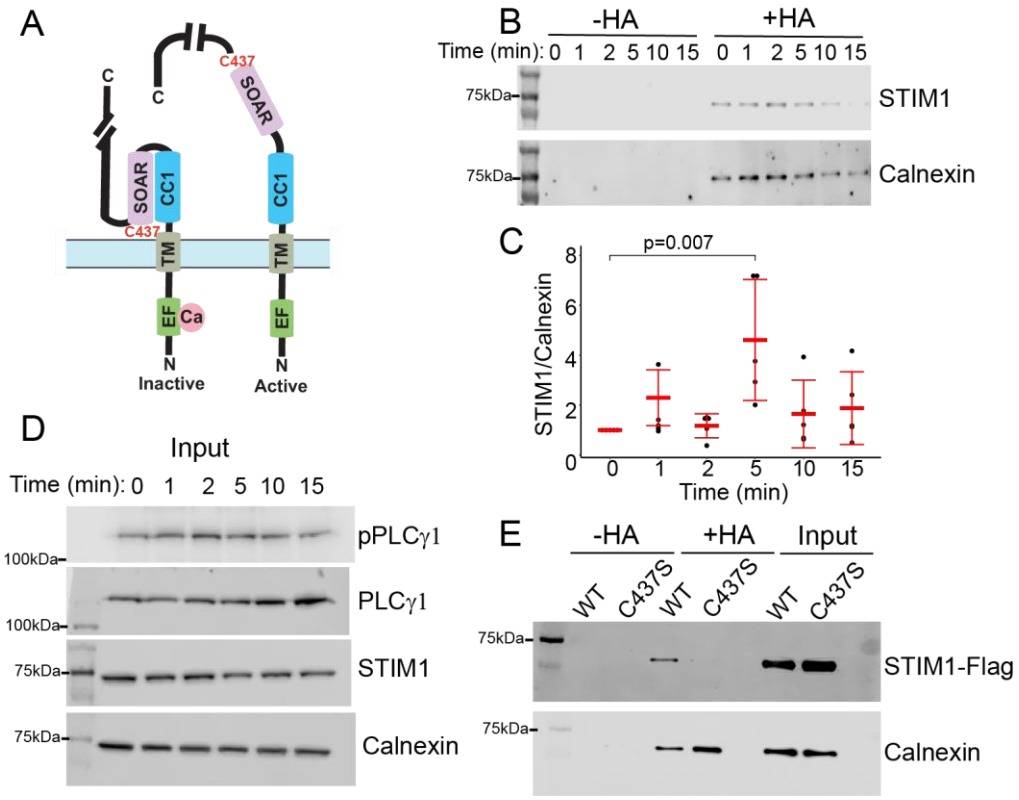

Figure 3.1. STIM1 is dynamically S-acylated at cysteine 437. A) Schematic representation of the inactive and active (extended) conformation of STIM1. The locations of the EF hand, coiled-coil 1 (CC1) and STIM1 Orai1 activation region (SOAR) of STIM1 are indicated. The location of cysteine 437 is noted at the C-terminus of the SOAR domain. For simplicity, one monomer of the dimeric STIM1 structure is presented. B) Jurkat T cells were treated with anti-CD3 antibody for 0, 1, 2, 5, 10, and 15 minutes and subjected to acyl-RAC. The reaction without hydroxylamine (-HA) as a negative control. Calnexin serves both as a positive control for S-acylation and a loading control. Representative of n=5. C) Quantification of fold change of S-acylation of STIM1 normalized to calnexin. Error bars indicate S.D. D) Input blots are shown for levels of pPLCγ1, PLCγ1, STIM1, and calnexin. The pPLCγ1 blot is indicative of the time course of TCR activation. E) HEK STIM double knockout (DKO) cells were transfected with WT or C437S STIM1-FLAG and acyl-RAC was performed after 5 minutes of calcium store depletion with thapsigargin. The blots are representative of four independent experiments.

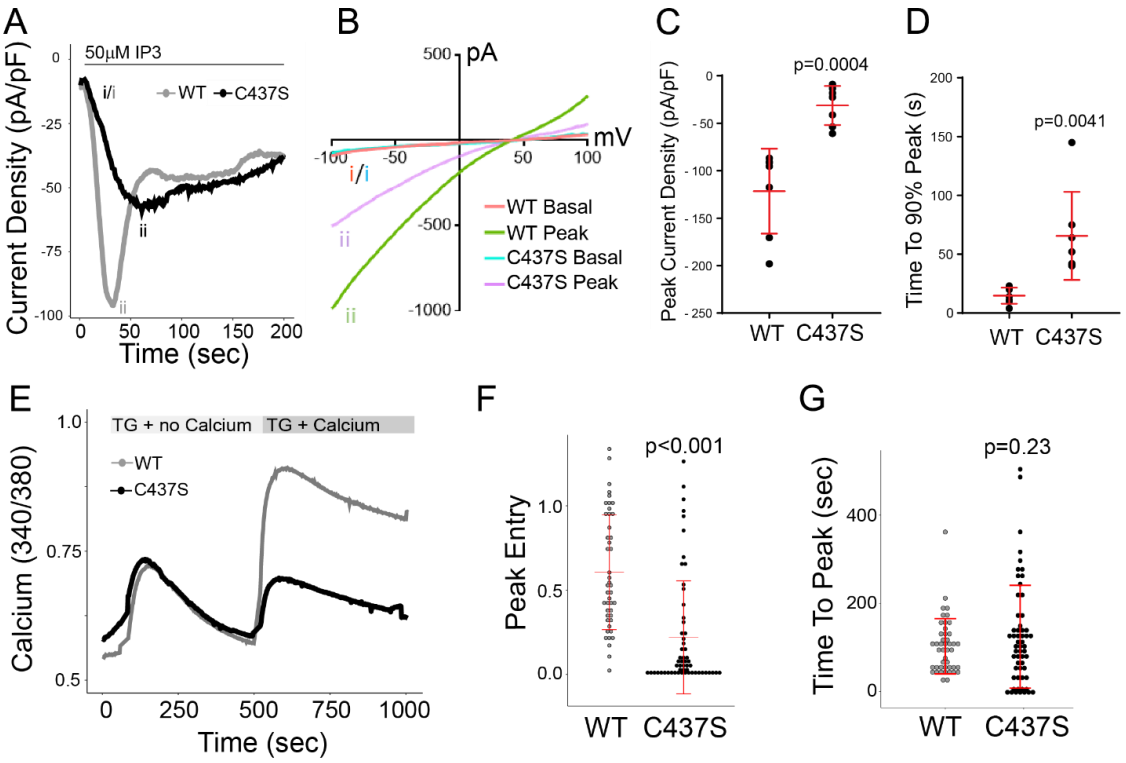

Figure 3.2. S-acylation of STIM1 facilitates store operated calcium entry. (A) Representative traces of CRAC channel currents in cells expressing WT STIM1-RFP (grey) and the acylation-deficient STIM1 mutant C473S (black). CRAC channel currents (representative of 7 experiments for each condition) were collected at −100 mV immediately upon entering whole-cell configuration. 50 μM IP3 was included in the pipette to activate IP3 receptors to induce ER Ca2+ store depletion. All panels in this figure include co-expression of WT Orai-YFP. (B) Representative current–voltage (I–V) relationships cell expressing WT or C437S STIM1-RFP. Labeling on the left corresponds to the time point that the I–V curve was collected on the trace in A. (C) Quantification of average peak current density of WT and C437S STIM1-RFP expressing cells (n=7 cells for each condition). Error bars indicate S.D. (D) Time to 90% peak current in cells expressing WT and C437S STIM1-RFP. (E) Fura-2 experiments were conducted in STIM double knockout (DKO) HEK293 cells expressing WT or C437S STIM1-RFP. Cells were first imaged in Ca2+-free medium, then treated with 10 μM thapsigargin (TG) in the absence of Ca2+ to induce Ca2+ store depletion. Cells were then incubated with 10 μM TG in the presence of 1 mM Ca2+ to induce Ca2+ entry. Single cell traces are shown as representatives of three individual experiments. There was no difference in basal Ca2+ or peak TG-induced Ca2+ release in the two conditions. (F) Quantification of peak Ca2+ entry in cells expressing WT or C437S STIM1-RFP. (G) Quantification of the time to peak Ca2+ entry in cells expressing WT and C437S STIM1. In E and F, each data point represents a single cell, and the data is pooled from three experiments. Error bars indicate S.D.. The p-values in panels C,D,F, and G are indicated above the C437S data and were calculated with an unpaired two-tailed t-test.

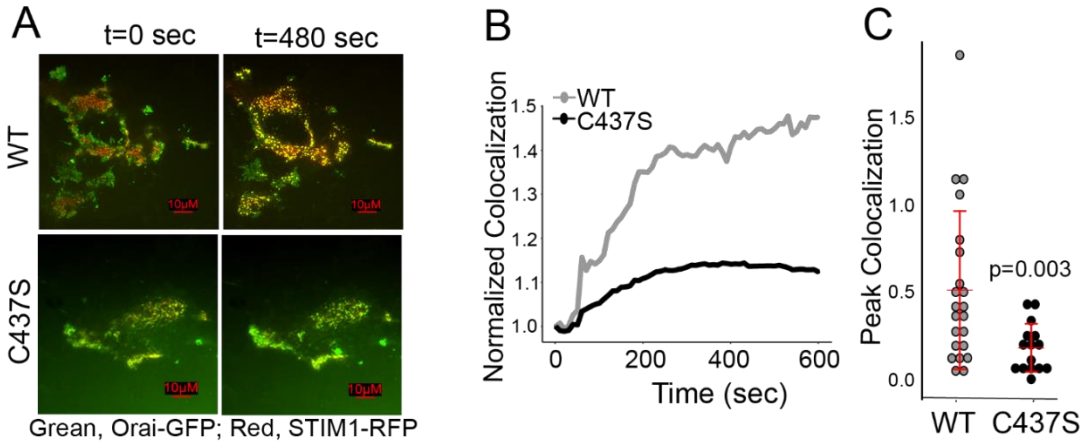

Figure 3.3. S-acylation of STIM1 is required for colocalization with Orai1. A) Representative TIRF images from six experiments of STIM DKO cells transfected with WT Orai-YFP (green) and either WT (top) or C437S (bottom) STIM1-mRFP (red). Thapsigargin was added after 60 seconds of baseline recording. See also supplementary videos 1 and 2. B) Quantification of WT and C437S STIM1-mRFP colocalization with Orai1-YFP using Pearson's correlation coefficient over time. Traces represent averages pooled from six separate experiments. The data was normalized to time zero. C) Peak normalized colocalization quantification of WT and C437S STIM1-mRFP and Orai1-YFP. Each data point represents a single cell and the data is pooled from 6 separate experiments. Error bars indicate S.D. The p-value was calculated with an unpaired two-tailed t-test.

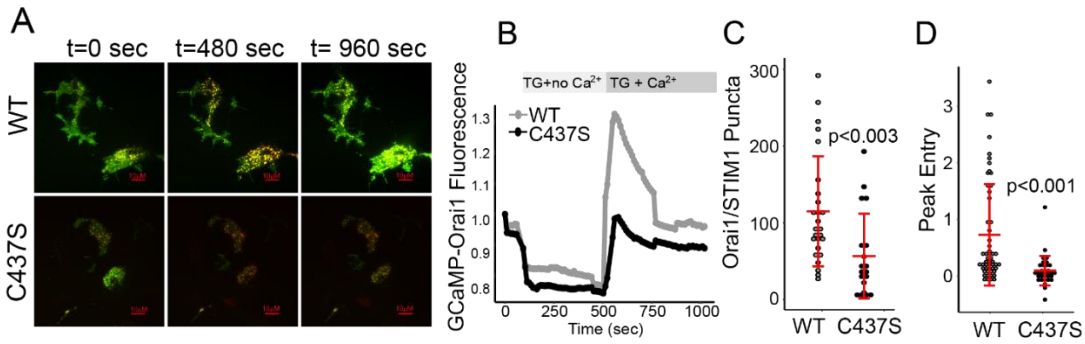

Figure 3.4. STIM1 S-acylation is required for the recruitment of active Orai1 to puncta. A) Representative TIRF images from six experiments of STIM DKO cells transfected with WT Orai-GCaMP6f (green) and either WT (top) or C437S (bottom) STIM1-mRFP (red). Cells were first imaged in Ca2+-free medium, then treated with 10 μM thapsigargin (TG) in the absence of Ca2+ to induce Ca2+ store depletion. Cells were then incubated with 10 μM TG in the presence of 1 mM Ca2+ to induce Ca2+ entry. See supplementary videos 3 and 4. B) Normalized Orai-GCaMP6f fluorescence of cells transfected with WT and C437S STIM1-mRFP over time. Traces represent averages pooled from six separate experiments. C) Quantification of the number of Orai1–GCaMP6f/STIM1 puncta which appear after Ca2+ add-back. D) Peak normalized fluorescence of Orai1-GCaMP6f in cells expressing WT and C437S STIM1-mRFP. Each data point in Panels C,D represents a single cell and the data is pooled from 6 separate experiments. Error bars indicate S.D. The p-values were calculated using an unpaired two-tailed t-test.

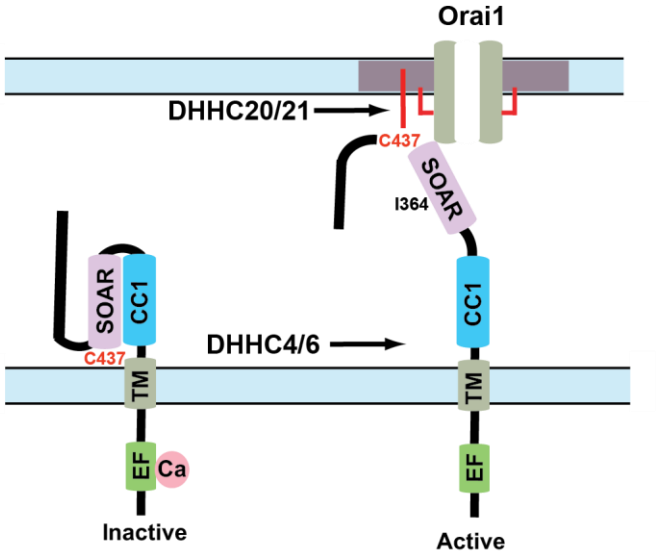

Figure 3.5. S-acylation of STIM1 C437 and CRAC channel function. Two potential models for the regulation of STIM1 by S-acylation at C437. In the first model, ER-localized DHHC4 or DHHC6 S-acylate C437 facilitating and/or stabilizing the extended conformation of STIM1. In the second model, S-acylation of C437 by the plasma membrane-localized DHHC20 or DHHC21 both stabilizes the extended conformation and promotes recruitment to lipid rafts where it can bind and gate S-acylated Orai1. The cholesterol binding residue isoleucine 364 is also highlighted. For clarity, the C-terminal PIP2 binding polybasic domain is not shown.

Chapter 4

DHHC21 is a STIM1 Palmitoyl Acyltransferase[4]

Abstract

Depletion of calcium from ER stores leads to the activation of calcium channels on the plasma membrane. This process is termed store-operated calcium entry (SOCE). The proteins STIM1 and STIM2 function as ER calcium sensors, and upon store-depletion, they undergo a conformational change which allows them to bind to and gate Orai calcium channels on the plasma membrane. We have shown that both Orai1 and STIM1 are dynamically S-acylated after store depletion, which is required for SOCE. This result implies a calcium-activated protein S-acyltransferase. Here we show that the protein acyltransferase DHHC21 is required for SOCE in vitro and in vivo. Plasma membrane-localized DHHC21 is dynamically recruited into Orai1/STIM1 puncta upon store depletion. Knockdown of DHHC21 expression inhibits SOCE and leads to reduced STIM1/Orai1 S-acylation. Using the *depilated* mouse model, we show that DHHC21 is required for STIM1 and Orai1 S-acylation and subsequent T cell signaling *in vivo*. Our results show that DHHC21 is rapidly activated by calcium/calmodulin leading to

[4] Goutham Kodakandla, Ying Fan, Michael X Zhu, Savannah West, Askar Akimzhanov[*], Darren Boehning[*]
Department of Biomedical Sciences, Cooper Medical School of Rowan University, Camden, USA, 08103
Department of Integrative Biology and Pharmacology, McGovern Medical School, University of Texas Health Sciences Center at Houston, Houston, Texas, 77030
Department of Biochemistry and Molecular Biology, McGovern Medical School, University of Texas Health Sciences Center at Houston, Houston, Texas, 77030
[*]Correspondence: Darren Boehning (boehning@rowan.edu) or Askar M. Akimzhanov (askar.m.akimzhanov@uth.tmc.edu)

dynamic S-acylation of calcium signaling proteins. These results further suggest that dynamic S-acylation has underappreciated and expansive roles in second messenger signaling.

Note: The data presented in this chapter is unpublished

Introduction

Intracellular calcium levels regulate many physiological functions. Store-operated calcium entry (SOCE) is a mechanism where the depletion of endoplasmic reticulum (ER) calcium stores leads to the activation of a calcium flux from the extracellular milieu [8, 19-21]. The ER calcium sensor Stromal Interaction Molecule 1 (STIM1) is activated upon depletion of calcium stores in ER lumen, which undergoes a conformational change to bind to the plasma membrane (PM), where it binds to and activates a calcium channel, Orai1 [173, 176, 194, 196]. This intermolecular complex between these two proteins is termed the calcium-release activated channel (CRAC) [21, 131, 308]. CRAC channels form macromolecular complexes near ER:PM junctions, which form the nexus of SOCE. These complexes have been termed ‘puncta’ owing to the punctate appearance in microscopy images [159]. Abnormalities in CRAC channel function lead to disorders in the immune and musculoskeletal systems, such as severe combined immunodeficiency (SCID), tubular aggregate myopathy, York platelet syndrome, and Stormorken syndrome [25, 131, 132, 154, 302, 309].

The mechanisms by which STIM1 and Orai1 proteins colocalize near ER:PM subdomains upon store-depletion have been a long-standing debate in the field. One prominent hypothesis is the diffusion trap model, which postulates a stochastic binding of activated STIM1 to Orai1 in these subdomains, where STIM1 ‘traps’ Orai1 channels to

induce SOCE [184, 185]. However, this model does not explain the active targeting of STIM1 to phosphatidylinositol 4,5-bisphosphate (PIP2) domains in membrane lipid rafts [235]. In addition, studies have also shown that both Orai1 and STIM1 exist in dynamic equilibrium, where these proteins can transfer between different puncta [184]. We have shown that S-acylation of Orai1 and STIM1 regulates CRAC channel formation [245, 246]. S-acylation is the reversible addition of lipid moieties to intracellular cysteine residues of target proteins [254]. S-acylation is mediated by a set of enzymes known as palmitoyl acyltransferases (PATs). PATs are also known as DHHC enzymes owing to the aspartate-histidine-histidine-cysteine motif in the active site of these enzymes [262, 298]. S-acylation affects protein stability, trafficking to subcellular compartments, and shuttling between membrane subdomains [310-314]. We have shown that S-acylation actively targets Orai1 and STIM1 to puncta providing an additional level of regulation to SOCE [245, 246]. Our findings also called into question the validity of the diffusion trap model.

Several DHHC enzymes are active in the plasma membrane, including DHHC5, DHHC20 and DHHC21. We have shown that DHHC21 is essential for T cell calcium signaling by S-acylating components of the T cell receptor (TCR) complex [253]. We also exploited the mouse model *depilated*, which has an in-frame deletion of a single phenylalanine residue in DHHC21 which eliminates a calmodulin-binding site [252, 253]. *Depilated* mice have significant deficits in T cell signaling and differentiation into effector T cell lineages. In vitro, T cells from *depilated* mice have defective TCR signaling, including defective Lck, PLC-γ1, ZAP-70, and ERK signaling after TCR ligation [250, 252]. Calcium transients induced by TCR ligation are significantly reduced

in T cells from *depilated* mice, however, the underlying mechanisms remain to be explored.

Based upon our previous findings in *depilated* mice, in this study we examined the hypothesis that DHHC21 is the PAT for STIM1. We show that STIM1 S-acylation is significantly abrogated in spleens from homozygous *depilated* mice. This is associated with defects in splenocyte SOCE. We also show that DHHC21 is recruited into STIM1 puncta, and this is altered in *depilated* splenocytes. We conclude that DHHC21 is the primary PAT for STIM1 *in vitro* and *in vivo*.

Material and Methods

Cells, Antibodies, and Constructs

HEK293T WT cells were purchased from American Type Culture Collection (ATCC) and cultured in Dulbecco's Modified Eagle Medium (DMEM) supplemented with 10% fetal bovine serum (FBS), 1% L-glutamine, and 1% pencillin-streptomycin. DHHC21 knockout cells were generated using CRISPR-Cas9 plasmids obtained from Genscript Inc. The sgRNA sequences used in these plasmids for knockout of DHHC21 are 5' AAGTGGTAGGGAACTCGCAG 3', 5' ATGAGACTAGCAGCCTTTAT 3'. These cells were maintained similarly to HEK293T WT cells. For experimental manipulations, cells were plated on polystyrene tissue culture dishes or 6-well plates. For imaging, cells were plated on poly-L-lysine-coated coverslips in 6 well plates. Cells were transfected with 0.5 µg STIM1 and 0.5 µg DHHC21 per 35 mm well. All cells were maintained at 37ºC and 5% CO2 until use. Antibodies for immunoblotting and immunofluorescence imaging were purchased from commercially available sources: STIM1 (catalog no.: 4961S), calnexin (catalog no.: 2679), anti-rabbit immunoglobulin, horseradish

peroxidase–linked secondary antibody (catalog no.: 7074S), anti-mouse immunoglobulin, and horseradish peroxidase–linked secondary antibody (catalog no.: 7076P2) were from Cell Signaling Technology; anti-CD3 human antibody (catalog no.: 14-0037-82) was from eBiosciences. The secondary antibodies for super resolution STED imaging were obtained from Abberior Inc. DHHC21-eGFP plasmids were purchased from Genscript Inc. DHHC21-GFP and DHHC21-FLAG plasmids were cloned in house. The DHHC21-ΔF233 mutant was generated using q5 site-directed mutagenesis kit from New England Biolabs using primers (F: TCAGAAGTTTTTGGCACTCGTTG, R: GGTCTGCTGCCATGGCTT). Mutagenesis was confirmed using Sanger Sequencing (Eton Biosciences). STIM1-mRFP was a generous gift from David Holowka and Barbara Baird (Cornell University). Thiol-Sepharose beads used for acyl-RAC were obtained from Nanocs, Inc and activated according to the manufacturer's protocol before continuing with acyl-RAC protocol listed later. All other chemicals and reagents were purchased from Sigma–Aldrich or VWR

Mice: Wild type and Zdhhc21^{dep} mice in the C56BL/6 background were bred in our barrier vivarium under pathogen-free conditions in accordance with the recommendations in the Guide for the Care and Use of Laboratory Animals of the National Institutes of Health. The animals were handled according to the animal care protocol #2020-1252 approved by the Rowan University Institutional Animal Care and Use Committee. Mice used for experiments were males and females at 6–8 weeks old.

Acyl-RAC assay: Acyl-RAC assay was performed as previously described by our group [278]. Cell and tissue lysates were collected in lysis buffer (1% dodecyl-b-D-maltoside in DPBS, supplemented with cOmplete protease inhibitor cocktail (Roche), 10 µM ML211

(acyl protein thioesterase inhibitor), and 10 mM phenyl-methyl-sulfonyl-fluoride (PMSF)). The lysates were centrifuged at 4 C for 30 minutes at 20,000 xg. 500 µg of protein lysate were used for enrichment of the S-acylated proteome. Protein precipitation was performed using 2:1 methanol:chloroform, and the protein pellets were incubated with 0.2% methylmethanethiosulfonate (MMTS) for 15 minutes at 42 C. Excess MMTS in the protein lysates was removed by three rounds of protein precipitation using methanol and chloroform. The resulting protein pellets were dissolved in 2SHB buffer (2% SDS, 5 mM EDTA, 100 mM HEPES, pH 7.4). 5% of the final volume was saved for input and the remaining was used for acyl-RAC. 400 mM hydroxylamine (HA) was added to protein lysates to cleave the thioester bonds at pH 7. The lysates were incubated with thiol-Sepharose resin with rotation overnight at 4 C. The next day, the samples were washed using 1% SDS in buffer A (5 mM EDTA, 100 mM HEPES, pH 7.4) supplemented with 1% SDS. Proteins were eluted using 10 mM DTT in SDS buffer (1% SDS, 50 mM Tris-HCl, 10% glycerol, and 1% bromophenol blue) at 80º C with continuous shaking. Samples were then resolved on 10% SDS-PAGE gels and analyzed using Western blotting.

Co-Immunoprecipitation

Protein lysates we obtained from WT and depilated mice, as well as DHHC21-KO cells transfected with FLAG-tagged WT and ΔF233 versions of DHHC21 using lysis buffer used in acyl-RAC section earlier. Protein lysates (1 mg) were incubated with 3 µl of either anti-DHHC21 or anti-FLAG antibodies overnight at 4 C. Next day, 50 µl protein A agarose slurry (Pierce) was added to the samples and incubated for another hour at room temperature. After one hour, samples were washed using the lysis buffer. After 3 washes,

the agarose pellet was allowed to dry and subsequently quenched by boiling the samples with SDS buffer at 95 C for 5 minutes. Samples were loaded on 10% SDS-PAGE gels and analyzed using western blotting. Co-IP was confirmed using blotting with pulldown antibodies.

Super-Resolution Imaging

We performed STED super-resolution imaging using STEDYCON microscope (Abberior). Splenocytes from *depilated* and WT mice were obtained and immunofluorescence was performed on these cells as previously described elsewhere. Briefly, the cells were plated on poly-L-lysine coated coverslips and treated with anti-CD3 where required. After treatment, the cells were fixed using 4% ice-cold paraformaldehyde for 20 minutes at room temperature with rotation. The cells were quenched of PFA with 30 mM glycine/PBS solution for 5 minutes at RT with rotation. Next, the cells were washed 3 times with PBS with rotation. Cells were permeabilized with 0.25% Triton X-100 and 1% BSA in PBS for 10 minutes at RT with rotation. Cells were then incubated with 2% BSA in PBS for 1 hour at RT with rotation. Cells were washed 3 times with PBS for 5 minutes each, and then incubated with antibodies in PBS with 0.3% BSA. Cells were washed and mounted on glass slides sealed with nail polish. The secondary antibodies for STED imaging were STAR Red anti-mouse and STAR orange anti-rabbit and were obtained from Abberior Inc.

Fura-2 Imaging

Fura2 imaging on WT HEK293, DHHC21-KO HEK293, and mouse splenocytes was performed as previously described [245, 246]. Briefly, for adherent cells, 2 days before imaging, cells were seeded on poly-lysine coated coverslips in 6-well tissue culture

plates. Next day, these cells were transfected with DHHC21 and STIM1 plasmids. Imaging buffer was prepared for Fura-2 calcium imaging (1% bovine serum albumin, 107 mM NaCl, 20 mM HEPES, 2.5 mM MgCl2, 7.5 mM KCl, 11.5 mM glucose, and 1 mM CaCl2). Imaging buffer devoid of $CaCl_2$ was also prepared where needed for store-depletion. 24h after plasmid transfection, the cells were incubated with 5 µM Fura-2 for 30 minutes at RT, followed by de-esterification for 30 minutes at RT. Time-lapse images were recorded on a Nikon Ti-2 microscope using a 40X oil immersion objective. Cells were excited alternatively at 340 nm and 380 nm every 2 seconds for 16 minutes and the fluorescence emission was collected at 525 nm. The first minute of time-lapse was used to obtain baseline calcium level. 10 µM thapsigargin in calcium-free imaging buffer was added after 1 minute to induce store-depletion. After an additional 7 minutes, the buffer was replaced with calcium-replete imaging buffer with thapsigargin to measure calcium entry. The ratio of fluorescence at 340 to 380nm was used to quantify cellular calcium levels. Cells that did not respond to thapsigargin were excluded from our analyses. Peak entry was calculated by subtracting maximum fluorescence ratio (Rmax) after calcium addback from fluorescence ratio at time 0 (R_0) and normalized to R_0.

Total Internal Reflection Fluorescence Imaging (TIRF)

Cells were seeded on poly-L-lysine coated coverslips 2 days before TIRF imaging. Cells were transfected with WT or ΔF233 DHHC21-eGFP, WT STIM1-mRFP, and WT Orai1-Myc using Lipofectamine 3000 following manufacturer's protocol. A Nikon Eclipse Ti microscope equipped with TIRF illumination system was used for imaging. Coverslips were mounted on Attofluor chambers with imaging buffer replete with calcium for live imaging using a 60x oil-immersion TIRF objective. Cells were alternatively excited at

488nm and 561nm lasers every 5 seconds. The first minute of the recording was used to obtain baseline colocalization levels. The images were obtained for a duration of 8 minutes. After 1 minute, the imaging buffer was replaced with 10 μM thapsigargin in calcium-free imaging buffer. Cells that had puncta prior to store depletion or those that showed high colocalization in resting state were excluded from analysis. Colocalization analysis was performed using Nikon NIS Elements software. Using regions of interests around cells, we obtained Pearson's correlation coefficients between both channels for the entire time series. We normalized correlation coefficients to time zero by diving correlation coefficient at a given time (Rn) by time zero (R_0). These values were used to plot the colocalization time curve. Peak colocalization was calculated by subtracting peak colocalization after TG addition (Rmax) from colocalization just before TG addition (R_{60}) and dividing the difference to R_{60}. ((Rmax-R_{60})/R_{60}).

Confocal Imaging

DHHC21-KO cells plated on coverslips and transfected with WT and ΔF233 versions of DHHC21-eGFP were used for confocal imaging. The cells were imaged using the confocal mode on the STEDYCON microscope described above using 100x oil objective. Identical exposure parameters were used to obtain images from WT and F233 DHHC21 expressing cells.

Results

DHHC21 is Required STIM1 S-Acylation

We have previously shown that CRAC channel components Orai1 and STIM1 are S-acylated [245, 246] . *Depilated* mice an in-frame deletion of phenylalanine 233 (ΔF233)

residue in the C-terminal tail of DHHC21 that eliminates calmodulin binding [252]. This mutation leads to deficits in TCR signaling and T cell differentiation indicating a loss of function. We determined if *depilated* DHHC21 mutant mice has deficits in STIM1 S-acylation *in vivo*. We harvested spleens from wild-type and *depilated* mice and performed acyl-RAC. We found that STIM1 has significantly reduced S-acylation in *depilated* mice spleens (Fig 1A & 1B). We confirmed these results in cells transfected with WT and ΔF233 FLAG-tagged DHHC21 (Fig 1C). These results indicate DHHC21 is the primary PAT for STIM1 *in vitro* and *in vivo*.

DHHC21 is Required for Store-Operated Calcium Entry

We next examined SOCE in splenocytes obtained from depilated mice (Fig 2A). As shown in Fig 2B, C, & D, depilated mice have significantly higher baseline cytosolic calcium levels, lower ER calcium stores, and decreased calcium entry upon store-depletion. We generated a DHHC21 knockout HEK293 cell line to determine the role of DHHC21 in SOCE and confirmed a complete loss of expression (Fig 3A). DHHC21 knockout cells have significantly reduced SOCE induced by thapsigargin (Fig 3 B & C). We rescued DHHC21 KO cells with WT and ΔF233 DHH21. Expression of WT, but not ΔF233, rescued SOCE in DHHC21 KO cells (Fig 4A). The calcium entry deficits found in depilated mice splenocytes correlated with those observed in DHHC21-KO cells transfected with WT and ΔF233 DHHC21 (Fig 4 B, C, & D). We conclude that DHHC21 is required for SOCE, and the *depilated* ΔF233 results in a loss of DHHC21 function.

Co-Localization of WT and ΔF233 DHHC21 with STIM1

We performed TIRF imaging to determine if DHHC21 associates with STIM1 upon store depletion. We co-transfected with either WT or ΔF233 DHHC21, STIM1-mRFP, and

Orai1-Myc into DHHC21 KO cells. As shown in Fig 5A, and B, store depletion leads recruitment of WT DHHC21 into STIM1 puncta. We observed a significantly higher peak colocalization of ΔF233 DHHC21 compared to WT DHHC21 (Fig 5C). These results indicate that ΔF233 DHHC21 expresses and is trafficked to the plasma membrane, however it is bound to STIM1 at much higher levels under resting conditions and after store depletion (Fig 5A). To confirm this finding in splenocytes, we performed superresolution imaging on splenocytes obtained from WT and *depilated* mice. We treated splenocytes *in vitro* with anti-CD3 antibody to activate TCR signaling and SOCE prior to fixation and staining for DHHC21 and STIM1. As shown in Fig 6, we see a significantly higher colocalization between DHHC21 and STIM1 in splenocytes treated with anti-CD3. The co-localization of DHHC21 and STIM1 in *depilated* mice was even more pronounced, correlating with our results in the DHHC21 KO model. We also performed co-immunoprecipitation on splenocytes from WT and *depilated* mice to determine the binding between DHHC21 and STIM1. As shown in Fig 6E, immunoprecipitating with DHHC21 shows a higher binding with STIM1 in *depilated* cells compared to WT. Together, these results indicate ΔF233 DHHC21 can still bind its substrate STIM1, but presumably cannot release STIM1 because of an inability to transfer a lipid group the protein.

Discussion

S-acylation plays a crucial role in store-operated calcium by modifying the localization and activity of Orai1 and STIM1. Previously, we have shown that both Orai1 and STIM1 undergo S-acylation upon store-depletion [245, 246]. S-acylation directs these proteins to membrane subdomains where they form CRAC channels to promote SOCE. Cysteine

mutant versions of these proteins that cannot undergo S-acylation show deficits in SOCE. Previously, another group demonstrated that DHHC20 S-acylates Orai1 [265]. In this work, we show DHHC21 is the PAT that S-acylates STIM1 upon store-depletion. We also show that mutant version of DHHC21 that is functionally deficient cannot S-acylate STIM1 and shows impaired SOCE. It remains to be determined whether Orai1 can be S-acylated by DHHC21, or whether two different PATs are required for SOCE after store depletion.

DHHC21 is a plasma membrane localized palmitoyl acyltransferase. We have shown previously that DHHC21 plays a key role in S-acylation of many proteins involved in T cell receptor signaling. TCR components such as PLC-y1, Lck, and ZAP-70 undergo S-acylation upon treatment with anti-CD3 which activates the T cell receptor [253]. We have previously shown that shRNA-mediated knockdown of DHHC21 or CD4+ T cells isolated from *depilated* mice prevented the S-acylation of these proteins and downstream signaling events, which indicates DHHC21 plays a prominent role in TCR signaling [252]. This was a basis for our hypothesis that DHHC21 might mediate S-acylation of STIM1. The S-acylation of STIM1 by PM-localized DHHC21 strongly suggests that S-acylation of the STIM1 tail stabilizes its association with the plasma membrane. The polybasic domain of STIM1 has been shown to interact with the membrane phospholipids such as $PI(4,5)P_2$ and physically bind to the plasma membrane [178]. In addition, the Isoleucine 384 (I384) in the cholesterol binding domain in the SOAR/CAD domain of STIM1 has been shown to also bind to the plasma membrane upon store-depletion using thapsigargin [164]. This interaction was shown to enhance SOCE. Together, these domains stabilize the active conformation of STIM1. An overview of the role of

DHHC21 in SOCE is depicted in Figure 7. S-acylation is rapidly reversible after TCR ligation, suggesting a mechanism by which STIM1 can be inactivated after calcium entry through the action of acyl-protein thioesterases.

We find in our experiments that DHHC21 is crucial for SOCE. This was observed in DHHC21-KO HEK293 cells which show decreased overall calcium entry as well as lower peak calcium entry. This is even more stark in splenocytes obtained from WT and depilated mice. Splenocytes obtained from depilated mice show both higher baseline cytosolic calcium levels as well as reduced peak entry. We hypothesize that the inability of these depilated splenocytes to respond to TCR stimulation has helped these cells to sequester calcium through other mechanisms that are poorly controlled, which leads to this abnormal basal calcium levels. The residual entry observed in these cells may be due to the action of other PATs such as DHHC20. However, we observe a nearly complete loss of STIM1 S-acylation in spleens from *depilated* mice. Further experiments are warranted to determine the mechanism(s) by which SOCE is partially retained in *depilated* splenocytes.

Compared to WT DHHC21, we observed increased association between DHHC21-ΔF233 and STIM1 upon store-depletion using thapsigargin as well as ligation of splenocytes with anti-CD3. This was a somewhat unexpected finding. We hypothesize that DHHC21-ΔF233 is still competent to bind substrate (including STIM1), but it can no longer release the substrate because of a lack of enzymatic activity. Future work will evaluated this hypothesis using a reconstituted enzyme assay system we developed for DHHC5 [315].

Acknowledgements

We thank David Holowka and Barbara Baird (Cornell University) for the gift of the STIM1-mRFP plasmid. We wish to thank the members of the Boehning and Akimzhanov labs for many helpful discussions.

Funding

This work was supported by startup funding from Cooper Medical School of Rowan University (to D.B.) and National Institute of General Medical Sciences grant R01GM130840 (to D.B. and A.M.A.).

Data Availability

All data supporting this study are available from the corresponding authors upon request.

Figures

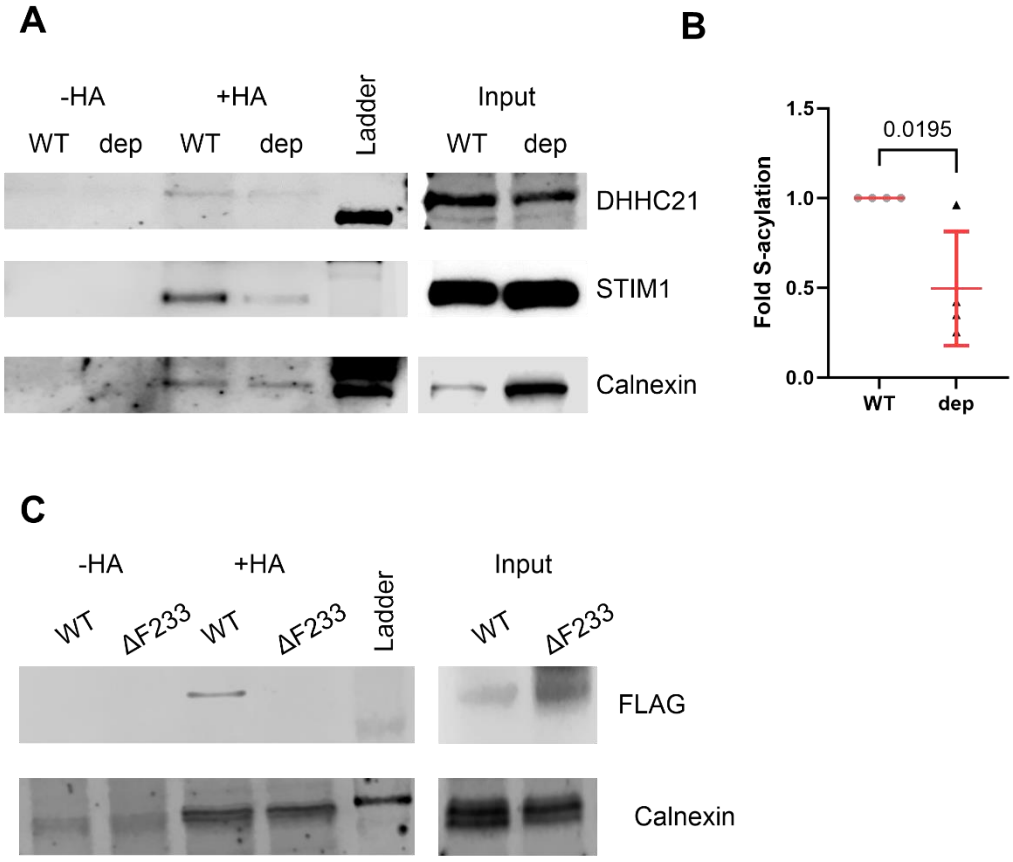

Figure 4.1. DHHC21 is the STIM1 protein acyltransferase. A) Spleens from C57BL6F1/J WT and *depilated* homozygous mice were collected, and acyl-RAC was performed. B) Quantification of fold S-acylation of STIM1 normalized to Calnexin from A. C) WT and F233 DHHC21-FLAG plasmids were co-expressed along with WT STIM1-mRFP, and WT Orai1-Myc in DHHC21-KO cells and acyl-RAC was performed as described in the methods section. -HA was used as a control and +HA was used for detecting S-acylation. Calnexin serves as both positive control as well as loading control. Statistical significance between the groups was calculated using student's t test. Error bars indicate S.D.

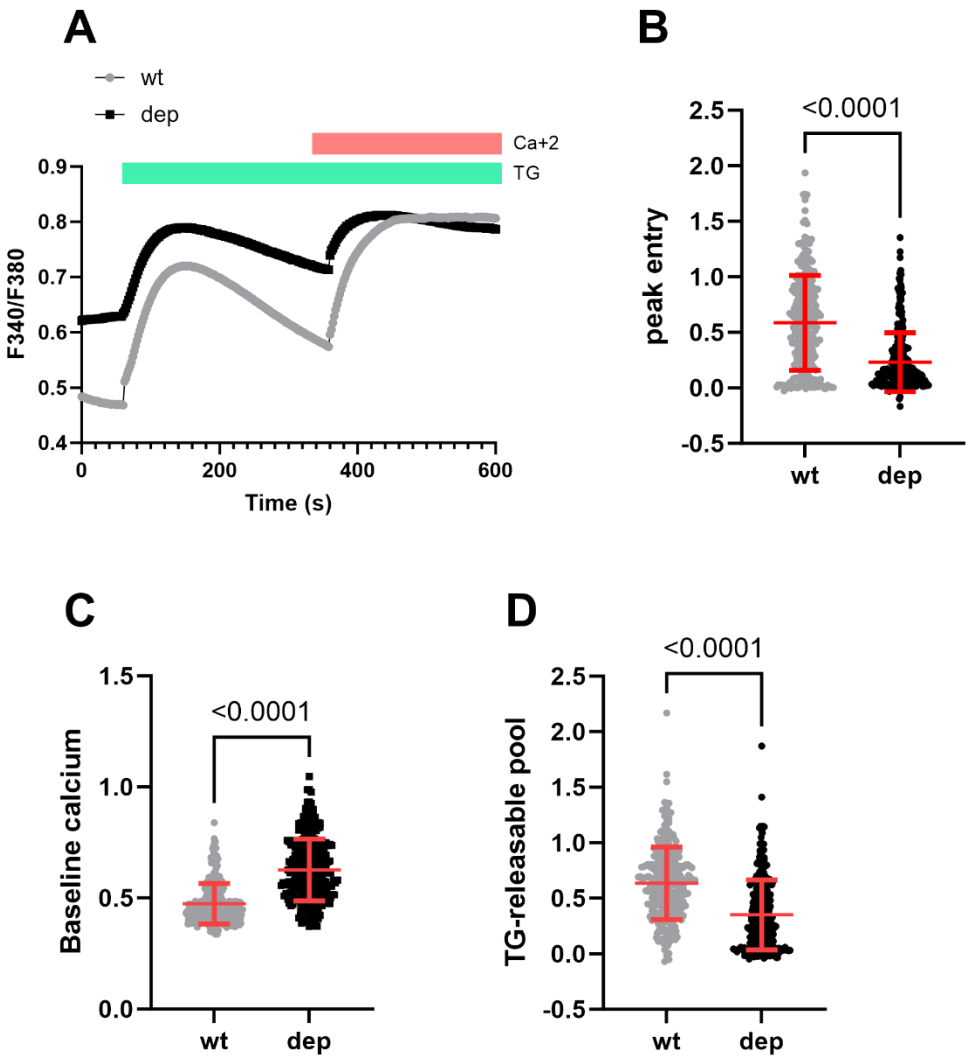

Figure 4.2. Depilated splenocytes show abnormal SOCE. A) Splenocytes were collected from C57BL6 WT and *depilated* homozygous mice and were used for Fura2 imaging using 10 µM thapsigargin (TG) for store-depletion and 1 mM calcium addback. F340/F380 ratios were used to quantify calcium levels in these cells. Baseline calcium levels, peak release, and peak entry was calculated from these F340/F380 values as described in the methods section. Statistical significance between the groups was calculated using student's t test. Error bars indicate S.D.

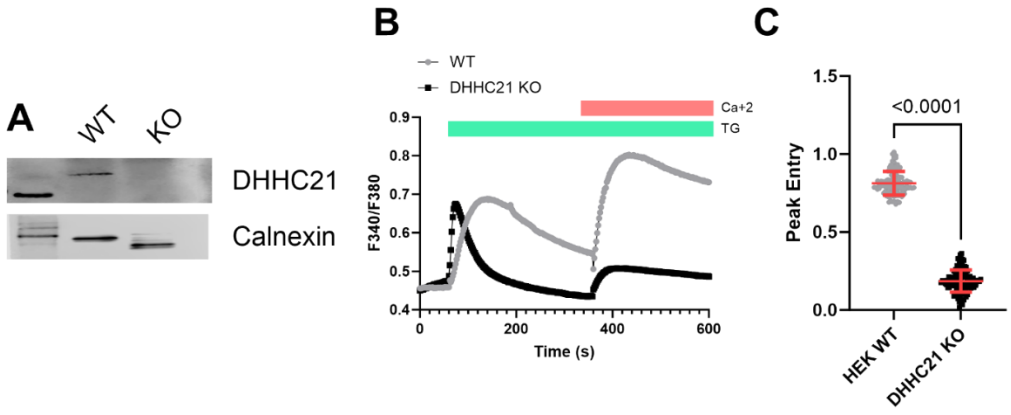

Figure 4.3. DHHC21 KO cells have impaired SOCE. CRISPR knockout HEK293 cells were generated and validated using Western blotting as well as Fura2 imaging. A) Western blotting was performed on whole cell lysates obtained from WT and DHHC-KO cells and probed for DHHC21 and calnexin. B) Fura2 imaging was performed on HEK WT and DHHC-KO cells as described in the methods. 10 µM thapsigargin (TG) in calcium free buffer was used to deplete ER calcium stores. 1 mM calcium was added back after 6 minutes to induce calcium entry. C) Peak calcium entry in WT and DHHC21 KO cells. Statistical significance between the groups was calculated using student's t test. Error bars indicate S.D.

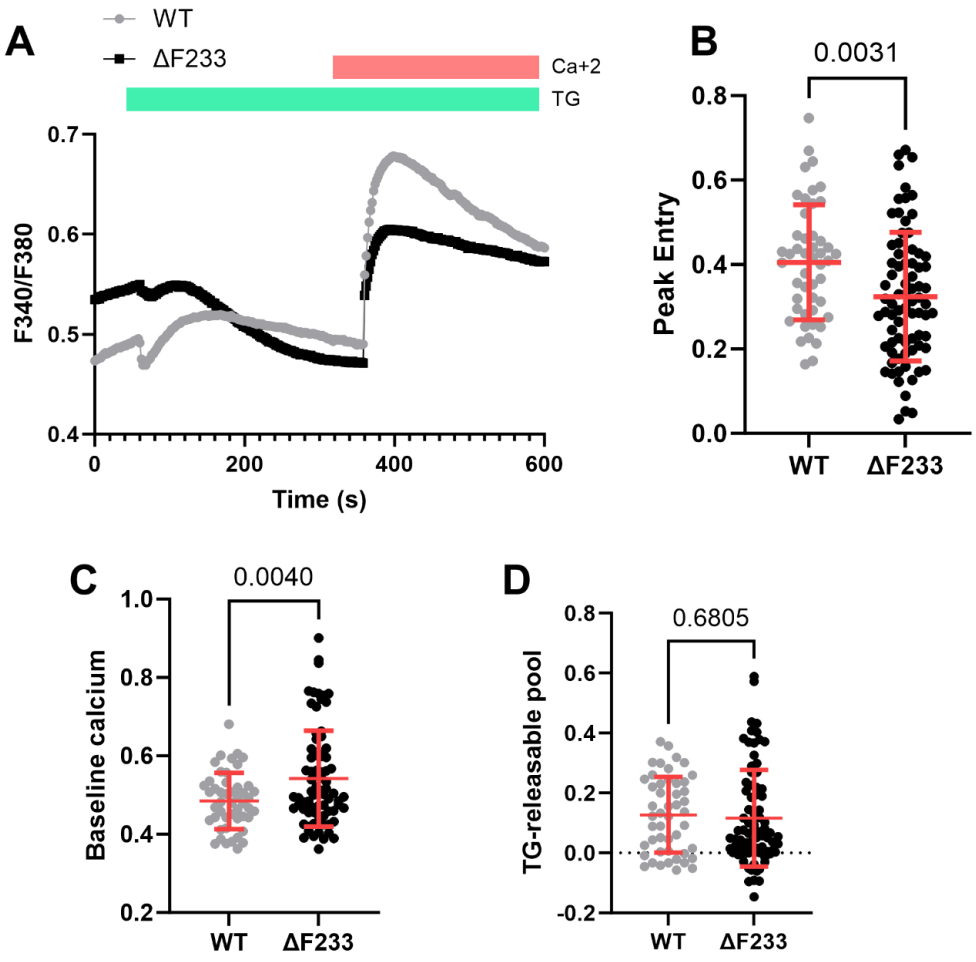

Figure 4.4. DHHC21-ΔF233 expression leads to a reduction in SOCE. WT or ΔF233 DHHC21-eGFP was co-expressed with STIM1-mRFP and Orai1-Myc in DHHC21-KO cells. A) Fura2 imaging was performed on these cells as described in the methods section. 10 µM thapsigargin (TG) in calcium free buffer was used to deplete ER calcium stores. 1 mM calcium was added back after 6 minutes to induce calcium entry. C, D, & E) Peak calcium entry, baseline calcium, and TG-releasable calcium pool was quantified WT and ΔF233 cells. Statistical significance between the groups was calculated using student's t test. Error bars indicate S.D.

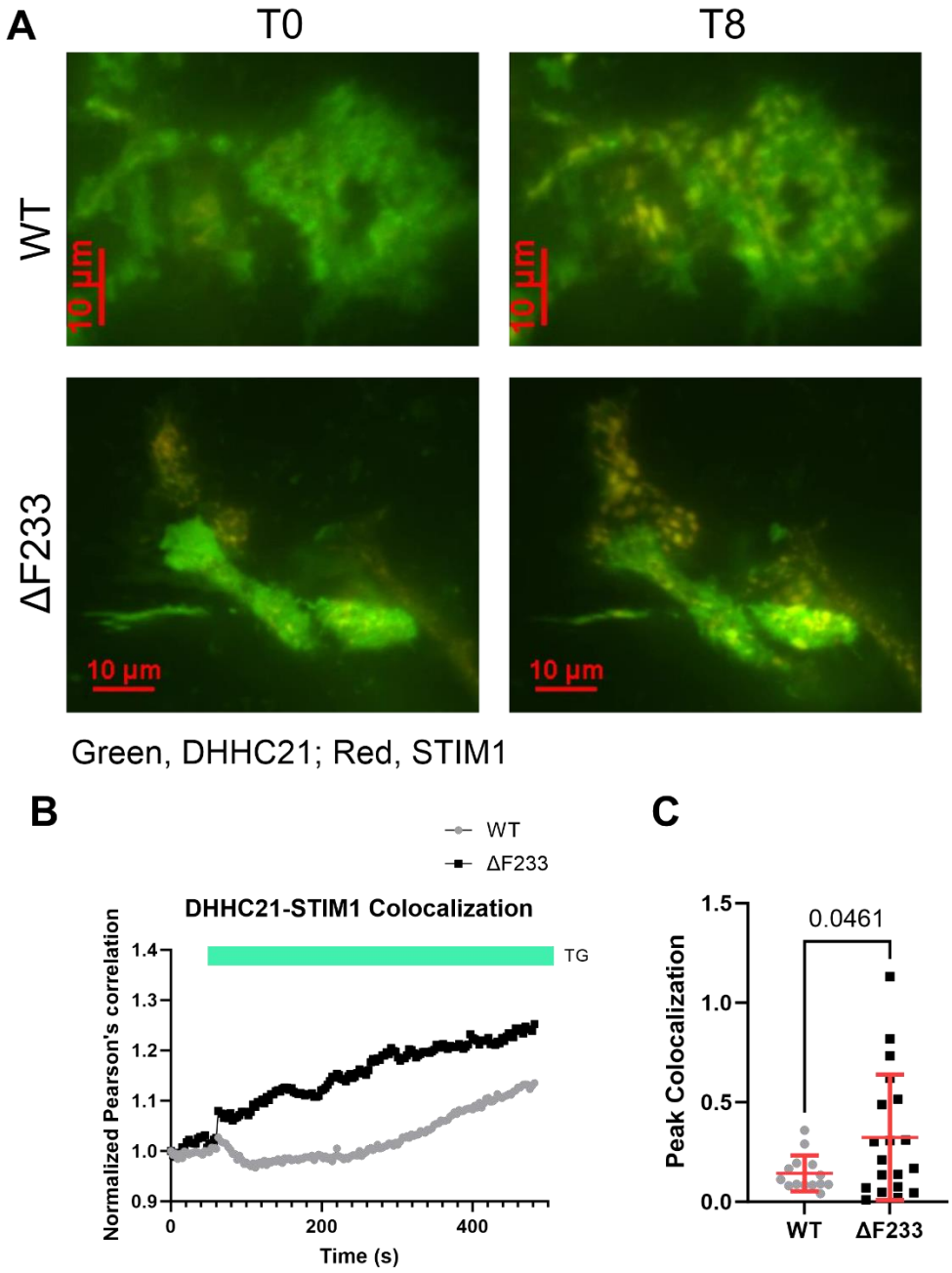

Figure 4.5. DHHC21-ΔF233 shows increased colocalization with STIM1 upon store-depletion. DHHC21-KO HEK293 cells were transfected with WT or ΔF233 DHHC21-eGFP, STIM1-mRFP, and Orai1-Myc plasmids, and store-depletion was induced using 10 µM thapsigargin (TG). Time-lapse images were recorded on TIRF as outlined in the methods section. A) Representative frames from the time lapse at time 0 and time 8 min are shown. C) Peak colocalization was quantified using Pearson's correlation values obtained from WT and ΔF233 expressing cells. Statistical significance between the groups was calculated using student's t test. Error bars indicate S.D.

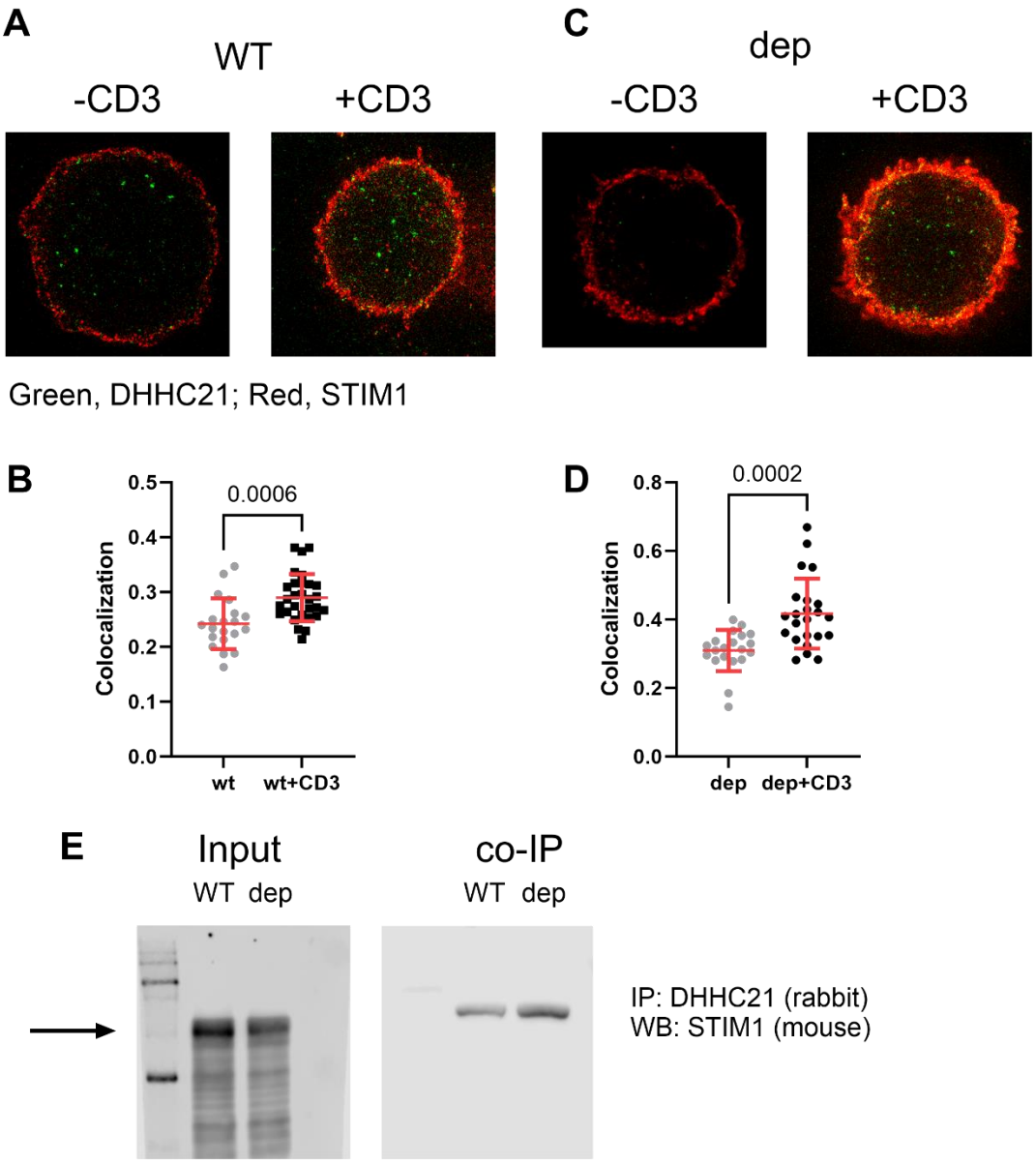

Figure 4.6. DHHC21 colocalizes with STIM1 in *depilated* splenocytes. Splenocytes were obtained from C57BL6F1/J WT and *depilated* homozygous mice and used for STED imaging and co-immunoprecipitation as detailed in the methods. A & C) Superresolution images of the splenocytes were used for Pearson's correlation analysis using ImageJ JACoP plugin. B & D) Pearson's correlation between DHHC21 and STIM1 obtained from A & C using JACoP plugin were analyzed using a student's t test. Error bars indicate S.D. E) Co-immunoprecipitation of STIM1 by DHHC21 from WT and *depilated* splenocytes. Arrow shows approximate molecular weight of STIM1 (~85 KDa).

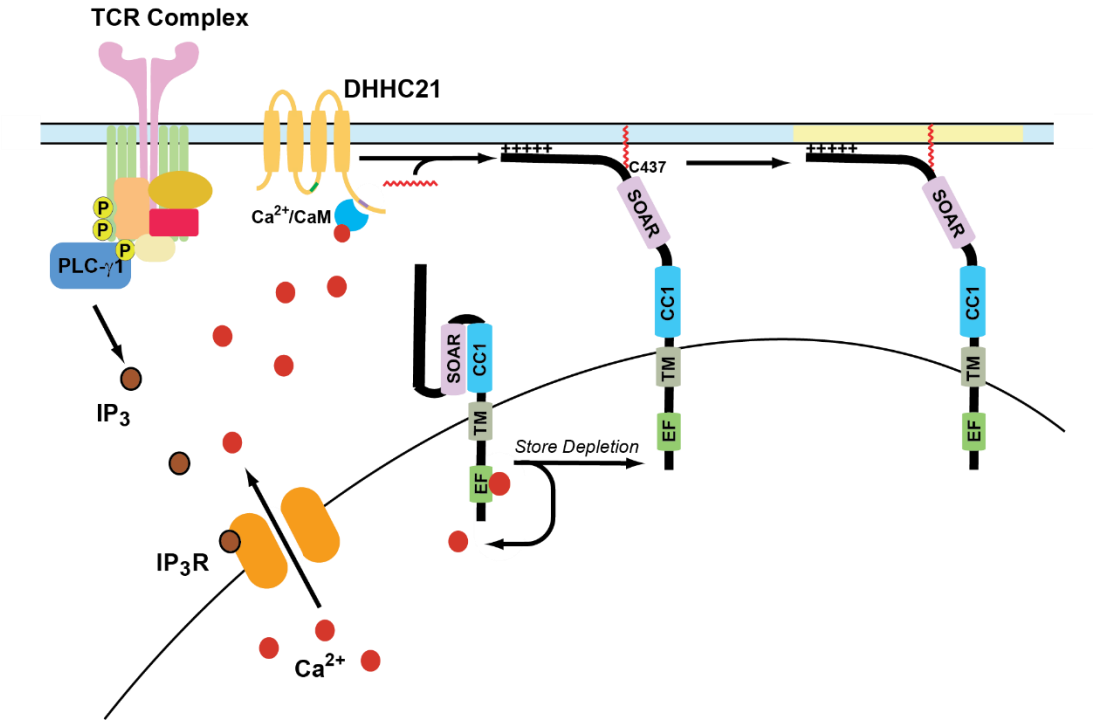

Figure 4.7. DHHC21 regulates SOCE by S-acylating STIM1. DHHC21 is a PM-resident palmitoyl acyltransferase which mediates S-acylation of STIM1. Activation of TCR complex leads to phosphorylation of PLCy1, which hydrolyses membrane phospholipids into IP_3 and diacylglycerol (DAG). IP3 then binds to IP_3 receptor (IP_3R) calcium channels which promote calcium release from the ER into the cytosol leading to store-depletion. The calcium released from the ER binds to the calmodulin (CaM) binding domain in DHHC21 and activates it. DHHC21 then catalyzes the S-acylation of STIM1 which recruits STIM1 to lipid rafts where it binds to and activates Orai1 channels to promote SOCE. One subunit of STIM1 dimer is presented here for simplicity.

Chapter 5

S-Acylation of SOCE-Associated Regulatory Factor Regulates Store-Operated Calcium Entry

Introduction

SARAF was initially discovered as an accessory protein bound to STIM1 in resting conditions, preventing its spontaneous and spurious activation [227, 230, 231]. SARAF is a single pass transmembrane ER protein that is found to be bound to C terminal inhibitory domain (CTID) of STIM1 in resting conditions. SARAF is an ER protein that interacts with the STIM1-Orai1 activating region (SOAR) domain of STIM1. Upon store depletion, the C-terminal inhibitory domain of STIM1 undergoes a conformational change that allows SARAF to dissociate from STIM1 [230]. This facilitates the translocation of the CRAC channels to specialized plasma membrane subdomains to form puncta. SARAF then binds to Orai1 in these subdomains to promote slow calcium-dependent inactivation [231]. SARAF may also have a role in immune responses and cardiac angiogenesis [316]. Another important function of SARAF is maintaining ER calcium concentration to prevent calcium overfilling after store depletion. Some reports also show siRNA-based knockdown of SARAF leads of perturbations in levels of cellular and ER calcium stores [317]. Most of the current knowledge about SARAF comes from a limited number of studies that focus on STIM1 and Orai1 in SOCE and not directly on SARAF. Some reports have also found that overexpression of SARAF protects mice from pressure overload induced cardiac hypertrophy [318, 319]. It is not known if S-acylation of SARAF plays a role in this process, but these reports show this effect is mediated through the interaction with Orai1 and STIM1. We hypothesized that SARAF

undergoes S-acylation upon store-depletion, which recruits it to CRAC puncta where it promotes slow calcium dependent inactivation.

Results and Discussion

To investigate the potential importance of SARAF S-acylation in SOCE, we followed a similar approach as shown in previous chapters on Orai1 and STIM1. We first developed a CRISPR knockout of SARAF in HEK293 cells using an all-in-one vector, which consists of the sgRNA against SARAF (ACCGCTATACCACCTCCCGC and CTGGGATGGGTATGATGTAC), eSpCas9, and GFP fluorescence protein for fluorescence-based sorting. We transfected the HEK293 cells with two different sgRNAs and selected GFP positive cells using Bio-Rad S3 cell sorter. The sorted cells were then serial diluted into 96 well plates. We picked single cell colonies and then analyzed for SARAF expression using western blotting and calcium imaging. From the data obtained, we selected one colony and used it for subsequent analysis. For DHHC enzymes to S-acylate their substrates, they need a cytosolic cysteine on the substrate. Based on the current structure available for SARAF, there is only one cytosolic cysteine (C320). We mutated this cysteine to a serine (C320S) using site-directed mutagenesis and used it to determine the role of S-acylation of SARAF on SOCE. For all other experiments, we used similar methods as chapters 1 and 2.

SARAF Undergoes S-Acylation Upon Store-Depletion

Based on S-acylation of Orai1 and STIM1, we hypothesized SARAF undergoes dynamic S-acylation upon store-depletion. We used Jurkat T cells and activated them using treatment with anti-CD3 to activate the T cell receptor. We performed acyl-resin assisted

capture (acyl-RAC) on cell lysates obtained from the activated T cells to determine if SARAF undergoes S-acylation. We found SARAF undergoes S-acylation as shown in Fig 1. The level of S-acylation peaks around 5 minutes (Fig 1B) after treatment with anti-CD3, which is consistent with the kinetics of S-acylation of both Orai1 and STIM1. To determine the specific residue where SARAF undergoes S-acylation, we performed acyl-RAC on SARAF KO cells. S-acylation can only occur on cytosolic cysteine residues. Based on this information, SARAF can be S-acylated only at C320 residue, as only this residue is exposed to the cytosol based on the currently available structure information. We substituted this cysteine to a serine using site-directed mutagenesis. We transfected SARAF KO cells with the WT and C320S plasmids and performed acyl-RAC on the cells after inducing store-depletion with thapsigargin. As shown in Fig 1C, C320S shows lower S-acylation levels compared to WT. These data show that SARAF undergoes stimulus-dependent S-acylation at its C320 residue.

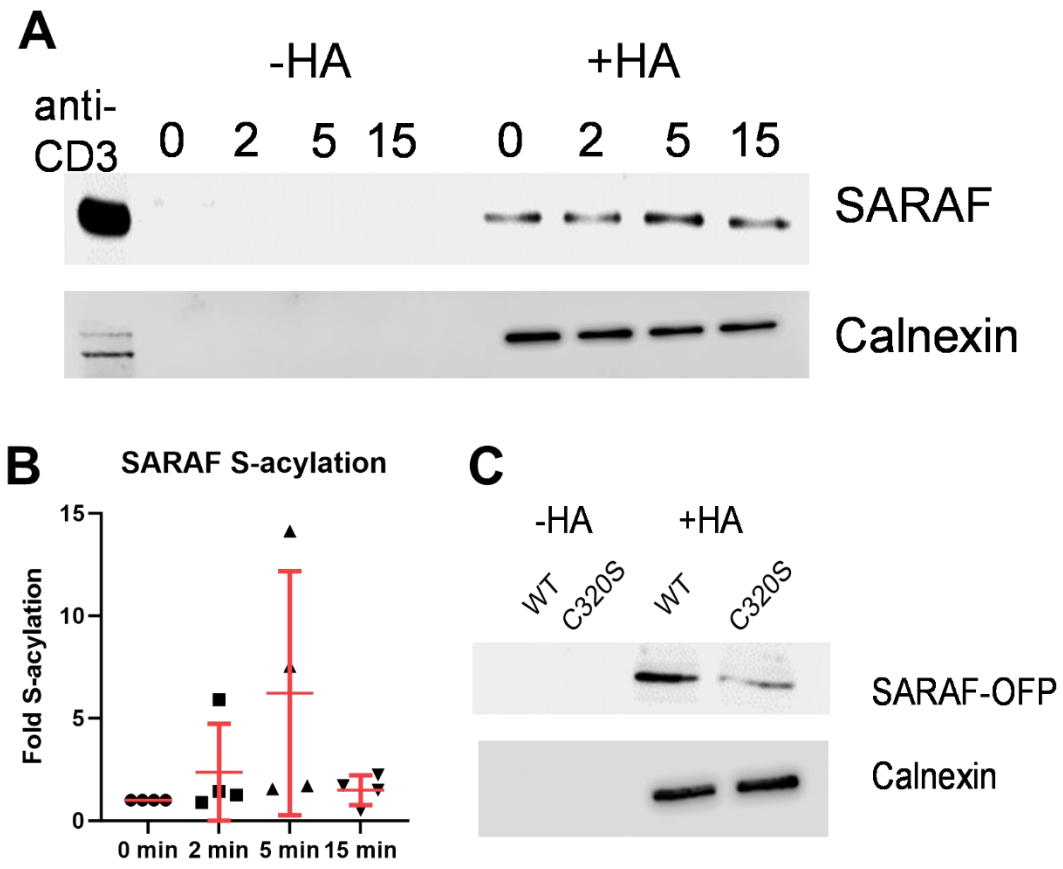

Figure 5.1. SARAF undergoes S-acylation at C320 residue. A) Jurkat T cells were treated with anti-CD3 antibody for 0, 2, 5, and 15 minutes and subjected to acyl-RAC. The reaction without hydroxylamine (-HA) serves as a negative control. Representative of n=3. B) Quantification of fold change of S-acylation of STIM1 normalized to calnexin. Error bars indicate S.D. C) HEK SARAF knockout (SARAF-KO) cells were transfected with WT or C320S SARAF-OFP and acyl-RAC was performed. The blots are representative of three independent experiments. Calnexin was used as both positive control for S-acylation as well as a loading control.

SARAF Knockout in HEK293 Cells Affects Basal Cytosolic Calcium Levels

To accurately assess the role of SARAF in cellular cytosolic calcium levels, we knocked out SARAF in HEK293 WT cells using CRISPR-Cas9 mediated genetic deletion. We used an all-in-one plasmid-based transfection method which carries the sgRNA against SARAF (ACCGCTATACCACCTCCCGC and CTGGGATGGGTATGATGTAC),

eSpCas9 enzyme, and eGFP as a selectable marker in a single plasmid. We confirmed SARAF knockout using western blotting and Fura-2 calcium imaging (Fig 2A). As shown in Fig 2B-C, knockout of SARAF leads to impaired basal calcium levels as well SOCE. The SARAF-KO cells also show higher peak entry than HEK293 WT cells (Fig 2D). The role of SARAF in basal calcium levels was also confirmed by an independent group who silenced SARAF using shRNA [317]. We believe SARAF controls the basal cytosolic calcium levels by preventing spontaneous activation of STIM1. This needs to be evaluated further using experiments between STIM1 and SARAF. Increased peak entry and baseline calcium levels in SARAF KO cells show that SARAF plays a significant role in promoting SOCE.

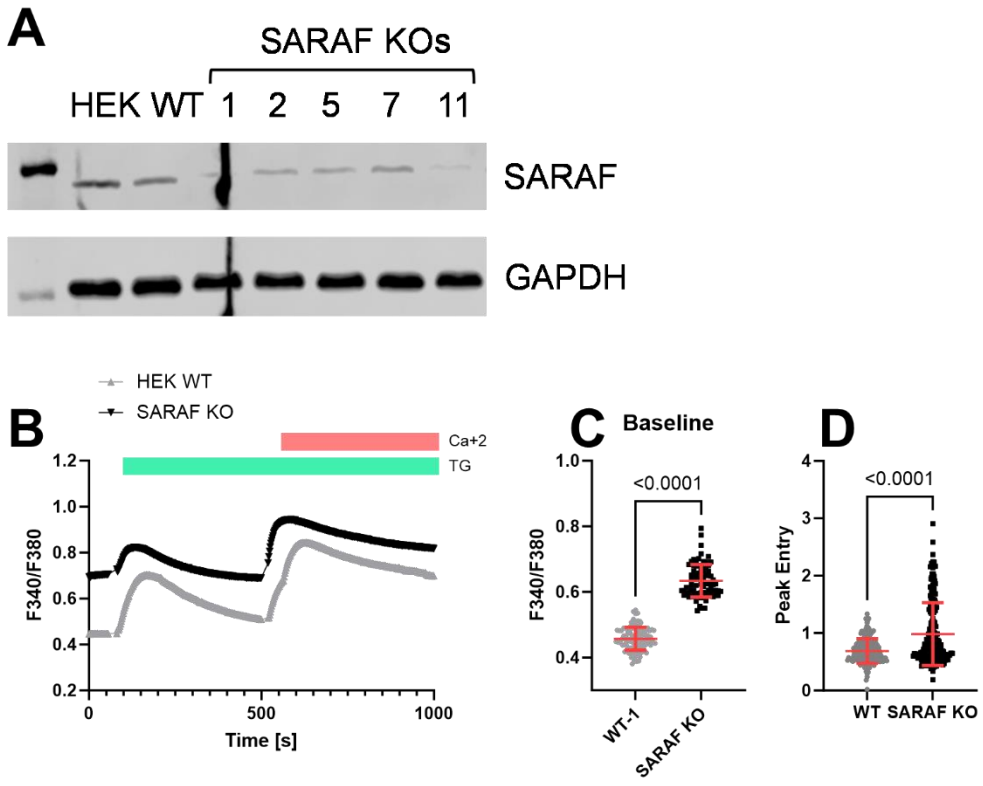

Figure 5.2. SARAF CRISPR knockout affects ER calcium levels and SOCE. SARAF CRISPR knockout was carried out in HEK293 cells using all-in-one plasmids obtained

from Genscript with sgRNA targeting SARAF, Cas9 protein, and eGFP for selection. ACCGCTATACCACCTCCCGC and CTGGGATGGGTATGATGTAC are the are the two sequences used. A) Whole cell lysates were collected from HEK293 SARAF-KO clones as indicated and were analyzed using western blotting. GAPDH was used as internal control. Clone 5 was selected for calcium imaging. B, C & D) Fura2 imaging was performed on clone 5 using thapsigargin mediated store-depletion paradigm. Baseline was calculated from the initial 60 seconds of recording. Peak entry was calculated using peak Fura2 ratio after calcium addback. Error bars indicate SD. $P<0.001$

SARAF C320S Shows Impaired SOCE

To determine the role of S-acylation of SARAF on SOCE, we transfected SARAF KO cells with the WT and C320S plasmids and performed Fura2 imaging on these cells after inducing store-depletion with thapsigargin. As shown in Fig 3A, C320S transfected cells show a significantly higher calcium entry upon store-depletion using thapsigargin. The C320S transfected cells also show higher baseline calcium levels as shown in Fig 3B. The peak entry observed in SARAF-C320S transfected cells is also significantly higher than the cells transfected with WT SARAF (Fig 3C).

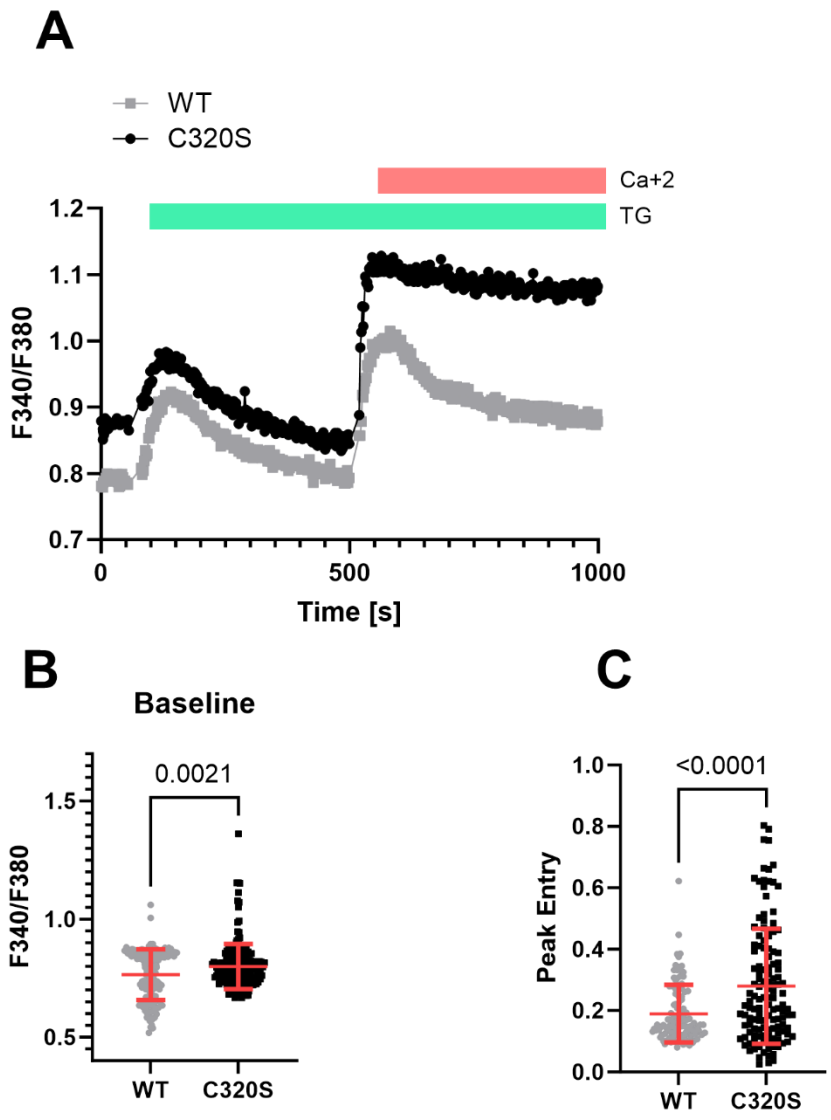

Figure 5.3. S-acylation of SARAF regulates store-operated calcium entry and peak calcium entry**.** A) HEK293 SARAF-KO cells were transfected with WT or C320S SARAF-OFP and were subjected to fura2 imaging using store-depletion paradigm. Representative single cell traces from n=3. B) Quantification of baseline from first 60 seconds of recording from A. C) Quantification of Peak entry from A. Error bars indicate SD. $p<0.001$

SARAF Colocalizes to CRAC Puncta Upon Store Depletion

We also performed TIRF imaging on the SARAF-KO cells transfected with WT SARAF-GFP and WT STIM1-mRFP to determine if SARAF colocalizes to CRAC puncta. We induced store-depletion in these cells using thapsigargin in calcium free media. As shown in Fig 4, store-depletion led to rapid and stimulus-dependent colocalization between STIM1 and SARAF. Addback of calcium in these cells increases the colocalization further (Fig 4B). This data, for the first time, shows stimulus-dependent translocation of SARAF to CRAC puncta.

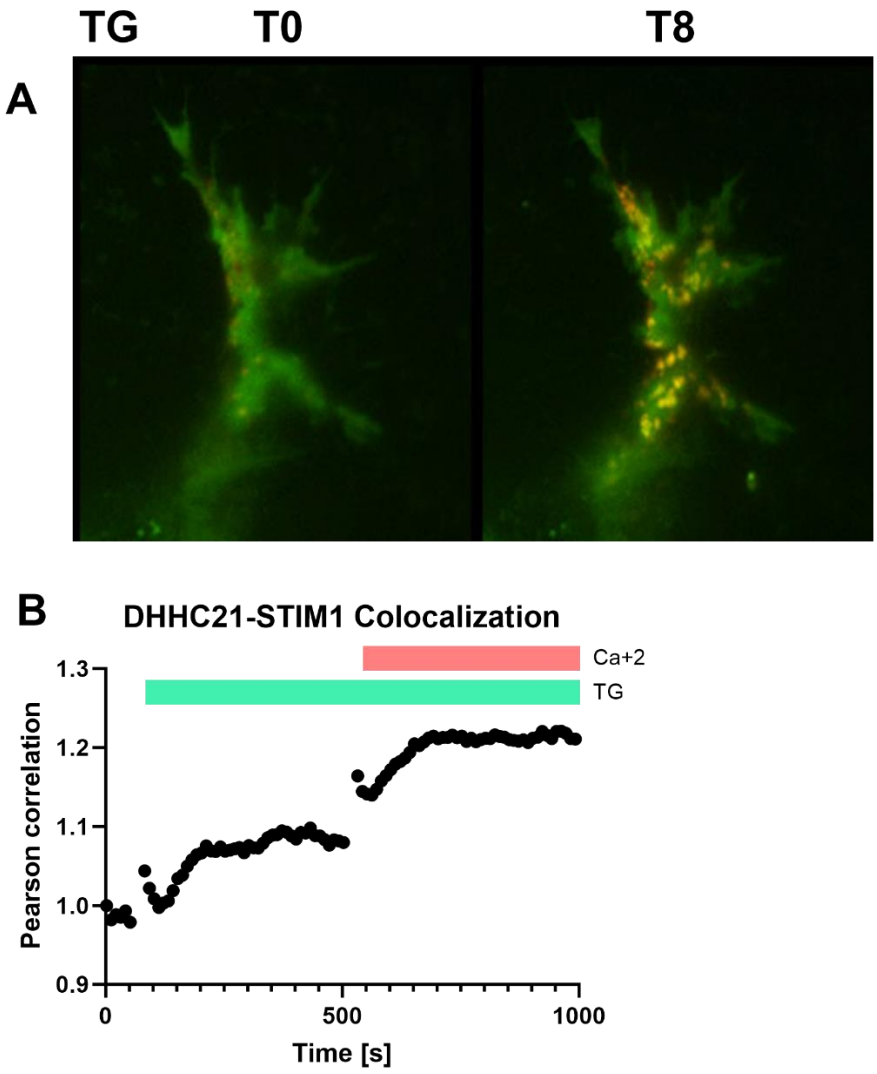

Figure 5.4. SARAF is recruited into CRAC puncta. A) HEK293 STIM DKO cells transfected with Orai1-Myc, STIM1-mRFP, and SARAF-GFP imaged using TIRF microscopy shows recruitment of SARAF in puncta after store depletion using thapsigargin (TG); T0 and T8 represent minutes after TG addition. B) Pearson correlation between STIM1-mRFP and SARAF-GFP was calculated and normalized to T0.

These preliminary experiments on SARAF were quite intriguing and worthy of additional studies. However, this study has faced challenges on many fronts. We show a stimulus-dependent increase of S-acylation of SARAF. However, we could not get a statistically significant increase at any timepoint. We believe the biggest challenge in these set of

experiments is the lack of validated antibodies against SARAF. The current set of antibodies include either polyclonal antibodies against a larger stretch of the protein or monoclonal antibodies generated using peptide sequences, both of which have drawbacks.

We believe S-acylation of SARAF helps its recruitment to the lipid rafts where Orai1 translocates to upon store-depletion. This translocation helps SARAF binding to Orai1 and inactivation of SOCE. We observed that SARAF knockout in HEK293 cells show higher baseline as well as peak calcium entry. SARAF is a predominantly ER-resident protein where it was shown to be bound to STIM1 in resting conditions to keep STIM1 in its inactive state. We believe the increased baseline is due to spurious activation of STIM1 as a result of absence of SARAF. This aberrant and consistent activation of STIM1 probably lead to a persistent calcium entry in these cells which results in higher-than-normal baseline calcium levels. The higher peak entry observed in these cells is due to the lack of slow-calcium dependent inactivation, which is mediated by SARAF binding to Orai1. The higher peak entry observed in SARAF-C320S transfected SARAF-KO cells is due to lack of S-acylation of SARAF.

Finally, we show SARAF is recruited to CRAC puncta upon store-depletion. This is the first time it's been shown that this protein can show stimulus-dependent translocation toward plasma membrane. We show this translocation using TIRF imaging done on STIM DKO cells transfected with STIM1-mRFP and SARAF-GFP. However, we were not able to determine the role of S-acylation of SARAF on its recruitment to CRAC puncta. From our Fura-2 calcium imaging data, we hypothesize the cysteine mutant of

SARAF will show a phenotype that shows impaired translocation, but it is yet to be determined. We hope to continue to investigate SARAF function in the future.

Chapter 6

Conclusions and Future Directions

Conclusions from Orai1, STIM1, and DHHC21 Projects

Since the discovery of store-operated calcium entry, questions have lingered on how this important mechanism is regulated. Orai1 and STIM1 from spatially distinct subcellular localization fuse together near the ER:PM junctions to form CRAC channels and promote calcium entry [7, 21, 174]. The ER resident STIM1 and PM resident Orai1 move to these junctions independently of each other to facilitate the calcium entry [18]. As we outlined earlier, many hypotheses were proposed to explain this complicated process. All these hypotheses have fallen short in explaining crucial aspects observed in how these proteins could shuttle between membrane subdomains. We proposed and showed some evidence for S-acylation to play a role in the formation and CRAC channels. Recently, we also found new evidence for DHHC21, a PM-resident palmitoyl acyltransferase, to regulate SOCE.

Our hypothesis that S-acylation plays a role in store-operated calcium entry was derived from the inability of current models to explain the specific characteristics that make this process unique. As explained earlier in the review, Orai1 and STIM1 proteins show distinct features upon store-depletion, such as decreased mobility in the membrane, targeting to membrane subdomains, and dynamic nature of CRAC puncta, among other observations [158, 184, 244]. We based our hypothesis that S-acylation, being a process that is controlled by a set of enzymes, gives a dynamic control to Orai1 and STIM1 function.

Orai1 undergoes S-acylation at residue C143 in the TM2-3 intracellular loop on the cytosolic side of the plasma membrane [245, 265]. How S-acylation of Orai1 regulates SOCE can be explained by the phenotype observed in the cysteine mutant version of Orai1, Orai1-C143S. As shown in Chapter 1, the S-acylation deficient C143S mutant of Orai1 shows a complete lack of calcium entry upon store depletion. In addition, this mutant also cannot form CRAC puncta with STIM1. A recent investigation into the S-acylation of Orai1 by an independent group confirmed some of our findings. They also reported that the cysteine mutant Orai1 loses its ability to localize to lipid rafts [265]. The conclusion from our study was that the cysteine mutant loses its ability to recruit to STIM1 in the specialized subdomains in the plasma membrane. Taken together, the data suggest that S-acylation targets Orai1 to membrane microdomains, such as lipid rafts, where it can be activated to allow calcium entry. The requirement of this channel to be in the lipid rafts adds specific context, especially in the case of T cell activation, where the T cell receptor (TCR) engages with many molecular mediators to successfully mount an immune response [130, 306, 310, 320]. These complexes, known as supramolecular activation complexes (SMAC), are arranged in concentric circles around the TCR and are enriched in lipid rafts [247, 248, 305]. Sustained calcium entry through the Orai1 channel is crucial for T cell activation [11, 131, 149, 302]. Hence, the S-acylation of Orai1 probably serves as a gatekeeping mechanism, keeping the channel from activation outside of these lipid rafts.

STIM1 is an ER-resident single-pass protein that has been proposed as the activator of CRAC channels. STIM1 in resting conditions is in a compact folded state, which hides the domains that are required for its binding to Orai1, such as the SOAR/CAD domain,

the polybasic domain, and the coiled-coil domains [173, 176, 183, 188, 297]. This is maintained by calcium binding to the EF-hand motif on its EF-hand motif in the luminal side of the ER [24, 191]. Upon store-depletion, calcium released from the EF-hand causes a conformational change which extends the polybasic domain toward the plasma membrane [178]. Several important interactions happen at these ER:PM junctions to regulate STIM1 binding to Orai1 as well as calcium entry. Firstly, the binding between the polybasic domain of STIM1 with the plasma membrane. The polybasic domain interacts with phosphoinositides in the plasma membrane, mainly phosphatidylinositol 4,5-bisphosphate (PIP_2). This binding stabilizes the binding between the SOAR/CAD domain of STIM1 with the plasma membrane which is mediated by the cholesterol binding domain within this SOAR region. The binding between cholesterol binding domain and plasma membrane facilitates binding between STIM1 and Orai1 at the plasma membrane [164]. Finally, the S-acylation of STIM1, which we have shown is mediated by the PM resident DHHC21 enzyme. We hypothesized that S-acylation of STIM1 in the plasma membrane, in a region adjacent to both the SOAR domain and the polybasic domain, confers the ability to fine tune the calcium entry through Orai1. We observed a partial loss of function phenotype in the cysteine mutant version of STIM1 (STIM1-C437S) [246]. This mutant shows basal calcium entry upon store-depletion, unlike the complete absence observed in the Orai1 cysteine mutant. In addition, this mutant also shows some puncta formation, albeit significantly lower than WT, upon store-depletion. This finding is consistent with the observation in experiments done using Orai and STIM knockout cells lines. STIM1 is capable of forming CRAC puncta independently of Orai1 in Orai triple knock out cells. But Orai1 is incapable of forming

puncta in the absence of STIM1 in experiments done in STIM double knock out cells [246]. Taken together, the data suggests S-acylation of STIM1 probably stabilizes the cytosolic domains of STIM1, SOAR/CAD and polybasic domains, near the plasma membrane, which facilitates the binding of STIM1 with Orai1 to propagate calcium influx.

In addition to Orai1 and STIM1, several other proteins regulate SOCE by performing a multitude of functions such as stabilizing the ER:PM junctions, organizing the microdomains, and calcium dependent inactivation of CRAC channels. These proteins include microtubule associated protein RP/EB family member 1 (MAPRE1) which helps STIM1 targeting toward microtubule plus ends [321], calcium release activated channel regulator 2A (CRACR2A) which binds to STIM1 at low calcium concentrations [322], SOCE-associated regulatory factor (SARAF) which promotes slow-calcium dependent inactivation of SOCE [226], EFHB, which promotes release of SARAF from STIM1 upon store refilling [234], STIMATE, which promotes STIM1 conformation change [323], among others. Of the proteins mentioned above, we were interested in SARAF, also known as TMEM66, for its role in inactivation of SOCE [226, 317]. In our preliminary studies, we found that SARAF undergoes S-acylation in T cells upon their activation, as well as store-depletion using thapsigargin. So, we analyzed the role of SARAF in SOCE using acyl-RAC, Fura-2 calcium imaging, as well as TIRF imaging. Here, we will highlight the unpublished results obtained from these experiments.

Unanswered Questions and Future Directions

Of the many topics not answered in our studies, we want to highlight a few that are more intriguing and necessitate scrutiny. We have discussed the role of DHHC enzymes in S-acylating CRAC channel components, including DHHC20 and DHHC21. But the enzymes that deacylated these proteins have not been studied yet. As explained earlier, S-acylation is reversible. DHHC enzyme S-acylate the target proteins and deacylating enzymes, mostly acyl protein thioesterases (APT) remove the lipid moiety from these proteins. APT enzymes have been thought to be constitutively active, where it's S-acylation by DHHC enzymes which controls the kinetics of the acylation-deacylation reversible cycle. For example, radiolabelling studies using tritiated palmitate have shown than palmitate incorporation has a half-life of 20 minutes whereas depalmitoylation is 10-20 times faster [313, 324]. Another difference between S-acylation and deacylation is the localization of proteins to undergo this process. Some reports suggested S-acylation is restricted to compartments where the DHHC enzymes reside, such as membranes, while deacylation can happen throughout the cell [325]. This gives credence to the constitutively active form of APT enzymes. However, the specific mechanisms how DHHC and APT enzymes coordinate these steps has not been explored.

How S-acylation drives the movement of these proteins to subdomains in the plasma membrane is also interesting. Addition of lipid moieties (long chain lipids) changes the hydrophobicity of the proteins. The result of this addition is an increased affinity toward phospholipids, cholesterol, or other moieties in membrane subdomains [326]. For example, addition of saturated lipids can result in translocation to cholesterol and sphingolipid-enriched membrane subdomains such as lipid rafts [259, 305]. Indeed,

previous work by our group has shown that S-acylation is critical for the assembly of the TCR complex in lipid rafts [130, 251, 253, 266].This might also help us understand the differences observed between cysteine mutants of Orai1 and STIM1, which show different calcium entry patters upon store-depletion.

Another interesting point of emphasis which we failed to make is the specific lipid moiety that is added to target proteins, and how the lipid moiety affects the protein behavior. The lipid moiety could range from saturated palmitate (C16:0, 74%) to monounsaturated oleate (C18:1, 4%) or saturated stearate (C16:0, 22%) among others [327]. The role of lipid moiety will help answer some differences observed in S-acylation of Orai1 and STIM1. For example, we hypothesized S-acylation of Orai1 helps it recruit to cholesterol rich lipid rafts, whereas STIM1 S-acylation increases its association with phospholipids. Palmitic acid has long known to have higher affinity toward cholesterol compared to other phospholipids [312, 314]. So, we can test if Orai1 S-acylation leads to addition of a palmitate group. On the other hand, stearic acid is known to recruit to plasma membrane domains that have poor phospatidylinositon-4,5-bisphosphate (PIP_2) [328]. Some reports have suggested the the CRAC channels translocate to these domains upon store-depletion for propagating SOCE currents [233]. We can hypothesize that STIM1 S-acylation leads to an addition of a stearic acid which helps this translocation. Delineating these hypotheses is crucial for understanding the role of S-acylation in SOCE.

We observed distinct SOCE patterns in cysteine mutants of Orai1 and STIM1 [245, 246]. As presented in chapters 1 and 2 respectively, the cysteine mutant of Orai1, Orai1-C143S, shows a complete lack of calcium entry upon store-depletion [245]. Compared to

Orai1, STIM1 cysteine mutant, STIM1-C437S, has a more subtle phenotype leading to a partial loss of function [246]. The phenotypic difference between mutant Orai1 and STIM1 can be explained by the membrane subdomains these proteins translocate to upon store-depletion. As explained earlier, we hypothesized (and others have shown) that Orai1 localizes to lipid rafts upon store-depletion [265]. The addition of palmitate or another saturated lipid group at the C143 residue probably mediates this translocation. Indeed, it has been shown that tritiated palmitate can be incorporated into Orai1 [265]. Thus, the complete loss of function in the cysteine mutant Orai1 is likely due to an inability to be recruited into lipid rafts where it can bind to STIM1.

We believe the S-acylation of STIM1 stabilizes the C-terminus of the active conformation at the plasma membrane. In addition to S-acylation, two other critical binding events happen between the C-terminus of STIM1 and the plasma membrane. In particular, STIM1 binds to membrane lipids on the inner leaflet via the polybasic domain and the cholesterol-binding domain [164, 178]. This functional redundancy of membrane-associated features in the C-terminus of STIM1 may explain the partial loss of function in the cysteine-mutant STIM1. Future work can test this hypothesis using different STIM1 mutants that lack the polybasic or CBD domains alone and in combination with the S-acylation mutant.

Finally, how the DHHC enzymes that S-acylate Orai1 and STIM1 are regulated is a question that remains unanswered. There is a dearth of information about how these enzymes are regulated. Previously, we have shown that DHHC5, an enzyme the S-acylates many signaling proteins involved in beta adrenergic receptor function, is itself regulated by S-acylation of several cysteines in the C-terminal tail. S-acylation of

DHHC5 in its C-terminal tail upon receptor stimulation increases its stability in the plasma membrane where it can S-acylate its target proteins [315]. In addition, the DHHC enzymes regulate each other, where one DHHC enzyme can S-acylate another DHHC enzyme, which in turn affects its localization, function, or stability. For example, DHHC16 S-acylated DHHC6, which is an ER membrane protein that S-acylates many ER proteins such as calnexin, E3 ligase gp78, and IP_3 receptor [329]. Our acyl-RAC experiments performed on the WT and F233 mutant version of DHHC21 shows interesting results. The F233 mutant cannot undergo S-acylation, whereas the WT can. All DHHC enzymes undergo auto-acylation, which involves these enzymes taking up the lipid moiety and then transferring it to the substrate. The lack of S-acylation of the F233 mutant indicates that this enzyme cannot undergo auto-acylation. Based on this data, we can hypothesize that calcium binding in the Calmodulin binding motif in the DHHC21 affects S-acylation of DHHC21 by a mechanism that is still to be explored. One possibility is that calcium binding in the C-terminal tail of DHHC21 prompts a conformational change that exposes the DHHC active site, where the enzyme can undergo auto-acylation. However, this needs to be tested. For most DHHC enzymes, the regulatory mechanisms are entirely unexplored. This remains a critical barrier to advancement in the S-acylation field and should be a primary focus of future studies.

References

1. Clapham, D.E., *Calcium signaling.* Cell, 2007. **131**(6): p. 1047-58.

2. Carafoli, E., *Calcium signaling: a tale for all seasons.* Proc Natl Acad Sci U S A, 2002. **99**(3): p. 1115-22.

3. Berridge, M.J., P. Lipp, and M.D. Bootman, *The versatility and universality of calcium signalling.* Nat Rev Mol Cell Biol, 2000. **1**(1): p. 11-21.

4. Hasselbach, W. and M. Makinose, *[The calcium pump of the "relaxing granules" of muscle and its dependence on ATP-splitting].* Biochem Z, 1961. **333**: p. 518-28.

5. Ebashi, S. and F. Lipmann, *Adenosine Triphosphate-Linked Concentration of Calcium Ions in a Particulate Fraction of Rabbit Muscle.* J Cell Biol, 1962. **14**(3): p. 389-400.

6. Rhee, S.G., *Regulation of phosphoinositide-specific phospholipase C.* Annu Rev Biochem, 2001. **70**: p. 281-312.

7. Parekh, A.B. and R. Penner, *Store depletion and calcium influx.* Physiol Rev, 1997. **77**(4): p. 901-30.

8. Parekh, A.B. and J.W. Putney, *Store-operated calcium channels.* Physiol Rev, 2005. **85**(2): p. 757-810.

9. Jousset, H., M. Frieden, and N. Demaurex, *STIM1 knockdown reveals that store-operated Ca2+ channels located close to sarco/endoplasmic Ca2+ ATPases (SERCA) pumps silently refill the endoplasmic reticulum.* J Biol Chem, 2007. **282**(15): p. 11456-64.

10. Negulescu, P.A. and T.E. Machen, *Release and reloading of intracellular Ca stores after cholinergic stimulation of the parietal cell.* Am J Physiol, 1988. **254**(4 Pt 1): p. C498-504.

11. Cheng, K.T., et al., *Local Ca^{2+} entry via Orai1 regulates plasma membrane recruitment of TRPC1 and controls cytosolic Ca^{2+} signals required for specific cell functions.* PLoS Biol, 2011. **9**(3): p. e1001025.

12. Quintana, A., et al., *Calcium microdomains at the immunological synapse: how ORAI channels, mitochondria and calcium pumps generate local calcium signals for efficient T-cell activation.* EMBO J, 2011. **30**(19): p. 3895-912.

13. Hogan, P.G., et al., *Transcriptional regulation by calcium, calcineurin, and NFAT.* Genes Dev, 2003. **17**(18): p. 2205-32.

14. Smedler, E. and P. Uhlen, *Frequency decoding of calcium oscillations.* Biochim Biophys Acta, 2014. **1840**(3): p. 964-9.

15. Barr, V.A., et al., *Dynamic movement of the calcium sensor STIM1 and the calcium channel Orai1 in activated T-cells: puncta and distal caps.* Mol Biol Cell, 2008. **19**(7): p. 2802-17.

16. Liou, J., et al., *Live-cell imaging reveals sequential oligomerization and local plasma membrane targeting of stromal interaction molecule 1 after Ca2+ store depletion.* Proc Natl Acad Sci U S A, 2007. **104**(22): p. 9301-6.

17. Penna, A., et al., *The CRAC channel consists of a tetramer formed by Stim-induced dimerization of Orai dimers.* Nature, 2008. **456**(7218): p. 116-20.

18. Wu, M.M., et al., *Ca2+ store depletion causes STIM1 to accumulate in ER regions closely associated with the plasma membrane.* J Cell Biol, 2006. **174**(6): p. 803-13.

19. Lewis, R.S. and M.D. Cahalan, *Mitogen-induced oscillations of cytosolic Ca2+ and transmembrane Ca2+ current in human leukemic T cells.* Cell Regul, 1989. **1**(1): p. 99-112.

20. Putney, J.W., Jr., *A model for receptor-regulated calcium entry.* Cell Calcium, 1986. **7**(1): p. 1-12.

21. Hoth, M. and R. Penner, *Depletion of intracellular calcium stores activates a calcium current in mast cells.* Nature, 1992. **355**(6358): p. 353-6.

22. Zweifach, A. and R.S. Lewis, *Mitogen-regulated Ca2+ current of T lymphocytes is activated by depletion of intracellular Ca2+ stores.* Proc Natl Acad Sci U S A, 1993. **90**(13): p. 6295-9.

23. Liou, J., et al., *STIM is a Ca2+ sensor essential for Ca2+-store-depletion-triggered Ca2+ influx.* Curr Biol, 2005. **15**(13): p. 1235-41.

24. Zhang, S.L., et al., *STIM1 is a Ca2+ sensor that activates CRAC channels and migrates from the Ca2+ store to the plasma membrane.* Nature, 2005. **437**(7060): p. 902-5.

25. Feske, S., et al., *Severe combined immunodeficiency due to defective binding of the nuclear factor of activated T cells in T lymphocytes of two male siblings.* Eur J Immunol, 1996. **26**(9): p. 2119-26.

26. Vig, M., et al., *CRACM1 is a plasma membrane protein essential for store-operated Ca2+ entry.* Science, 2006. **312**(5777): p. 1220-3.

27. Gwack, Y., et al., *A genome-wide Drosophila RNAi screen identifies DYRK-family kinases as regulators of NFAT.* Nature, 2006. **441**(7093): p. 646-50.

28. Yeromin, A.V., et al., *Molecular identification of the CRAC channel by altered ion selectivity in a mutant of Orai.* Nature, 2006. **443**(7108): p. 226-9.

29. Streb, H., et al., *Release of Ca2+ from a nonmitochondrial intracellular store in pancreatic acinar cells by inositol-1,4,5-trisphosphate.* Nature, 1983. **306**(5938): p. 67-9.

30. Berridge, M.J. and R.F. Irvine, *Inositol trisphosphate, a novel second messenger in cellular signal transduction.* Nature, 1984. **312**(5992): p. 315-21.

31. Joseph, S.K., et al., *myo-Inositol 1,4,5-trisphosphate. A second messenger for the hormonal mobilization of intracellular Ca2+ in liver.* J Biol Chem, 1984. **259**(5): p. 3077-81.

32. Aub, D.L., J.S. McKinney, and J.W. Putney, Jr., *Nature of the receptor-regulated calcium pool in the rat parotid gland.* J Physiol, 1982. **331**: p. 557-65.

33. Casteels, R. and G. Droogmans, *Exchange characteristics of the noradrenaline-sensitive calcium store in vascular smooth muscle cells or rabbit ear artery.* J Physiol, 1981. **317**: p. 263-79.

34. Matthews, G., E. Neher, and R. Penner, *Second messenger-activated calcium influx in rat peritoneal mast cells.* J Physiol, 1989. **418**: p. 105-30.

35. Penner, R., G. Matthews, and E. Neher, *Regulation of calcium influx by second messengers in rat mast cells.* Nature, 1988. **334**(6182): p. 499-504.

36. Thastrup, O., et al., *Thapsigargin, a novel molecular probe for studying intracellular calcium release and storage.* Agents Actions, 1989. **27**(1-2): p. 17-23.

37. Van Coppenolle, F., et al., *Ribosome-translocon complex mediates calcium leakage from endoplasmic reticulum stores.* J Cell Sci, 2004. **117**(Pt 18): p. 4135-42.

38. Grynkiewicz, G., M. Poenie, and R.Y. Tsien, *A new generation of Ca2+ indicators with greatly improved fluorescence properties.* J Biol Chem, 1985. **260**(6): p. 3440-50.

39. Gouy, H., et al., *Ca2+ influx in human T lymphocytes is induced independently of inositol phosphate production by mobilization of intracellular Ca2+ stores. A study with the Ca2+ endoplasmic reticulum-ATPase inhibitor thapsigargin.* Eur J Immunol, 1990. **20**(10): p. 2269-75.

40. Sarkadi, B., et al., *Calcium influx and intracellular calcium release in anti-CD3 antibody-stimulated and thapsigargin-treated human T lymphoblasts.* J Membr Biol, 1991. **123**(1): p. 9-21.

41. Mason, M.J., M.P. Mahaut-Smith, and S. Grinstein, *The role of intracellular Ca2+ in the regulation of the plasma membrane Ca2+ permeability of unstimulated rat lymphocytes.* J Biol Chem, 1991. **266**(17): p. 10872-9.

42. Takemura, H., et al., *Activation of calcium entry by the tumor promoter thapsigargin in parotid acinar cells. Evidence that an intracellular calcium pool and not an inositol phosphate regulates calcium fluxes at the plasma membrane.* J Biol Chem, 1989. **264**(21): p. 12266-71.

43. Fanger, C.M., et al., *Characterization of T cell mutants with defects in capacitative calcium entry: genetic evidence for the physiological roles of CRAC channels.* J Cell Biol, 1995. **131**(3): p. 655-67.

44. Serafini, A.T., et al., *Isolation of mutant T lymphocytes with defects in capacitative calcium entry.* Immunity, 1995. **3**(2): p. 239-50.

45. Randriamampita, C. and R.Y. Tsien, *Emptying of intracellular Ca2+ stores releases a novel small messenger that stimulates Ca2+ influx.* Nature, 1993. **364**(6440): p. 809-14.

46. Thomas, D. and M.R. Hanley, *Evaluation of calcium influx factors from stimulated Jurkat T-lymphocytes by microinjection into Xenopus oocytes.* J Biol Chem, 1995. **270**(12): p. 6429-32.

47. Zhang, C. and D.W. Thomas, *Stromal Interaction Molecule 1 rescues store-operated calcium entry and protects NG115-401L cells against cell death induced by endoplasmic reticulum and mitochondrial oxidative stress.* Neurochem Int, 2016. **97**: p. 137-45.

48. Yao, Y., et al., *Activation of store-operated Ca2+ current in Xenopus oocytes requires SNAP-25 but not a diffusible messenger.* Cell, 1999. **98**(4): p. 475-85.

49. Supattapone, S., et al., *Solubilization, purification, and characterization of an inositol trisphosphate receptor.* J Biol Chem, 1988. **263**(3): p. 1530-4.

50. Gill, D.L., *Calcium signalling: receptor kinships revealed.* Nature, 1989. **342**(6245): p. 16-8.

51. Irvine, R.F., *'Quantal' Ca2+ release and the control of Ca2+ entry by inositol phosphates--a possible mechanism.* FEBS Lett, 1990. **263**(1): p. 5-9.

52. Lee, E.H., et al., *Conformational coupling of DHPR and RyR1 in skeletal myotubes is influenced by long-range allosterism: evidence for a negative regulatory module.* Am J Physiol Cell Physiol, 2004. **286**(1): p. C179-89.

53. Montell, C., *The TRP superfamily of cation channels.* Sci STKE, 2005. **2005**(272): p. re3.

54. Montell, C., *Physiology, phylogeny, and functions of the TRP superfamily of cation channels.* Sci STKE, 2001. **2001**(90): p. re1.

55. Cosens, D.J. and A. Manning, *Abnormal electroretinogram from a Drosophila mutant.* Nature, 1969. **224**(5216): p. 285-7.

56. Hardie, R.C. and B. Minke, *The trp gene is essential for a light-activated Ca2+ channel in Drosophila photoreceptors.* Neuron, 1992. **8**(4): p. 643-51.

57. Montell, C., et al., *Rescue of the Drosophila phototransduction mutation trp by germline transformation.* Science, 1985. **230**(4729): p. 1040-3.

58. Montell, C. and G.M. Rubin, *Molecular characterization of the Drosophila trp locus: a putative integral membrane protein required for phototransduction.* Neuron, 1989. **2**(4): p. 1313-23.

59. Vaca, L., et al., *Activation of recombinant trp by thapsigargin in Sf9 insect cells.* Am J Physiol, 1994. **267**(5 Pt 1): p. C1501-5.

60. Amiri, H., G. Schultz, and M. Schaefer, *FRET-based analysis of TRPC subunit stoichiometry.* Cell Calcium, 2003. **33**(5-6): p. 463-70.

61. Hoenderop, J.G., et al., *Homo- and heterotetrameric architecture of the epithelial Ca2+ channels TRPV5 and TRPV6.* EMBO J, 2003. **22**(4): p. 776-85.

62. Kuzhikandathil, E.V., et al., *Functional analysis of capsaicin receptor (vanilloid receptor subtype 1) multimerization and agonist responsiveness using a dominant negative mutation.* J Neurosci, 2001. **21**(22): p. 8697-706.

63. Catterall, W.A., *From ionic currents to molecular mechanisms: the structure and function of voltage-gated sodium channels.* Neuron, 2000. **26**(1): p. 13-25.

64. Montell, C., et al., *A unified nomenclature for the superfamily of TRP cation channels.* Mol Cell, 2002. **9**(2): p. 229-31.

65. Walker, R.G., A.T. Willingham, and C.S. Zuker, *A Drosophila mechanosensory transduction channel.* Science, 2000. **287**(5461): p. 2229-34.

66. Sidi, S., R.W. Friedrich, and T. Nicolson, *NompC TRP channel required for vertebrate sensory hair cell mechanotransduction.* Science, 2003. **301**(5629): p. 96-9.

67. Denis, V. and M.S. Cyert, *Internal Ca(2+) release in yeast is triggered by hypertonic shock and mediated by a TRP channel homologue.* J Cell Biol, 2002. **156**(1): p. 29-34.

68. Palmer, C.P., et al., *A TRP homolog in Saccharomyces cerevisiae forms an intracellular Ca(2+)-permeable channel in the yeast vacuolar membrane.* Proc Natl Acad Sci U S A, 2001. **98**(14): p. 7801-5.

69. Phillips, A.M., A. Bull, and L.E. Kelly, *Identification of a Drosophila gene encoding a calmodulin-binding protein with homology to the trp phototransduction gene.* Neuron, 1992. **8**(4): p. 631-42.

70. Xu, X.Z., et al., *TRPgamma, a drosophila TRP-related subunit, forms a regulated cation channel with TRPL.* Neuron, 2000. **26**(3): p. 647-57.

71. Reuss, H., et al., *In vivo analysis of the drosophila light-sensitive channels, TRP and TRPL.* Neuron, 1997. **19**(6): p. 1249-59.

72. Niemeyer, B.A., et al., *The Drosophila light-activated conductance is composed of the two channels TRP and TRPL.* Cell, 1996. **85**(5): p. 651-9.

73. Leung, H.T., C. Geng, and W.L. Pak, *Phenotypes of trpl mutants and interactions between the transient receptor potential (TRP) and TRP-like channels in Drosophila.* J Neurosci, 2000. **20**(18): p. 6797-803.

74. Thastrup, O., et al., *Thapsigargin, a tumor promoter, discharges intracellular Ca2+ stores by specific inhibition of the endoplasmic reticulum Ca2(+)-ATPase.* Proc Natl Acad Sci U S A, 1990. **87**(7): p. 2466-70.

75. Ranganathan, R., et al., *Cytosolic calcium transients: spatial localization and role in Drosophila photoreceptor cell function.* Neuron, 1994. **13**(4): p. 837-48.

76. Hardie, R.C., *Excitation of Drosophila photoreceptors by BAPTA and ionomycin: evidence for capacitative Ca2+ entry?* Cell Calcium, 1996. **20**(4): p. 315-27.

77. Hardie, R.C. and P. Raghu, *Activation of heterologously expressed Drosophila TRPL channels: Ca2+ is not required and InsP3 is not sufficient.* Cell Calcium, 1998. **24**(3): p. 153-63.

78. Sokabe, T., et al., *Endocannabinoids produced in photoreceptor cells in response to light activate.* Sci Signal, 2022. **15**(755): p. eabl6179.

79. Liu, C.H., et al., *Rapid Release of Ca.* J Neurosci, 2020. **40**(16): p. 3152-3164.

80. Wes, P.D., et al., *TRPC1, a human homolog of a Drosophila store-operated channel.* Proc Natl Acad Sci U S A, 1995. **92**(21): p. 9652-6.

81. Zhu, X., et al., *Molecular cloning of a widely expressed human homologue for the Drosophila trp gene.* FEBS Lett, 1995. **373**(3): p. 193-8.

82. Wissenbach, U., et al., *Structure and mRNA expression of a bovine trp homologue related to mammalian trp2 transcripts.* FEBS Lett, 1998. **429**(1): p. 61-6.

83. Okada, T., et al., *Molecular and functional characterization of a novel mouse transient receptor potential protein homologue TRP7. Ca(2+)-permeable cation channel that is constitutively activated and enhanced by stimulation of G protein-coupled receptor.* J Biol Chem, 1999. **274**(39): p. 27359-70.

84. Okada, T., et al., *Molecular cloning and functional characterization of a novel receptor-activated TRP Ca2+ channel from mouse brain.* J Biol Chem, 1998. **273**(17): p. 10279-87.

85. Philipp, S., et al., *A mammalian capacitative calcium entry channel homologous to Drosophila TRP and TRPL.* EMBO J, 1996. **15**(22): p. 6166-71.

86. Vannier, B., et al., *The membrane topology of human transient receptor potential 3 as inferred from glycosylation-scanning mutagenesis and epitope immunocytochemistry.* J Biol Chem, 1998. **273**(15): p. 8675-9.

87. Zhu, X., et al., *trp, a novel mammalian gene family essential for agonist-activated capacitative Ca2+ entry.* Cell, 1996. **85**(5): p. 661-71.

88. Zitt, C., et al., *Expression of TRPC3 in Chinese hamster ovary cells results in calcium-activated cation currents not related to store depletion.* J Cell Biol, 1997. **138**(6): p. 1333-41.

89. Smani, T., et al., *A novel mechanism for the store-operated calcium influx pathway.* Nat Cell Biol, 2004. **6**(2): p. 113-20.

90. Itagaki, K., et al., *Cytoskeletal reorganization internalizes multiple transient receptor potential channels and blocks calcium entry into human neutrophils.* J Immunol, 2004. **172**(1): p. 601-7.

91. Lockwich, T., et al., *Stabilization of cortical actin induces internalization of transient receptor potential 3 (Trp3)-associated caveolar Ca2+ signaling complex and loss of Ca2+ influx without disruption of Trp3-inositol trisphosphate receptor association.* J Biol Chem, 2001. **276**(45): p. 42401-8.

92. Hofmann, T., et al., *Direct activation of human TRPC6 and TRPC3 channels by diacylglycerol.* Nature, 1999. **397**(6716): p. 259-63.

93. Lucas, P., et al., *A diacylglycerol-gated cation channel in vomeronasal neuron dendrites is impaired in TRPC2 mutant mice: mechanism of pheromone transduction.* Neuron, 2003. **40**(3): p. 551-61.

94. Jungnickel, M.K., et al., *Trp2 regulates entry of Ca2+ into mouse sperm triggered by egg ZP3.* Nat Cell Biol, 2001. **3**(5): p. 499-502.

95. Hofmann, T., et al., *Cloning, expression and subcellular localization of two novel splice variants of mouse transient receptor potential channel 2.* Biochem J, 2000. **351**(Pt 1): p. 115-22.

96. Vannier, B., et al., *Mouse trp2, the homologue of the human trpc2 pseudogene, encodes mTrp2, a store depletion-activated capacitative Ca2+ entry channel.* Proc Natl Acad Sci U S A, 1999. **96**(5): p. 2060-4.

97. Kiselyov, K., et al., *Functional interaction between InsP3 receptors and store-operated Htrp3 channels.* Nature, 1998. **396**(6710): p. 478-82.

98. Brough, G.H., et al., *Contribution of endogenously expressed Trp1 to a Ca2+-selective, store-operated Ca2+ entry pathway.* FASEB J, 2001. **15**(10): p. 1704-1710.

99. Petersen, C.C., et al., *Putative capacitative calcium entry channels: expression of Drosophila trp and evidence for the existence of vertebrate homologues.* Biochem J, 1995. **311 (Pt 1)**(Pt 1): p. 41-4.

100. Xu, X.Z., et al., *Coassembly of TRP and TRPL produces a distinct store-operated conductance.* Cell, 1997. **89**(7): p. 1155-64.

101. Venkatachalam, K. and C. Montell, *TRP channels.* Annu Rev Biochem, 2007. **76**: p. 387-417.

102. Hellmich, U.A. and R. Gaudet, *Structural biology of TRP channels.* Handb Exp Pharmacol, 2014. **223**: p. 963-90.

103. Gregorio-Teruel, L., et al., *Mutation of I696 and W697 in the TRP box of vanilloid receptor subtype I modulates allosteric channel activation.* J Gen Physiol, 2014. **143**(3): p. 361-75.

104. Baez-Nieto, D., et al., *Thermo-TRP channels: biophysics of polymodal receptors.* Adv Exp Med Biol, 2011. **704**: p. 469-90.

105. Lee, K.P., et al., *Molecular determinants mediating gating of Transient Receptor Potential Canonical (TRPC) channels by stromal interaction molecule 1 (STIM1).* J Biol Chem, 2014. **289**(10): p. 6372-6382.

106. Wedel, B.J., et al., *A calmodulin/inositol 1,4,5-trisphosphate (IP3) receptor-binding region targets TRPC3 to the plasma membrane in a calmodulin/IP3 receptor-independent process.* J Biol Chem, 2003. **278**(28): p. 25758-65.

107. Dionisio, N., et al., *Functional role of the calmodulin- and inositol 1,4,5-trisphosphate receptor-binding (CIRB) site of TRPC6 in human platelet activation.* Cell Signal, 2011. **23**(11): p. 1850-6.

108. Moore, T.M., et al., *Store-operated calcium entry promotes shape change in pulmonary endothelial cells expressing Trp1.* Am J Physiol, 1998. **275**(3): p. L574-82.

109. Barnes, P.J. and S.F. Liu, *Regulation of pulmonary vascular tone.* Pharmacol Rev, 1995. **47**(1): p. 87-131.

110. Lum, H. and A.B. Malik, *Regulation of vascular endothelial barrier function.* Am J Physiol, 1994. **267**(3 Pt 1): p. L223-41.

111. Kohn, E.C., et al., *Angiogenesis: role of calcium-mediated signal transduction.* Proc Natl Acad Sci U S A, 1995. **92**(5): p. 1307-11.

112. Huang, A.J., et al., *Endothelial cell cytosolic free calcium regulates neutrophil migration across monolayers of endothelial cells.* J Cell Biol, 1993. **120**(6): p. 1371-80.

113. Freichel, M., et al., *Lack of an endothelial store-operated Ca2+ current impairs agonist-dependent vasorelaxation in TRP4-/- mice.* Nat Cell Biol, 2001. **3**(2): p. 121-7.

114. Sakura, H. and F.M. Ashcroft, *Identification of four trp1 gene variants murine pancreatic beta-cells.* Diabetologia, 1997. **40**(5): p. 528-32.

115. Rosado, J.A. and S.O. Sage, *Coupling between inositol 1,4,5-trisphosphate receptors and human transient receptor potential channel 1 when intracellular Ca2+ stores are depleted.* Biochem J, 2000. **350 Pt 3**(Pt 3): p. 631-5.

116. Garcia, R.L. and W.P. Schilling, *Differential expression of mammalian TRP homologues across tissues and cell lines.* Biochem Biophys Res Commun, 1997. **239**(1): p. 279-83.

117. Mori, Y., et al., *Differential distribution of TRP Ca2+ channel isoforms in mouse brain.* Neuroreport, 1998. **9**(3): p. 507-15.

118. Liman, E.R., D.P. Corey, and C. Dulac, *TRP2: a candidate transduction channel for mammalian pheromone sensory signaling.* Proc Natl Acad Sci U S A, 1999. **96**(10): p. 5791-6.

119. Li, H.S., X.Z. Xu, and C. Montell, *Activation of a TRPC3-dependent cation current through the neurotrophin BDNF.* Neuron, 1999. **24**(1): p. 261-73.

120. Montell, C., *Visual transduction in Drosophila.* Annu Rev Cell Dev Biol, 1999. **15**: p. 231-68.

121. Colbert, H.A., T.L. Smith, and C.I. Bargmann, *OSM-9, a novel protein with structural similarity to channels, is required for olfaction, mechanosensation, and olfactory adaptation in Caenorhabditis elegans.* J Neurosci, 1997. **17**(21): p. 8259-69.

122. Caterina, M.J., et al., *Impaired nociception and pain sensation in mice lacking the capsaicin receptor.* Science, 2000. **288**(5464): p. 306-13.

123. Zitt, C., et al., *Cloning and functional expression of a human Ca2+-permeable cation channel activated by calcium store depletion.* Neuron, 1996. **16**(6): p. 1189-96.

124. Desai, P.N., et al., *Multiple types of calcium channels arising from alternative translation initiation of the Orai1 message.* Sci Signal, 2015. **8**(387): p. ra74.

125. Trebak, M., et al., *Signaling mechanism for receptor-activated canonical transient receptor potential 3 (TRPC3) channels.* J Biol Chem, 2003. **278**(18): p. 16244-52.

126. Ong, H.L., et al., *Dynamic assembly of TRPC1-STIM1-Orai1 ternary complex is involved in store-operated calcium influx. Evidence for similarities in store-operated and calcium release-activated calcium channel components.* J Biol Chem, 2007. **282**(12): p. 9105-16.

127. Jardin, I., et al., *Orai1 mediates the interaction between STIM1 and hTRPC1 and regulates the mode of activation of hTRPC1-forming Ca2+ channels.* J Biol Chem, 2008. **283**(37): p. 25296-25304.

128. Zeng, W., et al., *STIM1 gates TRPC channels, but not Orai1, by electrostatic interaction.* Mol Cell, 2008. **32**(3): p. 439-48.

129. Cheng, K.T., et al., *Functional requirement for Orai1 in store-operated TRPC1-STIM1 channels.* J Biol Chem, 2008. **283**(19): p. 12935-40.

130. Akimzhanov, A.M., et al., *T-cell receptor complex is essential for Fas signal transduction.* Proc Natl Acad Sci U S A, 2010. **107**(34): p. 15105-10.

131. Feske, S., et al., *A severe defect in CRAC Ca2+ channel activation and altered K+ channel gating in T cells from immunodeficient patients.* J Exp Med, 2005. **202**(5): p. 651-62.

132. McCarl, C.A., et al., *ORAI1 deficiency and lack of store-operated Ca2+ entry cause immunodeficiency, myopathy, and ectodermal dysplasia.* J Allergy Clin Immunol, 2009. **124**(6): p. 1311-1318.e7.

133. Ong, H.L., S.I. Jang, and I.S. Ambudkar, *Distinct contributions of Orai1 and TRPC1 to agonist-induced [Ca(2+)](i) signals determine specificity of Ca(2+)-dependent gene expression.* PLoS One, 2012. **7**(10): p. e47146.

134. Kim, M.S., et al., *Native Store-operated Ca2+ Influx Requires the Channel Function of Orai1 and TRPC1.* J Biol Chem, 2009. **284**(15): p. 9733-41.

135. Galán, C., et al., *STIM1, Orai1 and hTRPC1 are important for thrombin- and ADP-induced aggregation in human platelets.* Arch Biochem Biophys, 2009. **490**(2): p. 137-44.

136. Sabourin, J., et al., *Store-operated Ca2+ Entry Mediated by Orai1 and TRPC1 Participates to Insulin Secretion in Rat β-Cells.* J Biol Chem, 2015. **290**(51): p. 30530-9.

137. Schaar, A., et al., *Ca.* J Cell Sci, 2019. **132**(13).

138. Perrouin-Verbe, M.A., et al., *Overexpression of certain transient receptor potential and Orai channels in prostate cancer is associated with decreased risk of systemic recurrence after radical prostatectomy.* Prostate, 2019. **79**(16): p. 1793-1804.

139. Guéguinou, M., et al., *SK3/TRPC1/Orai1 complex regulates SOCE-dependent colon cancer cell migration: a novel opportunity to modulate anti-EGFR mAb action by the alkyl-lipid Ohmline.* Oncotarget, 2016. **7**(24): p. 36168-36184.

140. Sabourin, J., et al., *Ca.* J Mol Cell Cardiol, 2018. **118**: p. 208-224.

141. Feske, S., et al., *The duration of nuclear residence of NFAT determines the pattern of cytokine expression in human SCID T cells.* J Immunol, 2000. **165**(1): p. 297-305.

142. Feske, S., et al., *Impaired NFAT regulation and its role in a severe combined immunodeficiency.* Immunobiology, 2000. **202**(2): p. 134-50.

143. Berridge, M.J., *Inositol trisphosphate and calcium signalling.* Nature, 1993. **361**(6410): p. 315-25.

144. Clapham, D.E., *Intracellular calcium. Replenishing the stores.* Nature, 1995. **375**(6533): p. 634-5.

145. Dolmetsch, R.E., et al., *Differential activation of transcription factors induced by Ca2+ response amplitude and duration.* Nature, 1997. **386**(6627): p. 855-8.

146. Timmerman, L.A., et al., *Rapid shuttling of NF-AT in discrimination of Ca2+ signals and immunosuppression.* Nature, 1996. **383**(6603): p. 837-40.

147. Kiani, A., A. Rao, and J. Aramburu, *Manipulating immune responses with immunosuppressive agents that target NFAT.* Immunity, 2000. **12**(4): p. 359-72.

148. Crabtree, G.R., *Generic signals and specific outcomes: signaling through Ca2+, calcineurin, and NF-AT.* Cell, 1999. **96**(5): p. 611-4.

149. Feske, S., et al., *Gene regulation mediated by calcium signals in T lymphocytes.* Nat Immunol, 2001. **2**(4): p. 316-24.

150. Dykxhoorn, D.M. and J. Lieberman, *The silent revolution: RNA interference as basic biology, research tool, and therapeutic.* Annu Rev Med, 2005. **56**: p. 401-23.

151. Downward, J., *RNA interference.* BMJ, 2004. **328**(7450): p. 1245-8.

152. Zhang, S.L., et al., *Genome-wide RNAi screen of Ca(2+) influx identifies genes that regulate Ca(2+) release-activated Ca(2+) channel activity.* Proc Natl Acad Sci U S A, 2006. **103**(24): p. 9357-62.

153. Yeromin, A.V., et al., *A store-operated calcium channel in Drosophila S2 cells.* J Gen Physiol, 2004. **123**(2): p. 167-82.

154. Feske, S., et al., *A mutation in Orai1 causes immune deficiency by abrogating CRAC channel function.* Nature, 2006. **441**(7090): p. 179-85.

155. Roos, J., et al., *STIM1, an essential and conserved component of store-operated Ca2+ channel function.* J Cell Biol, 2005. **169**(3): p. 435-45.

156. Prakriya, M., et al., *Orai1 is an essential pore subunit of the CRAC channel.* Nature, 2006. **443**(7108): p. 230-3.

157. Xu, P., et al., *Aggregation of STIM1 underneath the plasma membrane induces clustering of Orai1.* Biochem Biophys Res Commun, 2006. **350**(4): p. 969-76.

158. Baba, Y., et al., *Coupling of STIM1 to store-operated Ca2+ entry through its constitutive and inducible movement in the endoplasmic reticulum.* Proc Natl Acad Sci U S A, 2006. **103**(45): p. 16704-9.

159. Luik, R.M., et al., *The elementary unit of store-operated Ca2+ entry: local activation of CRAC channels by STIM1 at ER-plasma membrane junctions.* J Cell Biol, 2006. **174**(6): p. 815-25.

160. Orci, L., et al., *From the Cover: STIM1-induced precortical and cortical subdomains of the endoplasmic reticulum.* Proc Natl Acad Sci U S A, 2009. **106**(46): p. 19358-62.

161. Smyth, J.T., et al., *Ca2+-store-dependent and -independent reversal of Stim1 localization and function.* J Cell Sci, 2008. **121**(Pt 6): p. 762-72.

162. Patterson, R.L., D.B. van Rossum, and D.L. Gill, *Store-operated Ca2+ entry: evidence for a secretion-like coupling model.* Cell, 1999. **98**(4): p. 487-99.

163. Grigoriev, I., et al., *STIM1 is a MT-plus-end-tracking protein involved in remodeling of the ER.* Curr Biol, 2008. **18**(3): p. 177-82.

164. Pacheco, J., et al., *A cholesterol-binding domain in STIM1 modulates STIM1-Orai1 physical and functional interactions.* Sci Rep, 2016. **6**: p. 29634.

165. Sharma, S., et al., *An siRNA screen for NFAT activation identifies septins as coordinators of store-operated Ca2+ entry.* Nature, 2013. **499**(7457): p. 238-42.

166. Chang, C.L., et al., *Feedback regulation of receptor-induced Ca2+ signaling mediated by E-Syt1 and Nir2 at endoplasmic reticulum-plasma membrane junctions.* Cell Rep, 2013. **5**(3): p. 813-25.

167. Giordano, F., et al., *PI(4,5)P(2)-dependent and Ca(2+)-regulated ER-PM interactions mediated by the extended synaptotagmins.* Cell, 2013. **153**(7): p. 1494-509.

168. Quintana, A., et al., *TMEM110 regulates the maintenance and remodeling of mammalian ER-plasma membrane junctions competent for STIM-ORAI signaling.* Proc Natl Acad Sci U S A, 2015. **112**(51): p. E7083-92.

169. Srikanth, S., et al., *Junctate is a Ca2+-sensing structural component of Orai1 and stromal interaction molecule 1 (STIM1).* Proc Natl Acad Sci U S A, 2012. **109**(22): p. 8682-7.

170. Treves, S., et al., *Junctate is a key element in calcium entry induced by activation of InsP3 receptors and/or calcium store depletion.* J Cell Biol, 2004. **166**(4): p. 537-48.

171. Ivanova, A. and P. Atakpa-Adaji, *Phosphatidylinositol 4,5-bisphosphate and calcium at ER-PM junctions - Complex interplay of simple messengers.* Biochim Biophys Acta Mol Cell Res, 2023. **1870**(6): p. 119475.

172. Mercer, J.C., et al., *Large store-operated calcium selective currents due to co-expression of Orai1 or Orai2 with the intracellular calcium sensor, Stim1.* J Biol Chem, 2006. **281**(34): p. 24979-90.

173. Kim, J.Y. and S. Muallem, *Unlocking SOAR releases STIM.* EMBO J, 2011. **30**(9): p. 1673-5.

174. Lioudyno, M.I., et al., *Orai1 and STIM1 move to the immunological synapse and are up-regulated during T cell activation.* Proc Natl Acad Sci U S A, 2008. **105**(6): p. 2011-6.

175. Zhou, Y., et al., *STIM1 gates the store-operated calcium channel ORAI1 in vitro.* Nat Struct Mol Biol, 2010. **17**(1): p. 112-6.

176. Stathopulos, P.B., et al., *Stored Ca2+ depletion-induced oligomerization of stromal interaction molecule 1 (STIM1) via the EF-SAM region: An initiation mechanism for capacitive Ca2+ entry.* J Biol Chem, 2006. **281**(47): p. 35855-62.

177. Stathopulos, P.B., L. Zheng, and M. Ikura, *Stromal interaction molecule (STIM) 1 and STIM2 calcium sensing regions exhibit distinct unfolding and oligomerization kinetics.* J Biol Chem, 2009. **284**(2): p. 728-32.

178. Yuan, J.P., et al., *SOAR and the polybasic STIM1 domains gate and regulate Orai channels.* Nat Cell Biol, 2009. **11**(3): p. 337-43.

179. Zheng, L., et al., *Biophysical characterization of the EF-hand and SAM domain containing Ca2+ sensory region of STIM1 and STIM2.* Biochem Biophys Res Commun, 2008. **369**(1): p. 240-6.

180. Huang, G.N., et al., *STIM1 carboxyl-terminus activates native SOC, I(crac) and TRPC1 channels.* Nat Cell Biol, 2006. **8**(9): p. 1003-10.

181. Park, C.Y., et al., *STIM1 clusters and activates CRAC channels via direct binding of a cytosolic domain to Orai1.* Cell, 2009. **136**(5): p. 876-90.

182. Kawasaki, T., I. Lange, and S. Feske, *A minimal regulatory domain in the C terminus of STIM1 binds to and activates ORAI1 CRAC channels.* Biochem Biophys Res Commun, 2009. **385**(1): p. 49-54.

183. Stathopulos, P.B., et al., *STIM1/Orai1 coiled-coil interplay in the regulation of store-operated calcium entry.* Nat Commun, 2013. **4**: p. 2963.

184. Wu, M.M., E.D. Covington, and R.S. Lewis, *Single-molecule analysis of diffusion and trapping of STIM1 and Orai1 at endoplasmic reticulum-plasma membrane junctions.* Mol Biol Cell, 2014. **25**(22): p. 3672-85.

185. Hoover, P.J. and R.S. Lewis, *Stoichiometric requirements for trapping and gating of Ca2+ release-activated Ca2+ (CRAC) channels by stromal interaction molecule 1 (STIM1).* Proc Natl Acad Sci U S A, 2011. **108**(32): p. 13299-304.

186. Covington, E.D., M.M. Wu, and R.S. Lewis, *Essential role for the CRAC activation domain in store-dependent oligomerization of STIM1.* Mol Biol Cell, 2010. **21**(11): p. 1897-907.

187. Muik, M., et al., *A Cytosolic Homomerization and a Modulatory Domain within STIM1 C Terminus Determine Coupling to ORAI1 Channels.* J Biol Chem, 2009. **284**(13): p. 8421-6.

188. Fahrner, M., et al., *A coiled-coil clamp controls both conformation and clustering of stromal interaction molecule 1 (STIM1).* J Biol Chem, 2014. **289**(48): p. 33231-44.

189. Stathopulos, P.B., et al., *Structural and mechanistic insights into STIM1-mediated initiation of store-operated calcium entry.* Cell, 2008. **135**(1): p. 110-22.

190. Yang, X., et al., *Structural and mechanistic insights into the activation of Stromal interaction molecule 1 (STIM1).* Proc Natl Acad Sci U S A, 2012. **109**(15): p. 5657-62.

191. Zheng, L., et al., *Auto-inhibitory role of the EF-SAM domain of STIM proteins in store-operated calcium entry.* Proc Natl Acad Sci U S A, 2011. **108**(4): p. 1337-42.

192. Muik, M., et al., *Dynamic coupling of the putative coiled-coil domain of ORAI1 with STIM1 mediates ORAI1 channel activation.* J Biol Chem, 2008. **283**(12): p. 8014-22.

193. Yu, J., et al., *An aromatic amino acid in the coiled-coil 1 domain plays a crucial role in the auto-inhibitory mechanism of STIM1.* Biochem J, 2013. **454**(3): p. 401-9.

194. Muik, M., et al., *STIM1 couples to ORAI1 via an intramolecular transition into an extended conformation.* EMBO J, 2011. **30**(9): p. 1678-89.

195. Ma, G., et al., *Inside-out Ca(2+) signalling prompted by STIM1 conformational switch.* Nat Commun, 2015. **6**: p. 7826.

196. Zhou, Y., et al., *Initial activation of STIM1, the regulator of store-operated calcium entry.* Nat Struct Mol Biol, 2013. **20**(8): p. 973-81.

197. Gonzalez-Cobos, J.C., et al., *Store-independent Orai1/3 channels activated by intracrine leukotriene C4: role in neointimal hyperplasia.* Circ Res, 2013. **112**(7): p. 1013-25.

198. Mignen, O., J.L. Thompson, and T.J. Shuttleworth, *Both Orai1 and Orai3 are essential components of the arachidonate-regulated Ca2+-selective (ARC) channels.* J Physiol, 2008. **586**(1): p. 185-95.

199. Mignen, O., J.L. Thompson, and T.J. Shuttleworth, *The molecular architecture of the arachidonate-regulated Ca2+-selective ARC channel is a pentameric assembly of Orai1 and Orai3 subunits.* J Physiol, 2009. **587**(Pt 17): p. 4181-97.

200. Thompson, J.L. and T.J. Shuttleworth, *Molecular basis of activation of the arachidonate-regulated Ca2+ (ARC) channel, a store-independent Orai channel, by plasma membrane STIM1.* J Physiol, 2013. **591**(14): p. 3507-23.

201. Vig, M., et al., *CRACM1 multimers form the ion-selective pore of the CRAC channel.* Curr Biol, 2006. **16**(20): p. 2073-9.

202. Navarro-Borelly, L., et al., *STIM1-Orai1 interactions and Orai1 conformational changes revealed by live-cell FRET microscopy.* J Physiol, 2008. **586**(22): p. 5383-401.

203. Gwack, Y., et al., *Biochemical and functional characterization of Orai proteins.* J Biol Chem, 2007. **282**(22): p. 16232-43.

204. Mignen, O., J.L. Thompson, and T.J. Shuttleworth, *Orai1 subunit stoichiometry of the mammalian CRAC channel pore.* J Physiol, 2008. **586**(2): p. 419-25.

205. Ji, W., et al., *Functional stoichiometry of the unitary calcium-release-activated calcium channel.* Proc Natl Acad Sci U S A, 2008. **105**(36): p. 13668-73.

206. Madl, J., et al., *Resting state Orai1 diffuses as homotetramer in the plasma membrane of live mammalian cells.* J Biol Chem, 2010. **285**(52): p. 41135-42.

207. Hou, X., et al., *Crystal structure of the calcium release-activated calcium channel Orai.* Science, 2012. **338**(6112): p. 1308-13.

208. Hou, X., et al., *Cryo-EM structure of the calcium release-activated calcium channel Orai in an open conformation.* Elife, 2020. **9**.

209. Hou, X., S.R. Burstein, and S.B. Long, *Structures reveal opening of the store-operated calcium channel Orai.* Elife, 2018. **7**.

210. Li, Z., et al., *Graded activation of CRAC channel by binding of different numbers of STIM1 to Orai1 subunits.* Cell Res, 2011. **21**(2): p. 305-15.

211. Li, Z., et al., *Mapping the interacting domains of STIM1 and Orai1 in Ca2+ release-activated Ca2+ channel activation.* J Biol Chem, 2007. **282**(40): p. 29448-56.

212. Prakriya, M. and R.S. Lewis, *Regulation of CRAC channel activity by recruitment of silent channels to a high open-probability gating mode.* J Gen Physiol, 2006. **128**(3): p. 373-86.

213. Yamashita, M. and M. Prakriya, *Divergence of Ca(2+) selectivity and equilibrium Ca(2+) blockade in a Ca(2+) release-activated Ca(2+) channel.* J Gen Physiol, 2014. **143**(3): p. 325-43.

214. McNally, B.A., et al., *Gated regulation of CRAC channel ion selectivity by STIM1.* Nature, 2012. **482**(7384): p. 241-5.

215. Dong, H., et al., *Pore waters regulate ion permeation in a calcium release-activated calcium channel.* Proc Natl Acad Sci U S A, 2013. **110**(43): p. 17332-7.

216. Gudlur, A., et al., *STIM1 triggers a gating rearrangement at the extracellular mouth of the ORAI1 channel.* Nat Commun, 2014. **5**: p. 5164.

217. Zhang, S.L., et al., *Mutations in Orai1 transmembrane segment 1 cause STIM1-independent activation of Orai1 channels at glycine 98 and channel closure at arginine 91.* Proc Natl Acad Sci U S A, 2011. **108**(43): p. 17838-43.

218. Yamashita, M., et al., *STIM1 activates CRAC channels through rotation of the pore helix to open a hydrophobic gate.* Nat Commun, 2017. **8**: p. 14512.

219. Zheng, H., et al., *Differential roles of the C and N termini of Orai1 protein in interacting with stromal interaction molecule 1 (STIM1) for Ca2+ release-activated Ca2+ (CRAC) channel activation.* J Biol Chem, 2013. **288**(16): p. 11263-72.

220. Zhou, Y., et al., *Pore architecture of the ORAI1 store-operated calcium channel.* Proc Natl Acad Sci U S A, 2010. **107**(11): p. 4896-901.

221. Yamashita, M., et al., *Orai1 mutations alter ion permeation and Ca2+-dependent fast inactivation of CRAC channels: evidence for coupling of permeation and gating.* J Gen Physiol, 2007. **130**(5): p. 525-40.

222. Alavizargar, A., et al., *Molecular Dynamics Simulations of Orai Reveal How the Third Transmembrane Segment Contributes to Hydration and Ca(2+) Selectivity in Calcium Release-Activated Calcium Channels.* J Phys Chem B, 2018. **122**(16): p. 4407-4417.

223. Yeung, P.S., et al., *Mapping the functional anatomy of Orai1 transmembrane domains for CRAC channel gating.* Proc Natl Acad Sci U S A, 2018. **115**(22): p. E5193-E5202.

224. McNally, B.A., et al., *Structural determinants of ion permeation in CRAC channels.* Proc Natl Acad Sci U S A, 2009. **106**(52): p. 22516-21.

225. Matias, M.G., et al., *Animal Ca2+ release-activated Ca2+ (CRAC) channels appear to be homologous to and derived from the ubiquitous cation diffusion facilitators.* BMC Res Notes, 2010. **3**: p. 158.

226. Palty, R., et al., *SARAF inactivates the store operated calcium entry machinery to prevent excess calcium refilling.* Cell, 2012. **149**(2): p. 425-38.

227. Albarran, L., et al., *Role of STIM1 in the surface expression of SARAF.* Channels (Austin), 2017. **11**(1): p. 84-88.

228. Albarran, L., et al., *Store-operated Ca2+ Entry-associated Regulatory factor (SARAF) Plays an Important Role in the Regulation of Arachidonate-regulated Ca2+ (ARC) Channels.* J Biol Chem, 2016. **291**(13): p. 6982-8.

229. Albarran, L., et al., *SARAF modulates TRPC1, but not TRPC6, channel function in a STIM1-independent manner.* Biochem J, 2016. **473**(20): p. 3581-3595.

230. Jha, A., et al., *The STIM1 CTID domain determines access of SARAF to SOAR to regulate Orai1 channel function.* J Cell Biol, 2013. **202**(1): p. 71-9.

231. Albarran, L., et al., *Dynamic interaction of SARAF with STIM1 and Orai1 to modulate store-operated calcium entry.* Sci Rep, 2016. **6**: p. 24452.

232. Lopez, E., et al., *STIM1 phosphorylation at Y(316) modulates its interaction with SARAF and the activation of SOCE and I(CRAC).* J Cell Sci, 2019. **132**(10).

233. Maleth, J., et al., *Translocation between PI(4,5)P2-poor and PI(4,5)P2-rich microdomains during store depletion determines STIM1 conformation and Orai1 gating.* Nat Commun, 2014. **5**: p. 5843.

234. Albarran, L., et al., *EFHB is a Novel Cytosolic Ca2+ Sensor That Modulates STIM1-SARAF Interaction.* Cell Physiol Biochem, 2018. **51**(3): p. 1164-1178.

235. Calloway, N., et al., *Stimulated association of STIM1 and Orai1 is regulated by the balance of PtdIns(4,5)P_2 between distinct membrane pools.* J Cell Sci, 2011. **124**(Pt 15): p. 2602-10.

236. Zhang, W., et al., *The Penta-EF-Hand ALG-2 Protein Interacts with the Cytosolic Domain of the SOCE Regulator SARAF and Interferes with Ubiquitination.* Int J Mol Sci, 2020. **21**(17).

237. Mullins, F.M., et al., *STIM1 and calmodulin interact with Orai1 to induce Ca2+-dependent inactivation of CRAC channels.* Proc Natl Acad Sci U S A, 2009. **106**(36): p. 15495-500.

238. Hauser, C.T. and R.Y. Tsien, *A hexahistidine-Zn2+-dye label reveals STIM1 surface exposure.* Proc Natl Acad Sci U S A, 2007. **104**(10): p. 3693-7.

239. Park, M.K., et al., *Perinuclear, perigranular and sub-plasmalemmal mitochondria have distinct functions in the regulation of cellular calcium transport.* EMBO J, 2001. **20**(8): p. 1863-74.

240. Marriott, I. and M.J. Mason, *ATP depletion inhibits capacitative Ca2+ entry in rat thymic lymphocytes.* Am J Physiol, 1995. **269**(3 Pt 1): p. C766-74.

241. Chvanov, M., et al., *ATP depletion induces translocation of STIM1 to puncta and formation of STIM1-ORAI1 clusters: translocation and re-translocation of STIM1 does not require ATP.* Pflugers Arch, 2008. **457**(2): p. 505-17.

242. Ercan, E., et al., *A conserved, lipid-mediated sorting mechanism of yeast Ist2 and mammalian STIM proteins to the peripheral ER.* Traffic, 2009. **10**(12): p. 1802-18.

243. Walsh, C.M., et al., *Role of phosphoinositides in STIM1 dynamics and store-operated calcium entry.* Biochem J, 2009. **425**(1): p. 159-68.

244. Qin, X., et al., *Increased Confinement and Polydispersity of STIM1 and Orai1 after Ca(2+) Store Depletion.* Biophys J, 2020. **118**(1): p. 70-84.

245. West, S.J., et al., *S-acylation of Orai1 regulates store-operated Ca2+ entry.* J Cell Sci, 2022. **135**(5).

246. Kodakandla, G., et al., *Dynamic S-acylation of the ER-resident protein stromal interaction molecule 1 (STIM1) is required for store-operated Ca(2+) entry.* J Biol Chem, 2022. **298**(9): p. 102303.

247. Jardin, I., G.M. Salido, and J.A. Rosado, *Role of lipid rafts in the interaction between hTRPC1, Orai1 and STIM1.* Channels (Austin), 2008. **2**(6): p. 401-3.

248. Dionisio, N., et al., *Lipid rafts are essential for the regulation of SOCE by plasma membrane resident STIM1 in human platelets.* Biochim Biophys Acta, 2011. **1813**(3): p. 431-7.

249. Wozniak, A.L., et al., *Requirement of biphasic calcium release from the endoplasmic reticulum for Fas-mediated apoptosis.* J Cell Biol, 2006. **175**(5): p. 709-14.

250. West, S.J., D. Boehning, and A.M. Akimzhanov, *Regulation of T cell function by protein S-acylation.* Front Physiol, 2022. **13**: p. 1040968.

251. Akimzhanov, A.M. and D. Boehning, *Rapid and transient palmitoylation of the tyrosine kinase Lck mediates Fas signaling.* Proc Natl Acad Sci U S A, 2015. **112**(38): p. 11876-80.

252. Bieerkehazhi, S., et al., *Ca2+-dependent protein acyltransferase DHHC21 controls activation of CD4+ T cells.* J Cell Sci, 2022. **135**(5).

253. Fan, Y., et al., *Regulation of T cell receptor signaling by protein acyltransferase DHHC21.* Mol Biol Rep, 2020. **47**(8): p. 6471-6478.

254. Chamberlain, L.H. and M.J. Shipston, *The physiology of protein S-acylation.* Physiol Rev, 2015. **95**(2): p. 341-76.

255. Chen, J.J., Y. Fan, and D. Boehning, *Regulation of Dynamic Protein S-Acylation.* Front Mol Biosci, 2021. **8**: p. 656440.

256. Essandoh, K., et al., *Palmitoylation: A Fatty Regulator of Myocardial Electrophysiology.* Front Physiol, 2020. **11**: p. 108.

257. Fraser, N.J., et al., *Therapeutic targeting of protein S-acylation for the treatment of disease.* Biochem Soc Trans, 2020. **48**(1): p. 281-290.

258. Ladygina, N., B.R. Martin, and A. Altman, *Dynamic palmitoylation and the role of DHHC proteins in T cell activation and anergy.* Adv Immunol, 2011. **109**: p. 1-44.

259. Resh, M.D., *Fatty acylation of proteins: The long and the short of it.* Prog Lipid Res, 2016. **63**: p. 120-31.

260. Duncan, J.A. and A.G. Gilman, *A cytoplasmic acyl-protein thioesterase that removes palmitate from G protein alpha subunits and p21(RAS).* J Biol Chem, 1998. **273**(25): p. 15830-7.

261. Lin, D.T. and E. Conibear, *ABHD17 proteins are novel protein depalmitoylases that regulate N-Ras palmitate turnover and subcellular localization.* Elife, 2015. **4**: p. e11306.

262. Jennings, B.C. and M.E. Linder, *DHHC protein S-acyltransferases use similar ping-pong kinetic mechanisms but display different acyl-CoA specificities.* J Biol Chem, 2012. **287**(10): p. 7236-45.

263. Kullmann, W., *Kinetics of chymotrypsin- and papain-catalysed synthesis of [leucine]enkephalin and [methionine]enkephalin.* Biochem J, 1984. **220**(2): p. 405-16.

264. Ulusu, N.N., *Evolution of Enzyme Kinetic Mechanisms.* J Mol Evol, 2015. **80**(5-6): p. 251-7.

265. Carreras-Sureda, A., et al., *S-acylation by ZDHHC20 targets ORAI1 channels to lipid rafts for efficient Ca2+ signaling by Jurkat T cell receptors at the immune synapse.* Elife, 2021. **10**.

266. Tewari, R., et al., *T cell receptor-dependent S-acylation of ZAP-70 controls activation of T cells.* J Biol Chem, 2021. **296**: p. 100311.

267. Hogan, P.G. and A. Rao, *Store-operated calcium entry: Mechanisms and modulation.* Biochem Biophys Res Commun, 2015. **460**(1): p. 40-9.

268. Feske, S., *CRAC channels and disease - From human CRAC channelopathies and animal models to novel drugs.* Cell Calcium, 2019. **80**: p. 112-116.

269. Baba, Y. and T. Kurosaki, *Physiological function and molecular basis of STIM1-mediated calcium entry in immune cells.* Immunol Rev, 2009. **231**(1): p. 174-88.

270. Tian, L., et al., *Palmitoylation gates phosphorylation-dependent regulation of BK potassium channels.* Proc Natl Acad Sci U S A, 2008. **105**(52): p. 21006-11.

271. Young, J.E. and A.D. Albert, *Rhodopsin palmitoylation in bovine rod outer segment disk membranes of different age/spatial location.* Exp Eye Res, 2001. **73**(5): p. 735-7.

272. Chini, B. and M. Parenti, *G-protein-coupled receptors, cholesterol and palmitoylation: facts about fats.* J Mol Endocrinol, 2009. **42**(5): p. 371-9.

273. Lynes, E.M., et al., *Palmitoylated TMX and calnexin target to the mitochondria-associated membrane.* EMBO J, 2012. **31**(2): p. 457-70.

274. Wang, Y., et al., *Palmitoylation as a Signal for Delivery.* Adv Exp Med Biol, 2020. **1248**: p. 399-424.

275. Blanc, M., F.P.A. David, and F.G. van der Goot, *SwissPalm 2: Protein S-Palmitoylation Database.* Methods Mol Biol, 2019. **2009**: p. 203-214.

276. Schmidt, M.F. and M.J. Schlesinger, *Fatty acid binding to vesicular stomatitis virus glycoprotein: a new type of post-translational modification of the viral glycoprotein.* Cell, 1979. **17**(4): p. 813-9.

277. Wan, J., et al., *Palmitoylated proteins: purification and identification.* Nat Protoc, 2007. **2**(7): p. 1573-84.

278. Tewari, R., et al., *Detection of Protein S-Acylation using Acyl-Resin Assisted Capture.* J Vis Exp, 2020(158).

279. Hundt, M., et al., *Palmitoylation-dependent plasma membrane transport but lipid raft-independent signaling by linker for activation of T cells.* J Immunol, 2009. **183**(3): p. 1685-94.

280. Hundt, M., et al., *Impaired activation and localization of LAT in anergic T cells as a consequence of a selective palmitoylation defect.* Immunity, 2006. **24**(5): p. 513-22.

281. Paige, L.A., et al., *Reversible palmitoylation of the protein-tyrosine kinase p56lck.* J Biol Chem, 1993. **268**(12): p. 8669-74.

282. Yoast, R.E., et al., *The native ORAI channel trio underlies the diversity of Ca.* Nat Commun, 2020. **11**(1): p. 2444.

283. Zhang, X., et al., *Distinct pharmacological profiles of ORAI1, ORAI2, and ORAI3 channels.* Cell Calcium, 2020. **91**: p. 102281.

284. Lin, H., *Protein cysteine palmitoylation in immunity and inflammation.* FEBS J, 2021. **288**(24): p. 7043-7059.

285. Dynes, J.L., A. Amcheslavsky, and M.D. Cahalan, *Genetically targeted single-channel optical recording reveals multiple Orai1 gating states and oscillations in calcium influx.* Proc Natl Acad Sci U S A, 2016. **113**(2): p. 440-5.

286. Dong, T.X., et al., *T-cell calcium dynamics visualized in a ratiometric tdTomato-GCaMP6f transgenic reporter mouse.* Elife, 2017. **6**.

287. Bogeski, I., et al., *Differential redox regulation of ORAI ion channels: a mechanism to tune cellular calcium signaling.* Sci Signal, 2010. **3**(115): p. ra24.

288. Alansary, D., I. Bogeski, and B.A. Niemeyer, *Facilitation of Orai3 targeting and store-operated function by Orai1.* Biochim Biophys Acta, 2015. **1853**(7): p. 1541-50.

289. Hogan, P.G., R.S. Lewis, and A. Rao, *Molecular basis of calcium signaling in lymphocytes: STIM and ORAI.* Annu Rev Immunol, 2010. **28**: p. 491-533.

290. Katz, Z.B., et al., *Septins organize endoplasmic reticulum-plasma membrane junctions for STIM1-ORAI1 calcium signalling.* Sci Rep, 2019. **9**(1): p. 10839.

291. Roth, A.F., et al., *Global analysis of protein palmitoylation in yeast.* Cell, 2006. **125**(5): p. 1003-13.

292. El Ayadi, A., et al., *Ubiquilin-1 regulates amyloid precursor protein maturation and degradation by stimulating K63-linked polyubiquitination of lysine 688.* Proc Natl Acad Sci U S A, 2012. **109**(33): p. 13416-21.

293. Feng, X., et al., *Drosophila TRPML forms PI(3,5)P2-activated cation channels in both endolysosomes and plasma membrane.* J Biol Chem, 2014. **289**(7): p. 4262-72.

294. Garcia, M.I., et al., *Functionally redundant control of cardiac hypertrophic signaling by inositol 1,4,5-trisphosphate receptors.* J Mol Cell Cardiol, 2017. **112**: p. 95-103.

295. Gudlur, A., et al., *Calcium sensing by the STIM1 ER-luminal domain.* Nat Commun, 2018. **9**(1): p. 4536.

296. Hirve, N., et al., *Coiled-Coil Formation Conveys a STIM1 Signal from ER Lumen to Cytoplasm.* Cell Rep, 2018. **22**(1): p. 72-83.

297. van Dorp, S., et al., *Conformational dynamics of auto-inhibition in the ER calcium sensor STIM1.* Elife, 2021. **10**.

298. Mitchell, D.A., et al., *Protein palmitoylation by a family of DHHC protein S-acyltransferases.* J Lipid Res, 2006. **47**(6): p. 1118-27.

299. Ohno, Y., et al., *Intracellular localization and tissue-specific distribution of human and yeast DHHC cysteine-rich domain-containing proteins.* Biochim Biophys Acta, 2006. **1761**(4): p. 474-83.

300. Aicart-Ramos, C., R.A. Valero, and I. Rodriguez-Crespo, *Protein palmitoylation and subcellular trafficking.* Biochim Biophys Acta, 2011. **1808**(12): p. 2981-94.

301. Emrich, S.M., et al., *Omnitemporal choreographies of all five STIM/Orai and IP3Rs underlie the complexity of mammalian Ca(2+) signaling.* Cell Rep, 2021. **34**(9): p. 108760.

302. Feske, S., *Calcium signalling in lymphocyte activation and disease.* Nat Rev Immunol, 2007. **7**(9): p. 690-702.

303. Shaw, P.J. and S. Feske, *Regulation of lymphocyte function by ORAI and STIM proteins in infection and autoimmunity.* J Physiol, 2012. **590**(17): p. 4157-67.

304. Zheng, S., et al., *Calcium store refilling and STIM activation in STIM- and Orai-deficient cell lines.* Pflugers Arch, 2018. **470**(10): p. 1555-1567.

305. Pani, B. and B.B. Singh, *Lipid rafts/caveolae as microdomains of calcium signaling.* Cell Calcium, 2009. **45**(6): p. 625-33.

306. Yokosuka, T. and T. Saito, *The immunological synapse, TCR microclusters, and T cell activation.* Curr Top Microbiol Immunol, 2010. **340**: p. 81-107.

307. Garcia, M.I., J.J. Chen, and D. Boehning, *Genetically encoded calcium indicators for studying long-term calcium dynamics during apoptosis.* Cell Calcium, 2017. **61**: p. 44-49.

308. Hoth, M., *Calcium and barium permeation through calcium release-activated calcium (CRAC) channels.* Pflugers Arch, 1995. **430**(3): p. 315-22.

309. Feske, S., C. Picard, and A. Fischer, *Immunodeficiency due to mutations in ORAI1 and STIM1.* Clin Immunol, 2010. **135**(2): p. 169-82.

310. Kabouridis, P.S., A.I. Magee, and S.C. Ley, *S-acylation of LCK protein tyrosine kinase is essential for its signalling function in T lymphocytes.* EMBO J, 1997. **16**(16): p. 4983-98.

311. Resh, M.D., *Fatty acylation of proteins: new insights into membrane targeting of myristoylated and palmitoylated proteins.* Biochim Biophys Acta, 1999. **1451**(1): p. 1-16.

312. Melkonian, K.A., et al., *Role of lipid modifications in targeting proteins to detergent-resistant membrane rafts. Many raft proteins are acylated, while few are prenylated.* J Biol Chem, 1999. **274**(6): p. 3910-7.

313. Rocks, O., et al., *An acylation cycle regulates localization and activity of palmitoylated Ras isoforms.* Science, 2005. **307**(5716): p. 1746-52.

314. Levental, I., M. Grzybek, and K. Simons, *Greasing their way: lipid modifications determine protein association with membrane rafts.* Biochemistry, 2010. **49**(30): p. 6305-16.

315. Chen, J.J., et al., *DHHC5 Mediates β-Adrenergic Signaling in Cardiomyocytes by Targeting Gα Proteins.* Biophys J, 2020. **118**(4): p. 826-835.

316. Galeano-Otero, I., et al., *SARAF and Orai1 Contribute to Endothelial Cell Activation and Angiogenesis.* Front Cell Dev Biol, 2021. **9**: p. 639952.

317. Zomot, E., et al., *Bidirectional regulation of calcium release-activated calcium (CRAC) channel by SARAF.* J Cell Biol, 2021. **220**(12).

318. Dai, F., et al., *Overexpression of SARAF Ameliorates Pressure Overload-Induced Cardiac Hypertrophy Through Suppressing STIM1-Orai1 in Mice.* Cell Physiol Biochem, 2018. **47**(2): p. 817-826.

319. Sanlialp, A., et al., *Saraf-dependent activation of mTORC1 regulates cardiac growth.* J Mol Cell Cardiol, 2020. **141**: p. 30-42.

320. Bijlmakers, M.J., *Protein acylation and localization in T cell signaling (Review).* Mol Membr Biol, 2009. **26**(1): p. 93-103.

321. Honnappa, S., et al., *An EB1-binding motif acts as a microtubule tip localization signal.* Cell, 2009. **138**(2): p. 366-76.

322. Srikanth, S., et al., *A novel EF-hand protein, CRACR2A, is a cytosolic Ca2+ sensor that stabilizes CRAC channels in T cells.* Nat Cell Biol, 2010. **12**(5): p. 436-46.

323. Jing, J., et al., *Proteomic mapping of ER-PM junctions identifies STIMATE as a regulator of Ca(2)(+) influx.* Nat Cell Biol, 2015. **17**(10): p. 1339-47.

324. Magee, A.I., et al., *Dynamic fatty acylation of p21N-ras.* EMBO J, 1987. **6**(11): p. 3353-7.

325. Rocks, O., et al., *The palmitoylation machinery is a spatially organizing system for peripheral membrane proteins.* Cell, 2010. **141**(3): p. 458-71.

326. Greaves, J. and L.H. Chamberlain, *Palmitoylation-dependent protein sorting.* J Cell Biol, 2007. **176**(3): p. 249-54.

327. Towler, D. and L. Glaser, *Acylation of cellular proteins with endogenously synthesized fatty acids.* Biochemistry, 1986. **25**(4): p. 878-84.

328. Laquel, P., et al., *Phosphoinositides containing stearic acid are required for interaction between Rho GTPases and the exocyst to control the late steps of polarized exocytosis.* Traffic, 2022. **23**(2): p. 120-136.

329. Abrami, L., et al., *Identification and dynamics of the human ZDHHC16-ZDHHC6 palmitoylation cascade.* Elife, 2017. **6**.

Appendix A

Abbreviations

acyl-RAC	acyl resin-assisted capture
BAPTA	l,2-bis(0-aminophenoxy)ethane-A;A^A',,A''-tetraacetic acid
BSA	bovine serum albumin
C-terminal	carboxy terminal
CaM	calmodulin
CRAC	calcium release-activated calcium
DHHC	aspartate-histidine-histidine-cysteine
DTT	dithiothreitol
EDTA	ethylene diamine-tetraacetic acid
EGTA	ethylene glycol-bis(P-aminoethyl ether)N,N,N',N'-tetraacetic acid
ER	endoplasmic reticulum
HA	hydroxylamine
HEK293	human embryonic kidney 293 cell line
IP3	inositol 1,4,5 trisphosphate
IP3R	inositol 1,4,5 trisphosphate receptor
mRFP	monomeric red fluorescence protein
PAT	protein acyltransferase
PBS	phosphate buffered saline
PIP2	phosphatidylinositol 4,5 bisphosphate
PLC	phospholipase C
PM	plasma membrane

PMSF	phenyl methyl sulfonyl fluoride
SDS-PAGE	sodium dodecyl sulfide polyacrylamide gel electrophoresis
SERCA	sarco-endoplasmic reticulum calcium ATPase
SOCE	store-operated calcium entry
STIM1	stromal interaction molecule 1
TCR	T-cell receptor
TG	thapsigargin
TIRF	total internal reflection fluorescence

Appendix B

Attributes

All experiments were performed, analyzed, presented by Goutham Kodakandla, with guidance from Dr. Darren Boehning, unless listed below.

Chapter 2

Fig 1: ABE was performed by Savannah West.

Fig 2: Electrophysiology experiments were conducted in the laboratory of Michael Zhu, UT-Houston

Chapter 3

Fig 2: Electrophysiology experiments were conducted in the laboratory of Michael Zhu, UT-Houston

Appendix C

Supplementary Figures

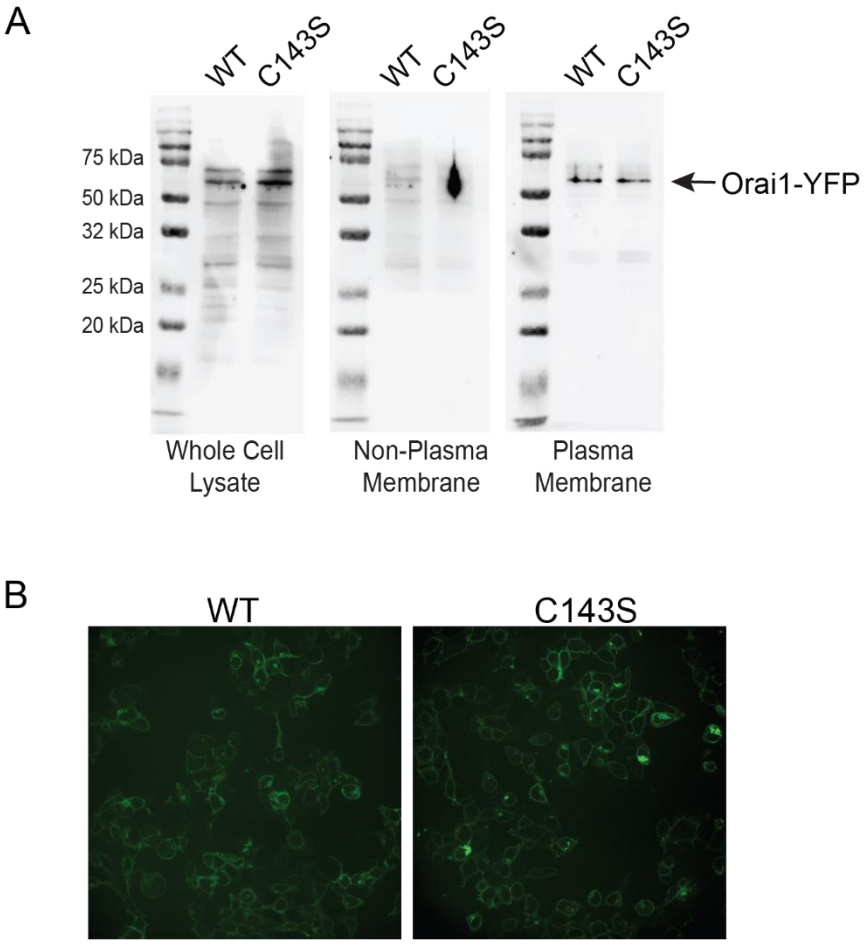

Figure C2.1. WT and C143S Orai1-YFP Expression. A) Cell surface biotinylation of wild-type and C143S mutant Orai1. "Non-plasma membrane" was not bound to streptavidin beads. "Plasma membrane" was eluted from the streptavidin beads. See methods for details. B) Confocal images of WT and C143S Orai1-YFP expressing HEK293T cells. Images were taken under identical conditions.

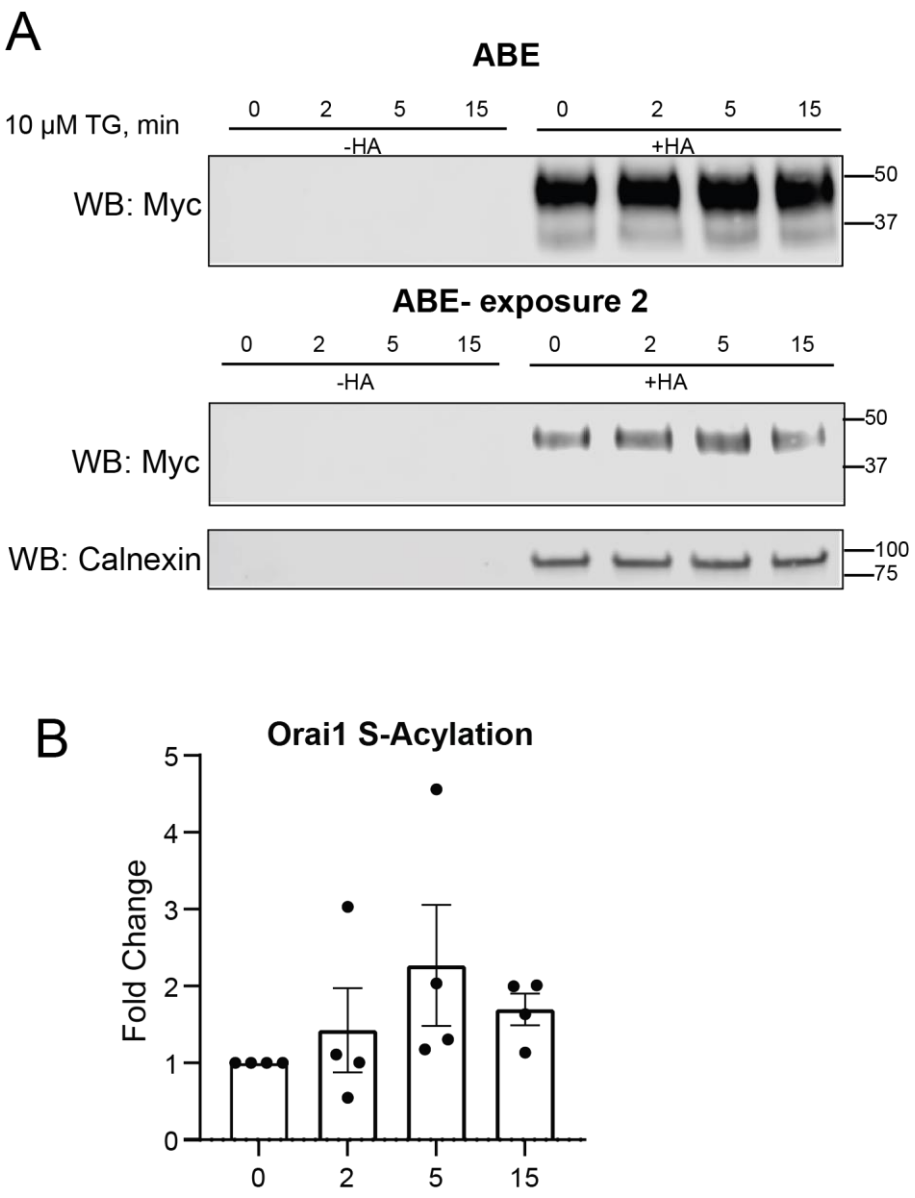

Figure C2.2. Orai1 is transiently S-acylated in HEK293T cells. A) HEK293T cells were transfected with Orai1-Myc and treated with 10 µM thapsigargin (TG) for 0, 2, 5, or 15 minutes, followed by ABE. Two exposures are shown, the first showing both bands that are present, and the second showing only the top band. The constitutively acylated protein calnexin is used as a positive control for ABE. B) Quantification of changes in Orai1 S-acylation (n=4). Error bars indicate S.E.M. There is no significance difference between the time points.

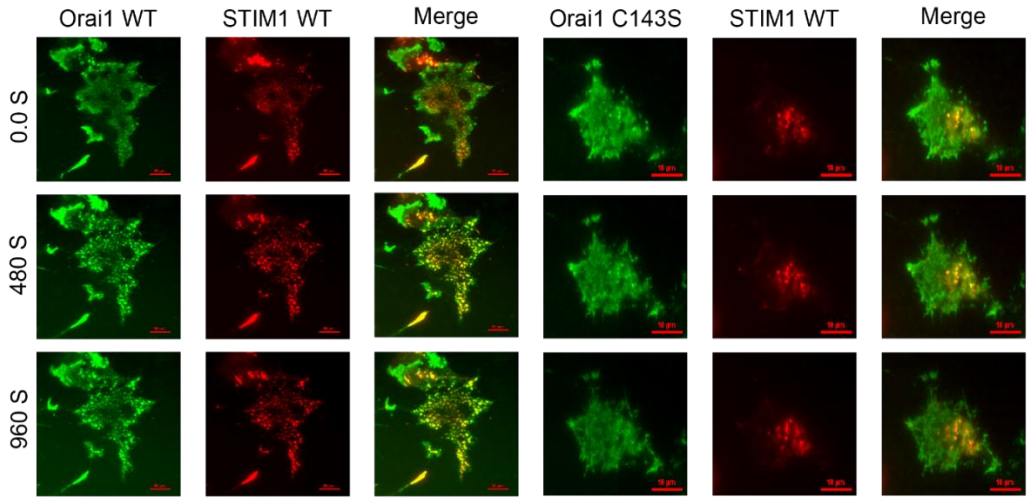

Figure C2.3. Individual channels from Figure 3. Shown are the individual Orai1-YFP, C143S-Orai1-YFP, and STIM1-mRFP channels obtained by TIRF microscopy as presented in Figure 3. Time (in seconds) is shown to the left of the panels. Thapsigargin (10 µM) was added at 60 seconds. A 10µm scale bar is shown.

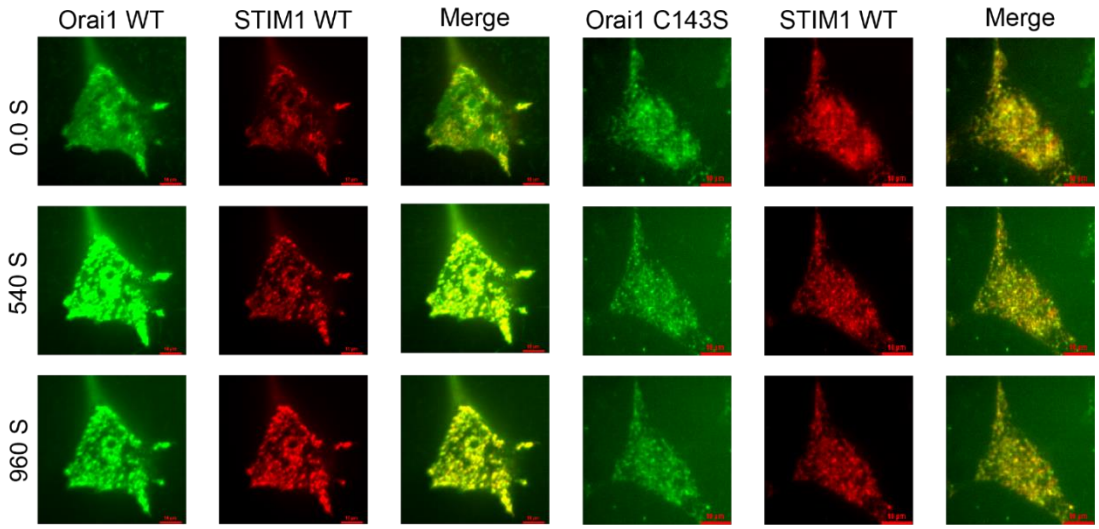

Figure C2.4. Individual channels from Figure 4. Shown are the individual Orai1-GCaMP6f, C143S-Orai1-GCaMP6f, and STIM1-mRFP channels obtained by TIRF microscopy as presented in Figure 3. Time (in seconds) is shown to the left of the panels. Thapsigargin (10 µM) was added at 60 seconds. A 10µm scale bar is shown.

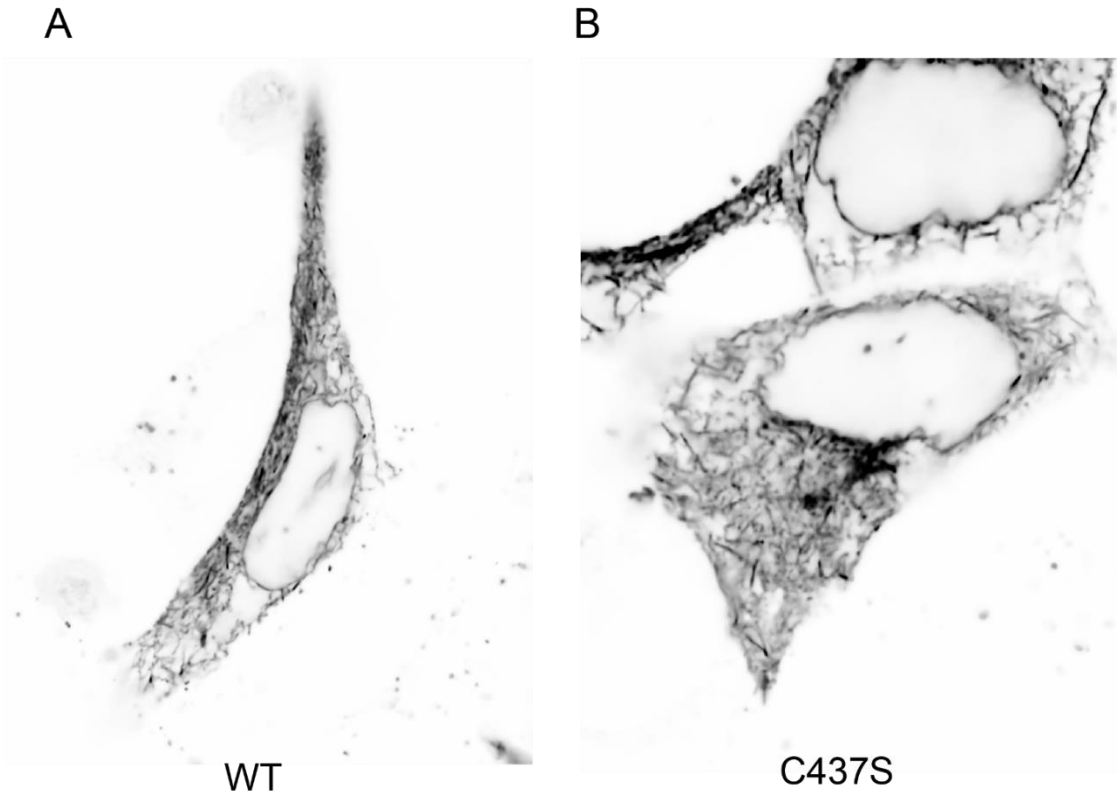

Figure C3.1. ER localization of WT and C437S STIM1. HEK293 STIM DKO cells were transfected with either WT or C437S STIM1-RFP and imaged by confocal microscopy. An inverted LUT was applied. Images were obtained with a 60X objective with 1.5X intermediate magnification.

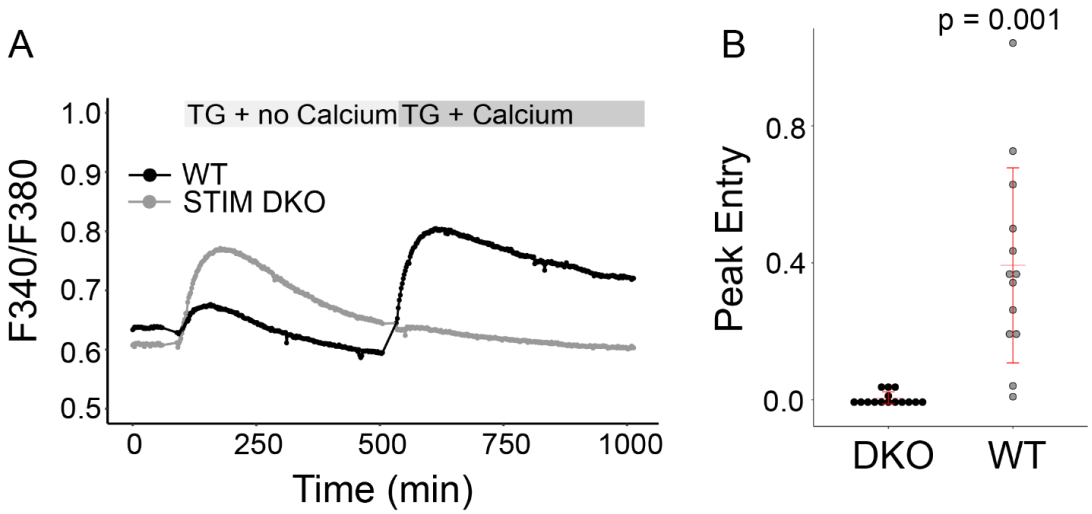

Figure C3.2. STIM1 DKO cells do not have SOCE. A) Fura-2 imaging of WT and STIM DKO HEK293 cells. Cells were first imaged in Ca2+-free medium, then treated with 10 µM thapsigargin (TG) in the absence of Ca2+ to induce Ca2+ store depletion. Cells were then incubated with 10 µM TG in the presence of 1 mM Ca2+ to induce Ca2+ entry. B) Quantified peak entry.

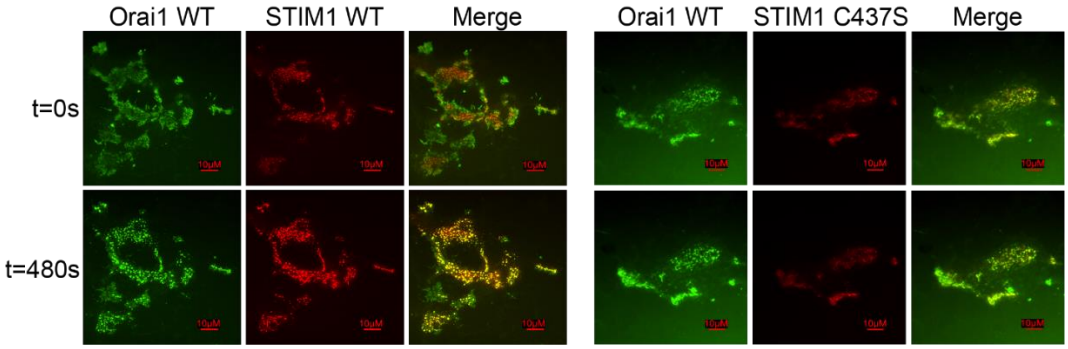

Figure C3.3. Individual channels from Figure 3. Shown are individual Orai1-YFP, STIM1-mRFP WT, and STIM1-mRFP C437S channels obtained by TIRF microscopy as presented in Figure 3. Time (in seconds) is shown to the left of the panels. Thapsigargin (10μM) was added at 60 seconds. A 10μm scale bar is shown.

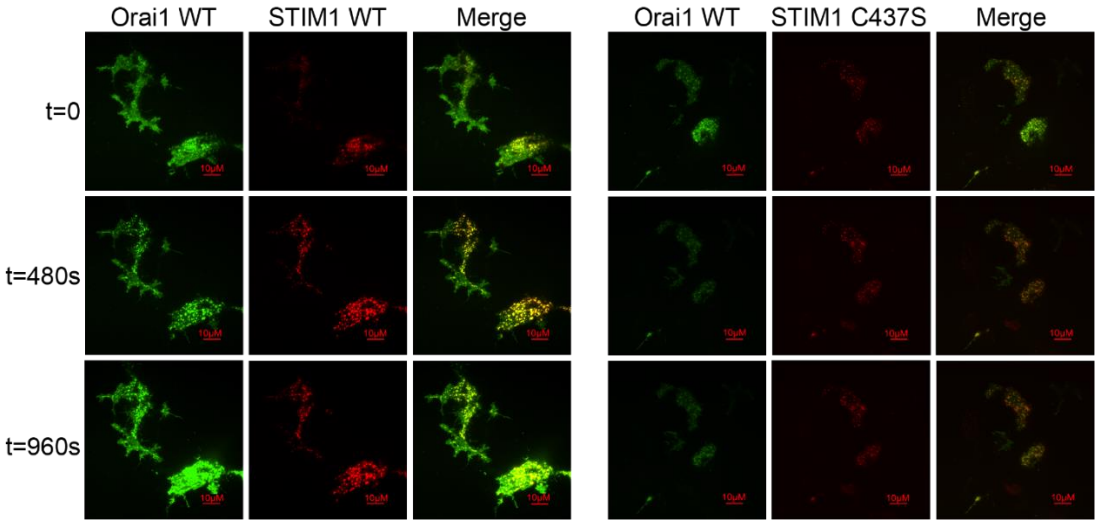

Figure C3.4. Individual channels from Figure 4. Shown are individual Orai1-GCaMP6f, STIM1-mRFP WT, and STIM1-mRFP C437S channels obtained by TIRF microscopy as presented in Figure 4. Time (in seconds) is shown to the left of the panels. Thapsigargin (10μM) in calcium-free media was added at 60 seconds. Calcium add-back with thapsigargin was at 500 seconds. A 10μm scale bar is shown.